國立交通大學

電子工程學系 電子研究所

博 士 論 文

電感耦合電漿氮化製程與氟化製程對鉿系高介電常數材料薄膜之效果

The Effect of Inductively-Coupled Plasma Nitridation and Fluorination Process to Hf-based Dielectric Thin Films

研 究 生：陳柏寧

指導教授：張國明 教授

中 華 民 國 九 十 九 年 七 月

電感耦合電漿氮化製程與氟化製程對鉿系高介電常數材料薄膜之效果

The Effect of Inductively-Coupled Plasma Nitridation and Fluorination Process to Hf-based Dielectric Thin Films

研 究 生：陳柏寧　　Student：Bwo-Ning Chen

指導教授：張國明　　Advisor：Kow-Ming Chang

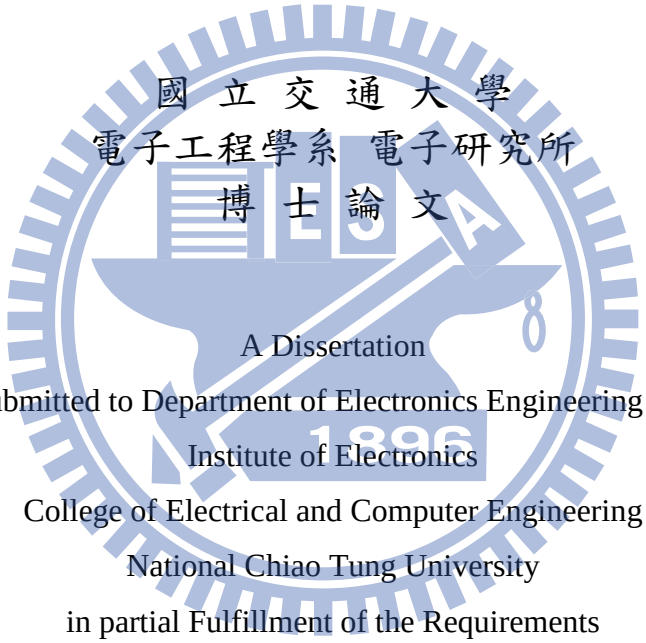

國 立 交 通 大 學

電子工程學系 電子研究所

博 士 論 文

A Dissertation

Submitted to Department of Electronics Engineering and

Institute of Electronics

College of Electrical and Computer Engineering

National Chiao Tung University

in partial Fulfillment of the Requirements

for the Degree of

Doctor of Philosophy

in

Electronics Engineering

July 2010

Hsinchu, Taiwan, Republic of China

中華民國九十九年七月

電感耦合電漿氮化製程與氟化製程對鉿系高介電常數材料薄膜之效果

學生：陳柏寧　　指導教授：張國明 博士

國立交通大學

電子工程學系電子研究所

中文摘要

在這篇論文中，我們致力於討論應用電感耦合電漿源對鉿系高介電常數材料作電漿氮化處理的應用，以期達到改善鉿系高介電常數材料之電特性，可靠度與熱穩定性之目的，然後再我們嘗試加入電感耦合電漿氟化處理的製程，以期進一步改善之前電漿氮化處理的效果，在我們的研究中，在調整到適合的實驗條件之下，電漿氮化與氟化製程的結合可以改善二氧化鉿（HfO_2）與及氧化鉿鋁（$HfAlO_x$）的電特性與可靠度。

首先，我們先專注於討論電感耦合電漿氮化製程對二氧化鉿高介電常數材料薄膜的效果，為了阻止雜質擴散，改善熱穩定度和增加鉿系閘極介電層介電常數之目的，利用氮化製程將氮摻雜入閘極介電質材料，這類的技術已被廣泛的研究，我們利用電感耦合電漿氮化製程以完成將氮摻雜進入二氧化鉿薄膜，實驗結果顯示二氧化鉿薄膜的電特性，可靠度與熱穩定度可以藉由電漿氮化製程而得到改善，在我們實驗步驟中，電漿製程之後整合了一個熱退火製程以減少由於電漿製程所帶給閘極介電層薄膜的傷害。

其次，因為二氧化鉿的熱穩定性不足以適應一般互補式金氧半導體元件製程，所以半導體元件製程中的熱製程，如源極/汲極的活化，將會使二氧化鉿作為閘極介電層材

料時發生漏電流增加以及橫向不均勻等問題，為了增加二氧化鉿材料的熱穩定性，將鋁摻雜進入二氧化鉿形成氧化鉿鋁是一個有效的方法，因此我們嘗試應用相似的電感耦合電漿氮化技術於氧化鉿鋁薄膜上，實驗結果，氧化鉿鋁的薄膜可以因為氮化而進一步改善其電特性，可靠度與熱穩定度。

最後，摻雜氟進入二氧化鉿閘極介電層可以改善金屬氧化物半導體元件結構的種種特性，如臨界電壓不穩，閘極漏電流，崩潰電壓和電容-電壓曲線的磁滯現象，沈積後電漿處理技術已被研究用來摻雜氟進入二氧化鉿薄膜，在我們的研究中，我們結合了電感耦合電漿氮化技術和電感耦合電漿氟化技術兩者，以氟化製程進一步改善氮化製程對二氧化鉿和氧化鉿鋁的製程效果，增強其薄膜的電特性與可靠度。

The Effect of Inductively-Coupled Plasma Nitridation and Fluorination Process to Hf-based Dielectric Thin Films

Student: Bwo-Ning Chen Advisor: Kow-Ming Chang

Department of Electronics Engineering

& Institute of Electronics

National Chiao-Tung University

Hsinchu, Taiwan R.O.C.

Abstract

In this dissertation, we concentrate our effect on applying plasma nitridation treatment in order to improve the electrical characteristics, the reliabilities and the thermal stability of Hf-based dielectric layers. Then we have tried to applied ICP fluorination process to enhance the improvement effect of the plasma treatment. The electrical characteristics and the reliabilities of HfO_2 thin films and $HfAlO_x$ thin films could be modified in adequate process conditions.

First, we are focus on the effect of ICP plasma nitridation process to the HfO_2 thin films. The incorporation of nitrogen into gate dielectrics by nitridation has been investigated with the aim of preventing dopant penetration, improving the thermal stability and enlarging the dielectric constant of Hf-based dielectrics. We use the plasma nitridation process to incorporate nitrogen into HfO_2 thin films. The experimental result indicates that the electrical characteristic, the reliability and the thermal stability of HfO_2 thin films could be improved by the plasma nitridation process. The post-nitridation annealing is integrated into the experimental steps for decreasing the plasma damage caused by the plasma treatment.

Secondly, since the thermal stability of the HfO_2 dielectric layers is quite low, so the thermal process, such as Source/Drain activation, would cause the high leakage current and lateral nonuniformity associated with grain boundaries after the deposition of HfO_2 thin films. In order to increase the crystallization temperature, Al could be added to HfO_2 to form Hf aluminates. We use similar plasma nitridation process to $HfAlO_x$ dielectric layers in order to incorporate nitrogen. The electrical characteristic, the reliability and the thermal stability of $HfAlO_x$ thin films could be improved by the plasma nitridation process.

Finally, the incorporation of fluorine into the HfO_2 gate dielectrics could improve the MOS structure characteristics including threshold voltage instability, gate leakage current, breakdown voltage and C-V hysteresis. The post-deposition plasma fluorination has been used to incorporate fluorine into the HfO_2 gate dielectrics. In our research, we combine the ICP nitridation process and the ICP fluorination process to enhance the electrical characteristics and the reliability of HfO_2 thin films and $HfAlO_x$ thin films.

致謝

首先在此感謝我的指導老師張國明教授，張國明老師在我這些年博士班以及碩士班學習生涯中，在研究方面與待人處事方面上都給予許多的指導與幫助，本論文得以完成首先要感謝老師不斷給我的支持。

在我這些日子的研究生活中，實驗室的學長同學與學弟們都給了我許多的幫助，特別在此先感謝實驗室的楊文誌學長在這幾年的指導與關心，另外感謝陳巨峰學長，鄧一中學長，曾明豪學長，游凱翔學長，王敬業學長，王漢邦學長，賴瓊惠學姐，林稔杰學長，趙高毅學長，林俊銘學長，朱俊宜學長，林志祥學長，陳在洼學長，郭俊銘學長等人在學術生活中前前後後的建議與關懷，感謝林建宏同學這些年大力地幫助與鼓勵，感謝黃士軒學弟，張知天大哥，曾文賢學弟，黃菘宏學弟，張庭嘉學弟，何伯慶學弟的支持，感謝葉星輝學弟，黃士銘學弟，湯鈞凱學弟，蘇明紳學弟，吳汶錦學弟，林協佑學弟在實驗操作上的鼎力相助，還有許多實驗室學長同學與學弟在這本論文一點一滴的建立中慷慨地給予了我很多的鼓勵，在此感謝。

另外感謝交通大學奈米中心以及國家奈米實驗室在實驗器材上的大力支持，感謝兩個機構中許倬綸先生等許許多多的研究人員這些年提供的幫助。交通大學電子工程所的各位教師與及林明霓小姐，李清音小姐等許多的行政人員，這些年來也不斷給予我許多的指導，在這裡謹向各位致意。

感謝我的家人，我的母親，我的姊姊，我的妹妹，以及我的姊夫和外甥女，還有所有不斷給予我幫助的各位家族成員與父執長輩，他們對我的耐心與支持是我能夠持續研究以及完成博士論文的最重要動力，感謝他們一直以來無間斷地關懷與包容，最後，感念我的父親，希望我所有的喜悅都與他共享。

Contents

Figure Captions

Chapter 1

Chapter 2

Chapter 3

Chapter 4

Chapter 5

Chapter 1

Introduction

1.1 Background and Motivation

1.1.1 The Application of High-k Dielectric in Modern IC Process

The continuing downsizing of silicon device has significantly reduced the thickness of the gate dielectric film. However, dielectric layer scaling companies the excessive off-state leakage current that would cause intolerable power consumption and overheat of the devices. To solve the issue about leakage current, a major resolution is to replace the silicon dioxide with a thicker dielectric layer that has a higher dielectric constant and maintains relatively low equivalent oxide thickness (EOT) [1.1]. Fig. 1.1 is the partial table from ITRS 2009, which indicates the predicted standard for high performance (HP) device technical requirements. According to this table, EOT of 0.75 nm is essential for 22 nm HP device technical CMOS technology. Fig. 1.2 and Fig 1.3 are also partial tables from ITRS 2009, which indicate the predicted standard for low operating power (LOP) device technical requirements and low standby power (LSTP) device technical requirements, respectively. In the LOP and LSTP device standard of 2012, even with integration of metal gate process, the EOT of dielectric layers would at least shrink to 1.0 nm. The above fact indicates the necessary to apply high-k dielectrics in CMOS process flow.

1.1.2 The Hf-based High-k Dielectric

To solve the challenge about the excessive leakage current, many kinds of high-k

dielectrics have emerged as the promising candidates to replace the ultrathin silicon dioxide dielectrics for the advanced CMOS technologies [1.2-1.5]. Among these dielectrics, HfO_2 is considered as a suitable gate dielectric material because of the acceptable band gap (~ 5.7 eV), the large dielectric constant (~ 25) and relatively high free energy of reaction with Si (47.6 kcal/mole at 727 ^oC) [1.6].

1.1.3 The Problems about Integration of High-k Dielectric

However, there are still several challenges which have to be considered in order to integrate these high-k dielectrics into a conventional CMOS process flow such as the interface SiO_2 regrowth and the thermal stability of these dielectrics [1.7]. The crystallization temperature of HfO_2 is quite low, so the thermal process, such as Source/Drain activation, would cause the high leakage current and lateral nonuniformity associated with grain boundaries after the deposition of HfO_2 thin films. The incorporation of Al in Hf-based dielectrics has been proven as an effective solution to the issue of thermal stability [1.8]. Fig. 1-4 shows that crystallization of pure HfO_2 dielectric would happen between 300 ^oC to 400 ^oC. Fig. 1-5 presents that with incorporation of Al in HfO_2 thin films, the EOT change of Hf-based dielectrics through thermal processes could be suppressed. The above experimental results prove the thermal stability of HfO_2 thin films could be improved by inducing Al in to thin films.

1.1.4 The Nitrogen Incorporation into Hf-based Thin Films

In high-k dielectrics, there is a high density of charge traps that could cause instability of the threshold voltage, Coulomb scattering of carriers in the channel and reliability problems. The main part of the charge traps is thought to be from oxygen vacancy in the hafnium-based

dielectric [1.9]. Nitrogen incorporation is the widely accepted technique to passivate those defects [1.10-1.11]. In the meantime, nitridation was also beneficial because nitridation decreased hot electron degradation, perhaps because nitrogen lessens the diffusion of hydrogen in the oxide [1.12]. The incorporation of nitrogen into gate dielectrics by nitridation also has been investigated with the aim of preventing dopant penetration [1.13-1.14]. Recently, the various nitridation processes have been shown to improve the thermal stability and the dielectric constant of Hf-based dielectrics [1.15-1.20]. Besides, the nitridation process also has been shown to improve the thermal stability of Hafnium-silicate thin films [1.21].

1.1.5 The Different Ways of Incorporating Nitrogen into Hf-based Thin Films

Thermal nitridation is usually performed at high temperature and hydrogen-containing species that act as electron traps could be added into the thin film. On the other hand, nitrogen could be incorporated into the dielectric layer by plasma nitridation process at lower temperature than by thermal nitridation process [1.22-1.23]. The source of plasma is various, in this dissertation, the inductively-coupled plasma (ICP) technology is used to incorporate nitrogen into Hf-based thin films. From Fig. 1-6, comparing to traditional plasma enhanced chemical vapor deposition (PECVD) system, the radical is firstly produced by ICP system then transport to surface of sample. So the radical density upon surface of sample in ICP system is higher than in traditional PECVD system. We could predict the effect of ICP plasma would be more apparent. The high density plasma effect is why we apply ICP technology in this dissertation.

1.1.6 The Fluorine Incorporation into Hf-based Thin Films

On the other hand, the incorporation of fluorine into the HfO_2 gate dielectrics could

improve the MOS structure characteristics including threshold voltage instability, gate leakage current, breakdown voltage and C-V hysteresis [1.10]. After the incorporation of fluorine, fluorine could effectively passivate charge trapping sites at HfO_2/SiO_2 interface. Strong hafnium-fluorine and silicon-fluorine bonds could be formed by fluorination [1.24-1.27]. Fluorine was found to substitute at the oxygen vacancy site and substitutional fluorine creates a shallow donor state [1.28-1.29]. As a result, the oxygen vacancy site could be passivated and the charged traps in high-k dielectric could be in stable state.

1.1.7 Motivation

In this research, firstly, we have tried to examine the plasma nitridation effect to the electrical properties, the reliabilities and the thermal stability of pure HfO_2 thin films. Secondly, we tried to apply the same plasma nitridation technology to $HfAlO_x$ thin films to see if the electrical properties, the reliabilities and the thermal stabilities of $HfAlO_x$ thin films could be modified by this plasma technology. Furthermore, we have tried to apply the plasma fluorination process to improve the characteristic of the nitrided HfO_2 and $HfAlO_x$ thin films.

1.2 Dissertation Organization

In this dissertation, we concentrated our effort to examine the effect of the plasma nitridation process and the plasma fluorination process to the electrical characteristics, the reliability and the thermal stability of pure HfO_2 and $HfAlO_x$ thin films.

In the chapter 1 of this dissertation, we describe the background and the motivation of our research. In the chapter 2, we apply the inductance-coupled plasma (ICP) nitridation technology to pure HfO_2 thin films in order to improve the electrical characteristics, the

reliabilities and the thermal stability of pure HfO_2 thin films. In the chapter 3, we examine the similar ICP nitridation process to $HfAlO_x$ thin films to observe the process effect to the electrical characteristics, the reliabilities and the thermal stability of $HfAlO_x$ thin films. Furthermore, in the chapter 4, we use the ICP fluorination process to improve the electrical characteristic and the reliabilities of the plasma-nitrided HfO_2 thin films. In the chapter 5, we use the similar plasma fluorination process to improve the electrical characteristic and the reliabilities of the plasma-nitrided $HfAlO_x$ thin films.

Finally, in the chapter 6, a conclusion is given, and the future work about this dissertation is proposed.

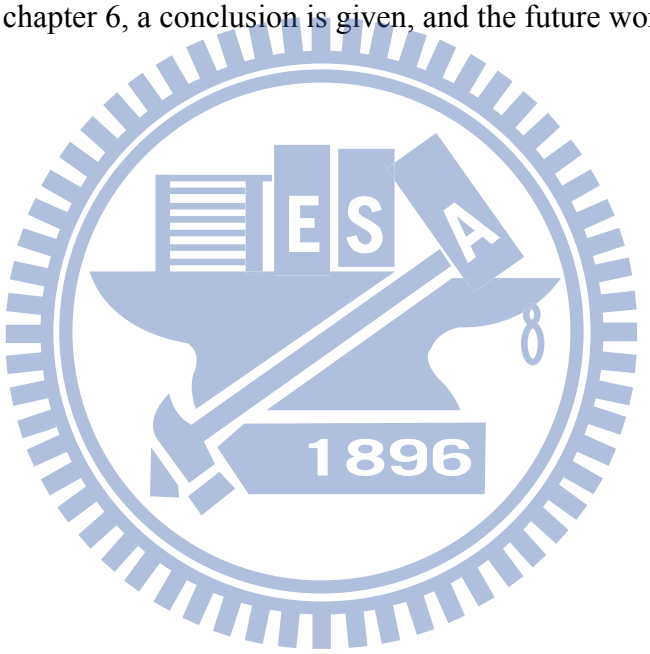

Table FEP2 High Performance Device Technical Requirements

Grey cells indicate the requirements projected only for indicated years

Year of Production	*2009*	*2010*	*2011*	*2012*	*2013*	*2014*	*2015*
MPU Printed Gate Length (nm)	47	41	35	31	28	25	22
MPU Physical Gate Length (nm)	29	27	24	22	20	18	17
Equivalent physical oxide thickness for bulk MPU/ASIC T_{ox} (nm) for 1.5E20-doped poly-Si [A, B, C]	1	0.9					
Equivalent physical oxide thickness for bulk MPU/ASIC T_{ox} (nm) for metal gate [A, B, C]	1	0.95	0.88	0.75	0.65	0.55	0.53
Gate dielectric leakage at 100 °C (A/cm^2) bulk high-performance [D, E, F]	6.5E+02	8.3E+02	9.0E+02	1.0E+03	1.1E+03	1.2E+03	1.3E+03
Metal gate work function for bulk MPU/ASIC $\lvert E_{CV} - \phi_m \rvert$ (eV) [G]	<0.2	<0.2	<0.15	<0.15	<0.15	<0.15	<0.15
Channel doping concentration (cm^{-3}), for bulk design [H]	3.70E+18	4.00E+18	4.50E+18	5.00E+18	5.70E+18	6.60E+18	7.50E+18
Bulk/DG on Bulk– Long channel hole mobility enhancement factor due to strain for MPU/ASIC [I]	1.9	2	2.1	2.2	2.3	2.3	2.3
Bulk/FDSOI/DG – Long channel electron mobility enhancement factor due to strain for MPU/ASIC [I]	1.8	1.8	1.8	1.8	1.8	1.8	1.8

Figure 1.1 The partial table from ITRS 2009, which indicates the predicted standard for high performance (HP) device technical requirements.

Ref: [1]. International Technology Roadmap for Semiconductors, presented at public.itrs.net (2009).

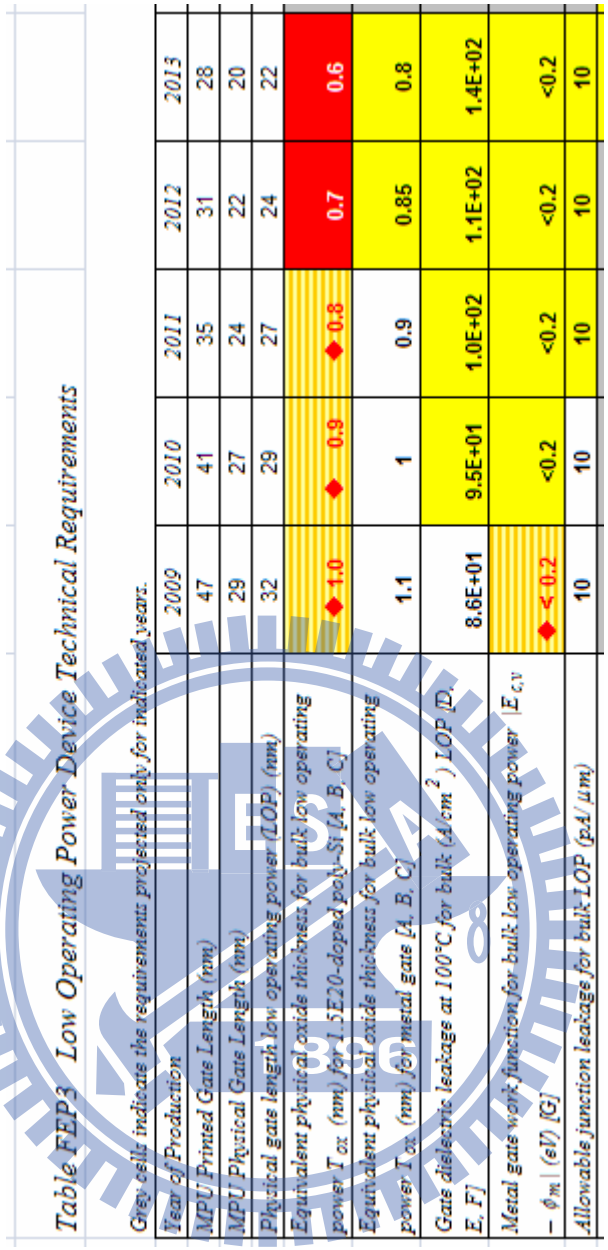

Table FEP3 Low Operating Power Device Technical Requirements

Grey cells indicate the requirements projected only for indicated years.

Year of Production	2009	2010	2011	2012	2013
MPU Printed Gate Length (nm)	47	41	35	31	28
MPU Physical Gate Length (nm)	29	27	24	22	20
Physical gate length low operating power (LOP) (nm)	32	29	27	24	22
Equivalent physical oxide thickness for bulk low operating power T_{ox} (nm) for 1.5E20-doped poly-Si [A, B, C]	1.0	0.9	0.8	0.7	0.6
Equivalent physical oxide thickness for bulk low operating power T_{ox} (nm) for metal gate [A, B, C]	1.1	1	0.9	0.85	0.8
Gate dielectric leakage at 100°C for bulk (A/cm^2) LOP [D, E, F]	8.6E+01	9.5E+01	1.0E+02	1.1E+02	1.4E+02
Metal gate work function for bulk low operating power $\lvert E_{cv} - \phi_m \rvert$ (eV) [G]	< 0.2	<0.2	<0.2	<0.2	<0.2
Allowable junction leakage for bulk LOP ($pA/\mu m$)	10	10	10	10	10

Figure 1.2 The partial table from ITRS 2009, which indicates the predicted standard for low operating power (LOP) device technical requirements.

Ref: [1]. International Technology Roadmap for Semiconductors, presented at public.itrs.net (2009).

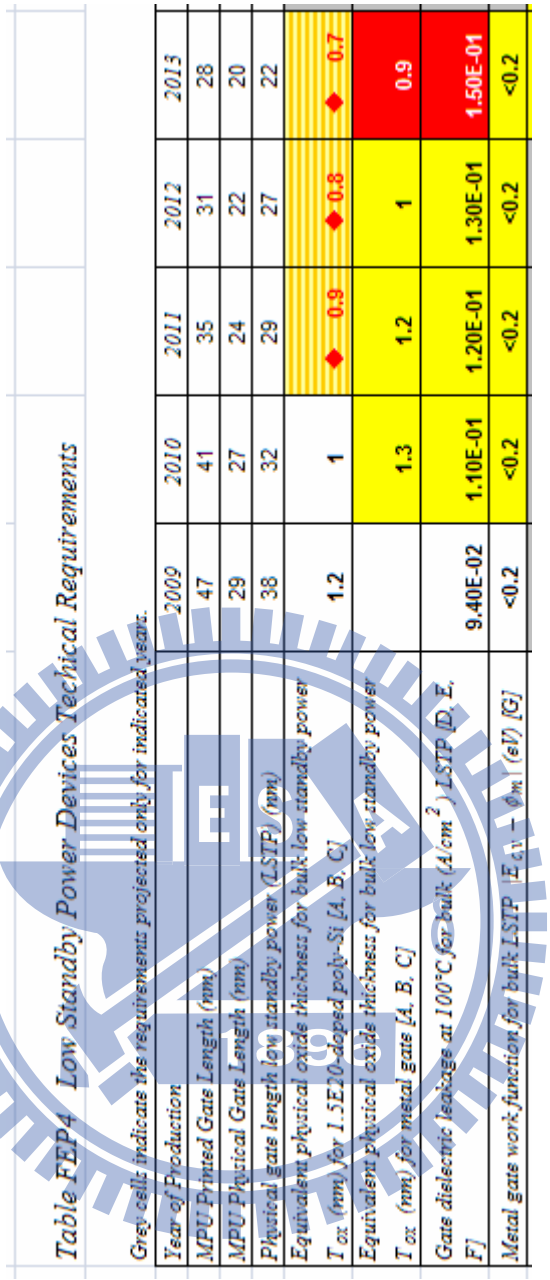

Table FEP4 Low Standby Power Devices Technical Requirements

Grey cells indicate the requirements projected only for indicated years.

Year of Production	2009	2010	2011	2012	2013
MPU Printed Gate Length (nm)	47	41	35	31	28
MPU Physical Gate Length (nm)	29	27	24	22	20
Physical gate length low standby power (LSTP) (nm)	38	32	29	27	22
Equivalent physical oxide thickness for bulk low standby power T_{ox} (nm) for 1.5E20-doped poly-Si [A, B, C]	1.2	1	◆ 0.9	◆ 0.8	◆ 0.7
Equivalent physical oxide thickness for bulk low standby power T_{ox} (nm) for metal gate [A, B, C]		1.3	1.2	1	0.9
Gate dielectric leakage at 100°C for bulk (A/cm^2) LSTP [D, E, F]	9.40E-02	1.10E-01	1.20E-01	1.30E-01	1.50E-01
Metal gate work function for bulk LSTP $\lvert E_{c1} - \Phi_m \rvert$ (eV) [G]	<0.2	<0.2	<0.2	<0.2	<0.2

Figure 1.3 The partial table from ITRS 2009, which indicates the predicted standard for low standby power (LSTP) device technical requirements.

Ref: [1]. International Technology Roadmap for Semiconductors, presented at public.itrs.net (2009).

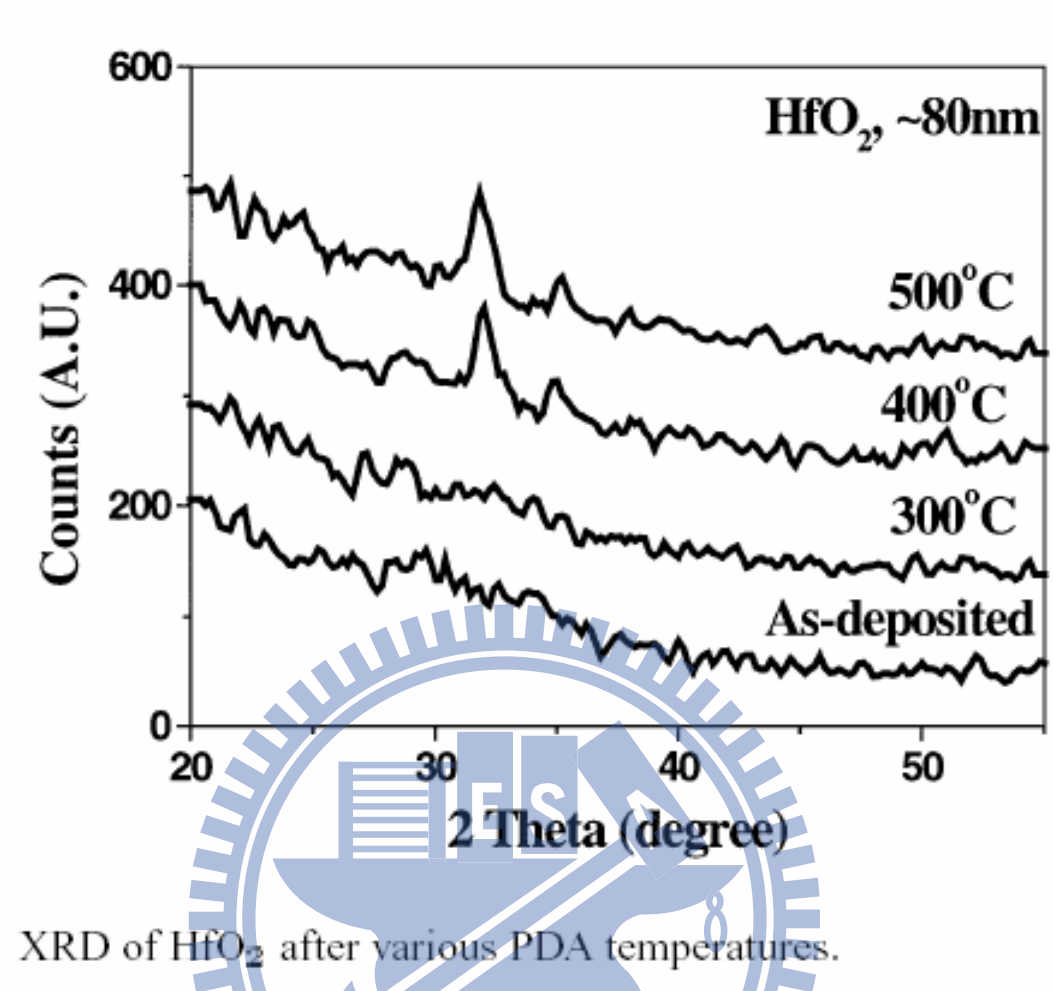

Figure 1.4 The XRD spectrum of HfO_2 dielectric after various PDA temperatures.

Ref: [8]. W. J. Zhu, T. Tamagawa, M. Gibson, T. Furukawa, and T. P. Ma, "Effect of Al inclusion in HfO_2 on the physical and electrical properties of the dielectrics", *IEEE Electron Dev. Lett.* **23**, p. 649 (2002).

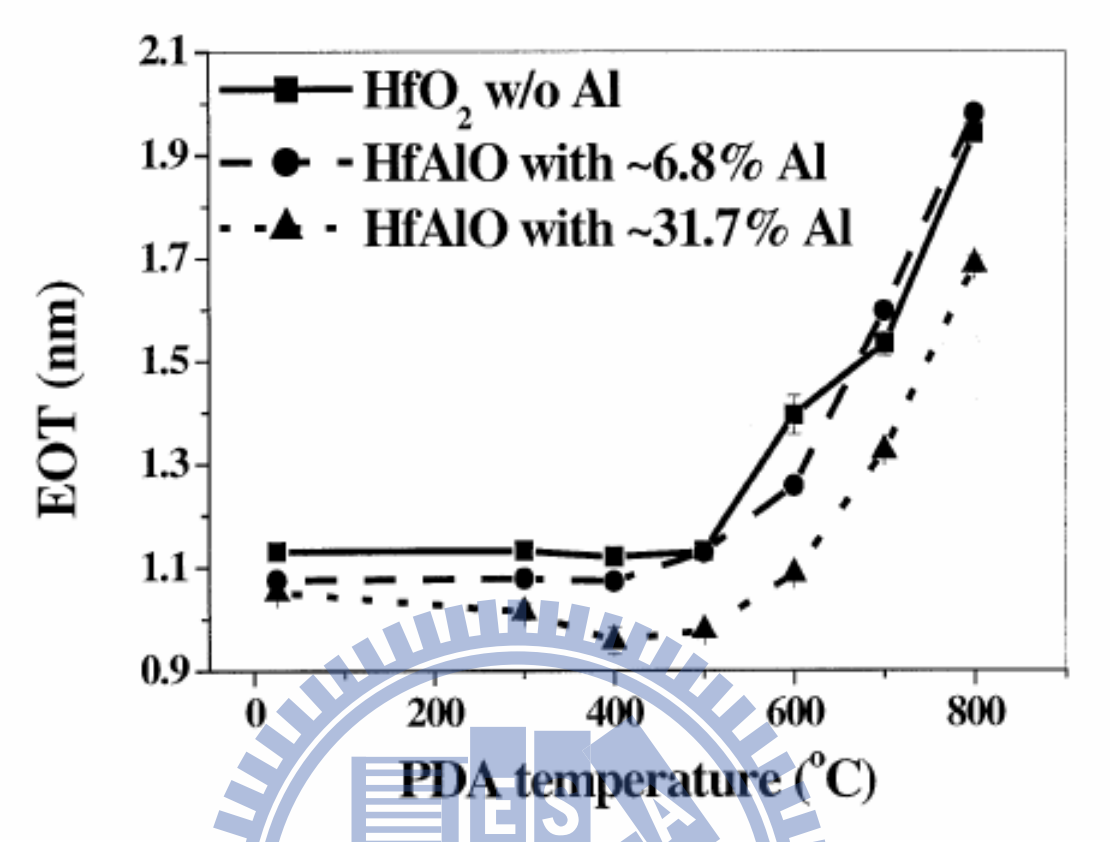

Figure 1.5 The EOT value of HfO_2 dielectric after various PDA temperatures.

Ref: [8]. W. J. Zhu, T. Tamagawa, M. Gibson, T. Furukawa, and T. P. Ma, "Effect of Al inclusion in HfO_2 on the physical and electrical properties of the dielectrics", *IEEE Electron Dev. Lett.* **23**, p. 649 (2002).

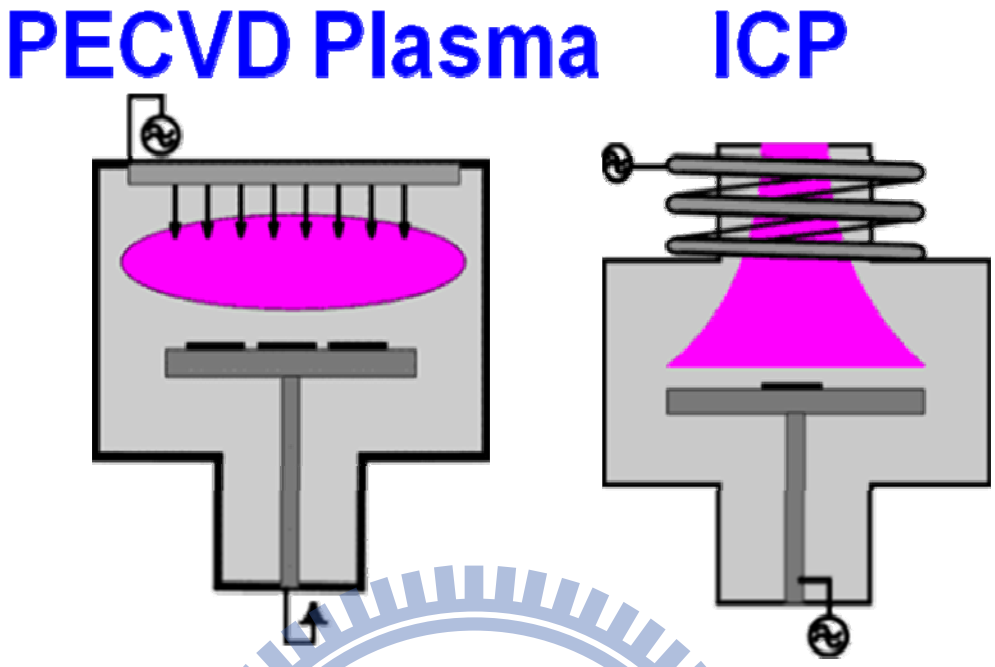

Figure 1.6 The plasma source of the plasma enhanced chemical vapor deposition (PECVD) system and inductively-coupled plasma (ICP) system.

Chapter 2

The Improvement Effect of the Plasma Nitridation Process to the Electrical Properties, the Reliability and the Thermal Stability of HfO_2 thin films

2.1 Introduction

The rapid advancement of complementary metal oxide semiconductor (CMOS) field effect transistor process during the past few years has forced the microelectronics industry to face serious technological challenges. According to the predictions of the International Technology Roadmap for Semiconductor, the equivalent oxide thickness (EOT) and gate leakage currents of conventional gate dielectrics will reach their physical limits [1]. To solve the challenge about the excessive leakage current, many kinds of high-k dielectrics have emerged as the promising candidates to replace the ultrathin silicon oxynitride dielectrics for the advanced CMOS technologies [2-5]. The pure HfO_2 is considered as a suitable gate dielectric material because of the acceptable band gap, which is wide enough to avoid the gate leakage forming the unacceptable power consumption, and the large dielectric constant, which is big enough to increase the physical thickness of the gate dielectric and maintain the relatively low EOT. However, there are several issues which have to be considered in order to integrate these Hf-based dielectrics into a conventional CMOS process flow such as the reliability and the thermal instability of these dielectrics [7, 30-31]. The incorporation of nitrogen into gate dielectrics by nitridation has been investigated with the aim of preventing dopant penetration [13-14]. Recently, the various nitridation processes have been shown to improve the thermal stability and the dielectric constant of Hf-based dielectrics [15-18, 21].

However, thermal nitridation is usually performed at high temperature and hydrogen-containing species that act as electron traps could be introduced into the thin film by thermal nitridation process. On the other hand, nitrogen could be incorporated by plasma nitridation process into the dielectric layer at lower temperature than by thermal nitridation process [22, 32]. The objective of this report is to examine the effect of different ICP plasma nitridation process to the electrical characteristics, the reliability and the thermal stability of HfO_2 thin films [33]. According to this study, the plasma nitridation process could be an effective technology to improve the electrical characteristics, the reliability and the thermal stability of pure HfO_2 thin films.

2.2 Experimental

In this research, Al/Ti/HfO_2/Si structures were fabricated to investigate the effect of the plasma nitridation to HfO_2 dielectrics. A Si wafer with standard initial RCA cleaning was placed into the chamber and a 6-nm HfO_2 layer was deposited on the wafer by the MOCVD system. Then the samples were annealed at 600 ℃ for 30 sec in pure N_2 gas by rapid temperature annealing (RTA) process and nitrided by an ICP plasma treatment at the substrate temperature of 300 ℃, the process pressure of the plasma nitridation process was set as 1.33 × 10^{-4} bar. Ar gas was added into the ICP chamber for activating the plasma while the nitridation process was performed. The flow rate of Ar was set as 10 sccm and the flow rate of the gas containing nitrogen, which is N_2, NH_3 or N_2O, was set as 100 sccm. In an ICP system, a rf current in the coils generates a changing magnetic field, then the magnetic field induces a changing electric field through inductive coupling. Therefore, the inductively coupled electric field accelerates electrons. The electronic mean free path might be shorter than the distance between the anode and the cathode, so there are enough ionizing collisions to produce high density plasma [34]. After the plasma nitridation, there was an annealing process whose

condition was at 600 ℃ for 30 sec in pure N_2 to eliminate the plasma damage [35-36]. A Ti film of 40 nm was deposited on the top side of the samples by sputtering. Then an Al film of 500 nm was thermally evaporated on the top side of the samples. The top electrodes were defined by a lithography process. Finally, the backside native oxide was stripped with diluted HF solution and the backside aluminum electrodes were evaporated by a thermal evaporation. The top area of the Al/Ti/HfO_2/Si MOS capacitors is 5000 μm^2. The capacitance-voltage (C-V) and the current density-voltage (J-V) characteristics of the MOS structures were measured by semiconductor parameter analyzer (HP4156C) and C-V measurement (HP4284) in order to evaluate the improvement effect of the plasma nitridation process and the best process condition. The experimental condition of the stress induced leakage current (SILC) measurement that was carried out in this study was set as constant voltage of 3 V for 180 sec. The stress condition of constant voltage stress (CVS) measurement carried out in this study was set as constant voltage of 3 V to observe the change of the gate leakage current while the stress was applied.

2.3 Results and Discussion

In the beginning of this work, different process time was tested to decide the most suitable process condition for various plasma nitridation processes. After the process time had been determined, the improvement effect of the plasma nitridation process to the reliability of pure HfO_2 thin films would be examined.

2.3.1 The Most Suitable Process Time

Figure 2.1 shows the C-V characteristics of the HfO_2 gate dielectrics treated in ICP N_2 plasma for different process times. The frequency used in the high frequency C-V

measurement was set as 50 kHz. The capacitors treated for 90 sec perform the maximum capacitance density among these samples with different process times. The EOT of HfO_2 thin films decrease from 3.6 nm to 2.3 nm after N_2 plasma nitridation. In addition, the capacitors treated for 30 sec and 60 sec also present the larger values than the capacitors without whole plasma nitridation process. The factor of improvement might be from that the PDA process [37-39] and the nitrogen incorporation in the HfO_2 dielectrics, which could enhance the electronic polarization as well as the ionic polarization, so the dielectric constant of the HfO_2 thin films increases just as Hf-silicate thin films [20, 40] and SiO_2 thin films [41]. Besides, the capacitance density of the samples treated for 120 sec is degraded. The reason could be the damage caused by the N_2 plasma.

The J-V characteristics of the HfO_2 capacitors treated by ICP N_2 plasma with different process times from 0 V to -2 V are described in Fig. 2.2. The gate leakage current density is suppressed while the treatment condition was 60 sec. The reduction of the leakage current could be attributed to the post-deposition annealing process [37-38]. The gate leakage current density of the samples not treated in ICP N_2 plasma at V_g of -1 V is about 3.74×10^{-4} A/cm^2 and the gate leakage current density of the capacitors treated in ICP N_2 plasma for 60 sec at V_g of -1 V is about 2.22×10^{-5} A/cm^2. Moreover, the leakage current densities of the samples treated in N_2 plasma for shorter or longer time are larger than the one treated for 60 sec. The effect of the nitridation process with shorter process time might be not enough. On the other hand, while the nitridation process time is longer than 60 sec, the plasma damage from the plasma nitridation could cause the increase of the gate leakage density. In summary, the best process time of the plasma nitridation in N_2 plasma is set as 60 sec. This appears that the samples treated in N_2 plasma for 60 sec display the most excellent value (the EOT of the samples is about 2.3 nm).

In Fig. 2.3 and Fig. 2.4, the C-V and the J-V characteristics of the HfO_2 gate dielectrics treated in ICP NH_3 plasma for different process times are presented. As mentioned before, the reason of the improvement effect in the NH_3 plasma nitridation process could be the same as the one in the N_2 plasma nitridation process [20, 37]. From the similar analysis, the best process time of the plasma nitridation in NH_3 plasma is set as 90 sec. The EOT of HfO_2 thin films decrease from 3.6 nm to 2.3 nm after NH_3 plasma nitridation. The gate leakage current density of the capacitors treated in ICP NH_3 plasma for 90 sec at V_g of -1 V is about 1.62×10^{-5} A/cm^2. This indicates that the samples treated in NH_3 plasma for 90 sec displays the most excellent value (the EOT of the samples is about 2.3 nm).

In Fig. 2.5 and Fig. 2.6, the C-V and the J-V characteristics of the HfO_2 gate dielectrics treated in ICP N_2O plasma for different process times are demonstrated. There could be other reasons for the improvement effect of the N_2O plasma nitridation process. Since a high concentration of oxygen vacancies causes electrons to be generated and a large leakage current to flow, treatment with plasma that contains oxygen could yield active oxygen atoms and reduce oxygen vacancies to improve the quality of dielectric films [34]. The EOT of HfO_2 thin films decrease from 3.6 nm to 2.7 nm after N_2O plasma nitridation. The gate leakage current density of the samples treated in ICP N_2O plasma for 60 sec at V_g of -1 V is about 2.37×10^{-5} A/cm^2 and the gate leakage current density of the capacitors treated in ICP N_2O plasma for 90 sec at V_g of -1 V is about 2.22×10^{-5} A/cm^2. So when the process time is set as 90 sec, the reduction of the gate leakage density of the nitrided sample would be more obvious. The decrease in the leakage current from nitridation process might be believed to be caused by electron trapping [42-43]. As mentioned above, the best process time of the plasma nitridation in N_2O plasma is set as 90 sec. The samples treated in N_2O plasma for 90 sec perform that the EOT of the samples is about 2.7 nm. The reason that the EOT of the sample

treated by N_2O plasma was bigger than the ones treated by N_2 or NH_3 plasma could be the excess oxygen in N_2O plasma to make the HfO_2 thin films become thicker.

2.3.2 Reliability

Figure 2.7 shows the hysteresis characteristics of the HfO_2 gate dielectrics treated in different ICP plasma. Hysteresis measurement was started from positive to negative bias (negative sweeping, 1 to −2 V), and then swept back from negative to positive bias (positive sweeping, −2 to 1 V) at a frequency of 50 kHz. The hysteresis phenomenon of the C-V curves can be observed for all samples, which is caused by the existence of negative charges trapped in the dielectric defect states when the capacitors are stressed [44]. These defect states are called slow trapping sites [45]. The hysteresis characteristic could be improved by various ICP plasma nitridation process as presented in Fig. 2.7. The C-V curve shift of the sample nitrided by N_2O plasma is about 6 mV and the voltage shift in the C-V curve of the sample nitrided by N_2 plasma is about 9 mV. That is, the hysteresis phenomenon of pure HfO_2 dielectrics could be restrained to be less than 10 mV by both N_2 and N_2O nitridation processes.

Figure 2.8 displays the SILC curve of p-type HfO_2 gate dielectrics treated with N_2 plasma process. After the samples stressed by constant voltage of 3 V for 180 sec, the degree of leakage current degradation could reflect the reliability of the samples. First, Fig. 2.8 presents that the degradation could be improved by N_2 plasma nitridation process. The increase of gate leakage current at -1 V of HfO_2 thim film changes from 159.06 % to 79.19 % after N_2 plasma nitridation. Secondly, since HfO_2 dielectric would recrystallize when suffering a high temperature process, the leakage current would increase after the extra high temperature RTA

process (800 ℃ for 30 sec in N_2). Even so, the degradation of the gate leakage would be slighter with N_2 plasma nitridation process.

As shown in Fig. 2.9, the SILC characteristics of p-type HfO_2 gate dielectrics nitrided by NH_3 plasma process present that the shift of leakage current because of the constant voltage stress could also be restrained by NH_3 plasma nitridation. The increase of gate leakage current at -1 V of HfO_2 thim film changes from 159.06 % to 50.00 % after NH_3 plasma nitridation. Furthermore, even when nitride sample suffered an additional high temperature RTA process (800 ℃ for 30 sec in N_2), the increase of the gate leakage current would be still suppressed.

Figure 2.10 describes the SILC curves of p-type HfO_2 gate dielectrics treated with N_2O plasma process. As Fig. 2.10 presents, the shift of leakage current due to the constant voltage stress could also be restrained by N_2O plasma nitridation. The increase of gate leakage current at -1 V of HfO_2 thim film changes from 159.06 % to 87.80 % after N_2O plasma nitridation. But the improvement effect of the N_2O plasma nitridation process to the SILC phenomenon of the HfO_2 thin films seems unapparent in comparison with other plasma nitridation process.

Figure 2.11 demonstrates the gate current shift of p-type HfO_2 gate dielectrics treated with N_2 plasma for different annealing process during CVS of 3 V. Figure 2.11 indicates that the gate current shift of the thin film treated with N_2 plasma for 60 sec is smaller than the one without nitridation. After N_2 plasma nitridation 60 sec, the gate leakage shift shrinks as 3.76 %. Besides, the sample with N_2 plasma treatment for 60 sec that suffered an additional thermal process of 800 ℃ also has smaller current shift. In other word, for substrate injection, the gate current shift could be suppressed by N_2 plasma nitridation.

The CVS characteristics of samples nitride by miscellaneous kinds of ICP plasma are described in Fig. 2.12. All the gate current shifts of the samples with nitridation could be decreased. The gate leakage shift shrinks as 11.64 % after 90 sec NH_3 plasma nitridation and the gate leakage shift shrinks as 14.36 % after 60 sec NH_3 plasma nitridation. Among all nitrided process, the ICP N_2 plasma nitridation process presents the best result. In summary, the improvement effect of the ICP N_2 plasma nitridation would be most obvious to the reliability of HfO_2 thin films.

2.3.3 Thermal Stability

The nitrogen was incorporated into the dielectric could maintain an amorphous homogeneous film without phase separation at high temperature [21]. The nitridation effect to the thinner HfO_2 thin films (the EOT of the samples was about 1.5 nm) was also corroborated in other experimental result.

In Figure 2.13 and Figure 2.14, the C-V and the J-V characteristics of the HfO_2 gate dielectrics treated by different plasma nitridation processes and thermal treatments have been shown. As demonstrated in Figure 2.14, for the samples which were just deposited in the ALD system and not nitrided, the C-V characteristic of the samples without the high temperature annealing (in N_2 at 850 ℃ for 30 sec) was very different from the samples with the annealing. So from the electrical characteristic, the original samples could not sustain the high temperature annealing. In the meantime, for the samples which were nitrided in N_2 plasma for 90 sec, the C-V characteristic of the samples without the high temperature annealing was very similar to the samples with the annealing. So it seemed to prove that the nitridation process could improve the thermal stability of the HfO_2 thin films. If the nitridation time had not been enough, the thermal stability of the high-k thin films would be

not enough either. Just like the samples treated in N_2 plasma for 30 sec could not sustain the high temperature annealing. In Figure 2.14, we observed that the J-V curve of the sample with nitridation which suffered high temperature annealing could maintain a lower value than the one without nitridation. The above electrical characteristics could also confirm the improved effect of the plasma nitridation to the thermally stability of the HfO_2 thin films.

2.3.4 Physical Analysis

Fig. 2.15 is XPS analysis of the Hf 4f electronic spectra of the samples treated in ICP N_2 plasma for 60 sec. For the nitrided HfO_2 thin films, the Hf 4f peaks of the XPS spectra would shift to lower binding energy because the binding energy of Hf-N bonds is lower than Hf-O bonds [60]. So it indicates that the presence of Hf-O-N bonds in HfO_2 thin films after ICP N_2 plasma nitridation.

2.4 Summary

According to above research, after the best process time was decided from the C-V and J-V characteristics, the improvement effect of the ICP plasma process to the reliability of pure HfO_2 thin films was verified from the hysteresis, SILC and CVS characteristics. For different ICP plasma nitridation process, the influence would be diverse. In conclusion, the ICP N_2 plasma nitridation process could achieve the best performance to the reliability of HfO_2 thin films. The EOT of HfO_2 changes from 3.6 nm to 2.3 nm and the gate leakage current density changes from 3.74×10^{-4} A/cm^2 to 2.22×10^{-5} A/cm^2 after N_2 plasma nitridation. Furthermore, the plasma nitridation could be also used to improve the thermal stability of the HfO_2 thin films to bear the high temperature process at 850 ℃ for at least 30 sec.

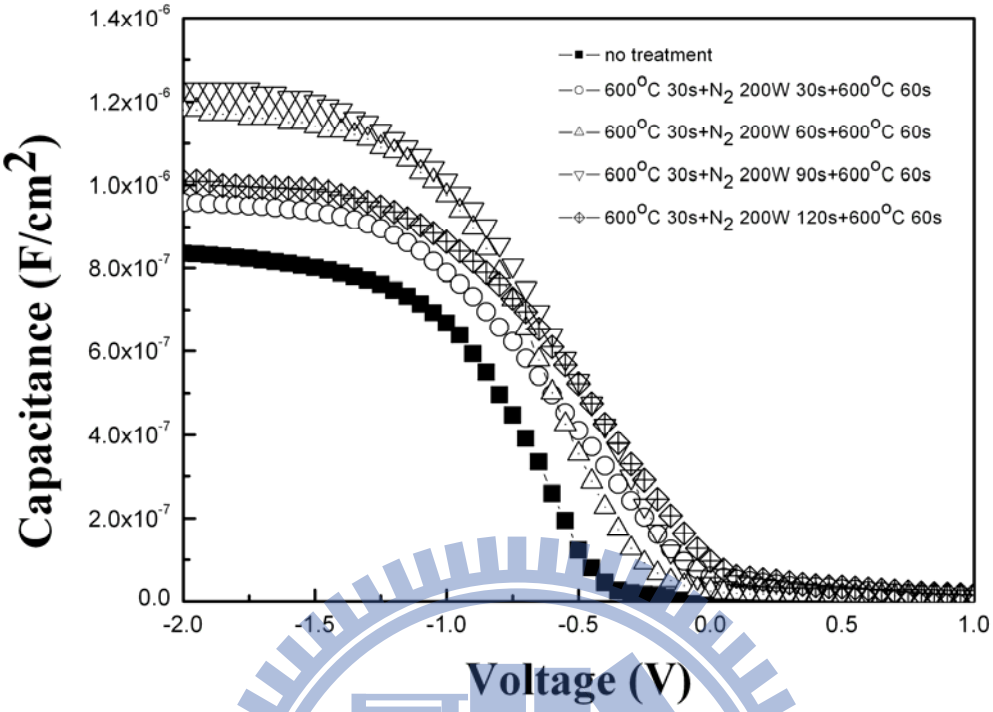

Figure 2.1 The C-V characteristics of the HfO_2 thin films treated in N_2 plasma for different process times.

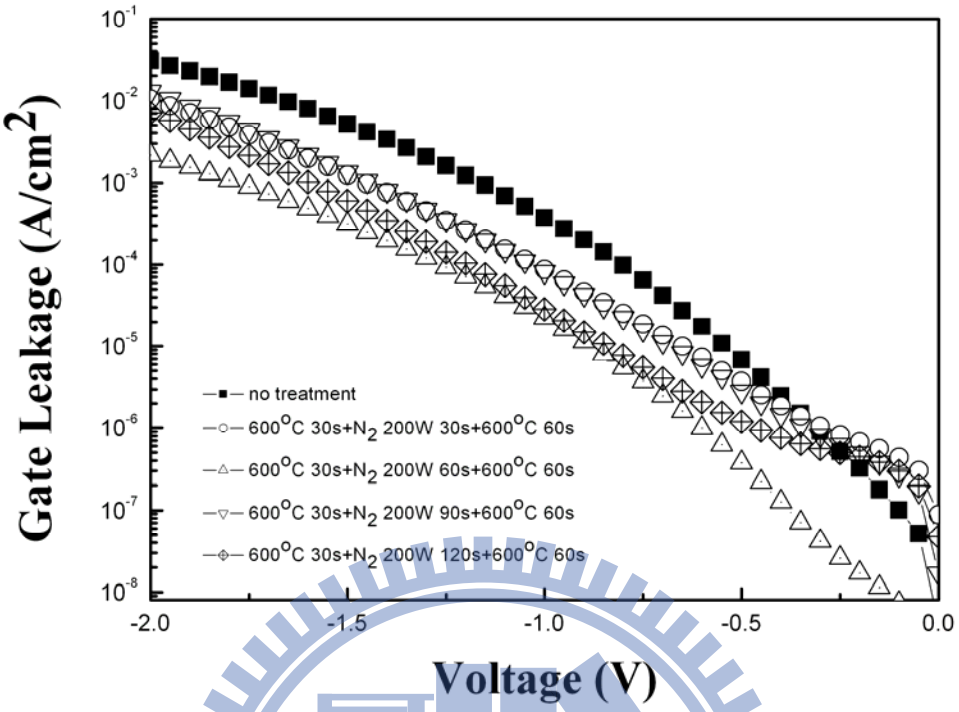

Figure 2.2 The J-V characteristics of the HfO_2 thin films treated in N_2 plasma for different process times.

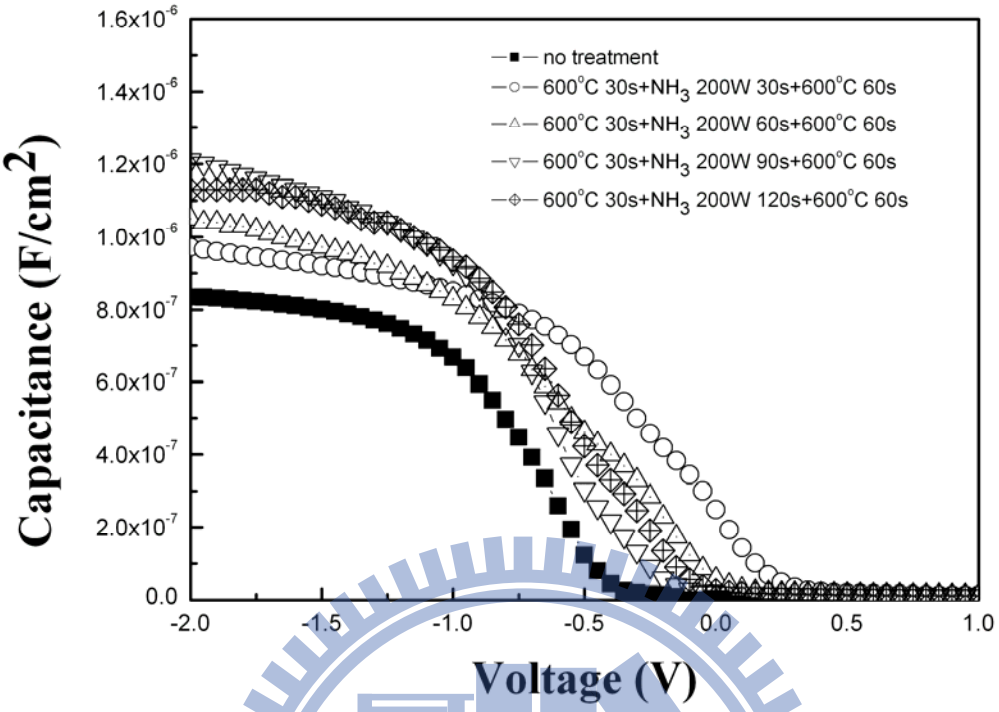

Figure 2.3 The C-V characteristics of the HfO_2 thin films treated in NH_3 plasma for different process times.

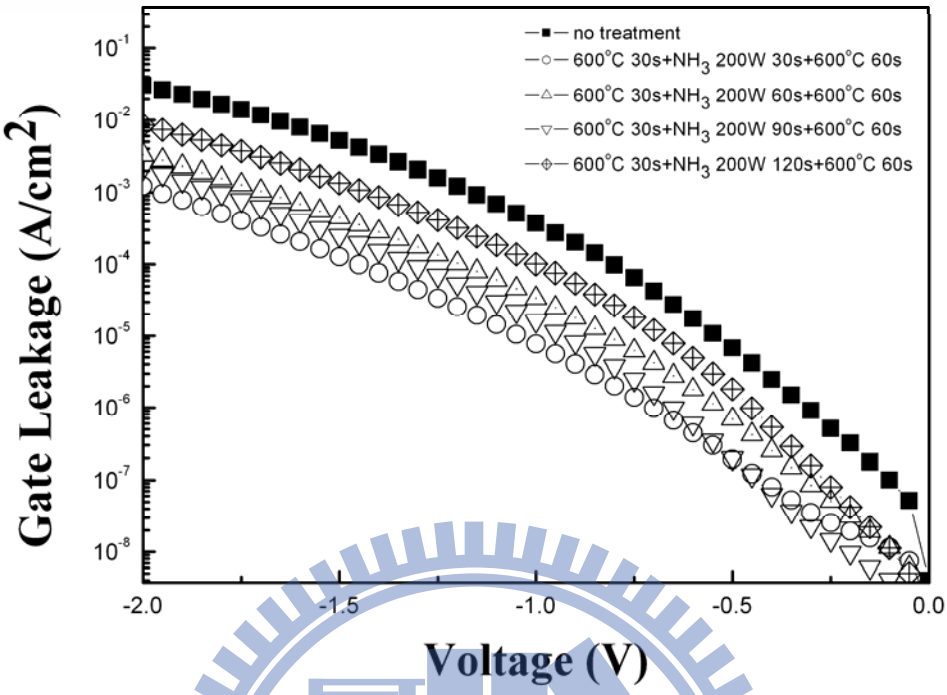

Figure 2.4 The J-V characteristics of the HfO_2 thin films treated in NH_3 plasma for different process times.

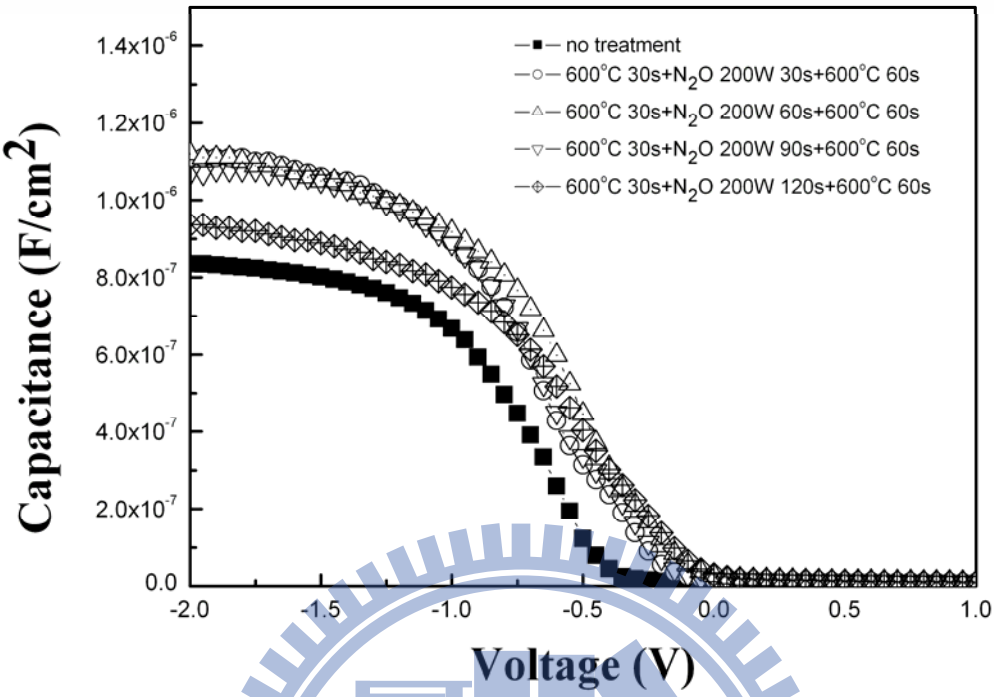

Figure 2.5 The C-V characteristics of the HfO_2 thin films treated in N_2O plasma for different process times.

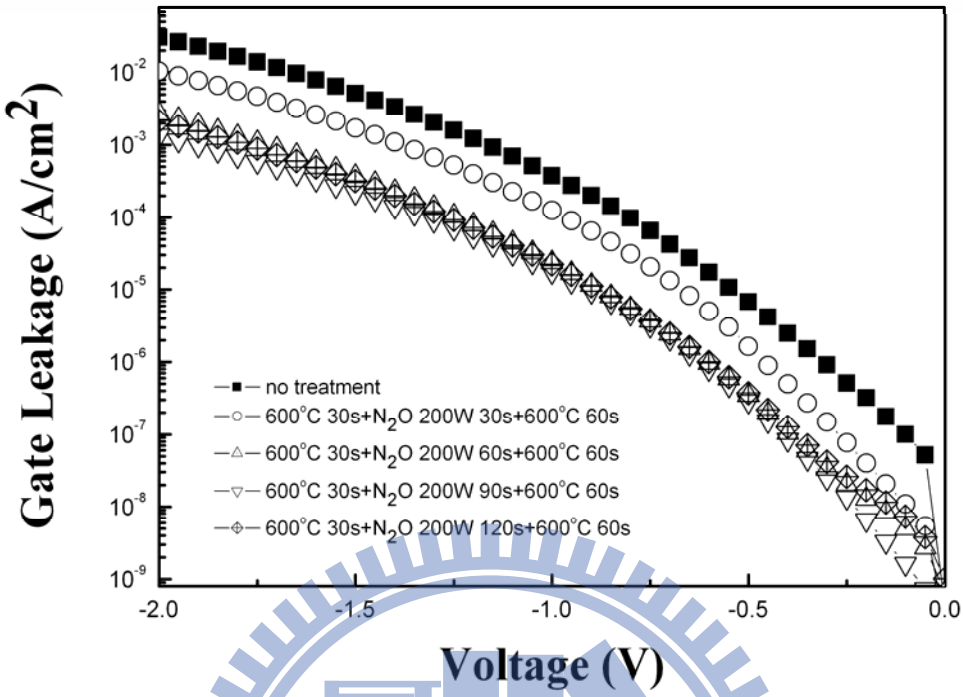

Figure 2.6 The J-V characteristics of the HfO_2 thin films treated in N_2O plasma for different process times.

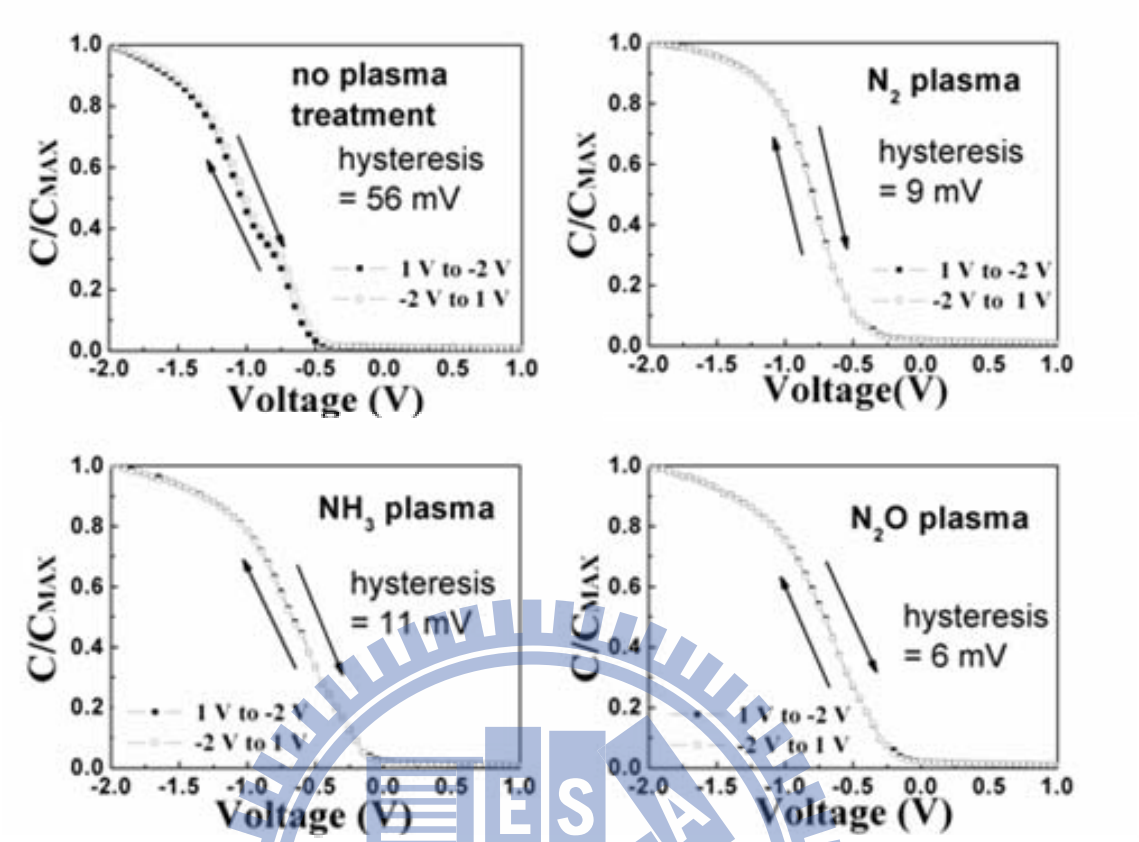

Figure 2.7 The hysteresis characteristics of the HfO_2 thin films nitrided by different ICP plasma process.

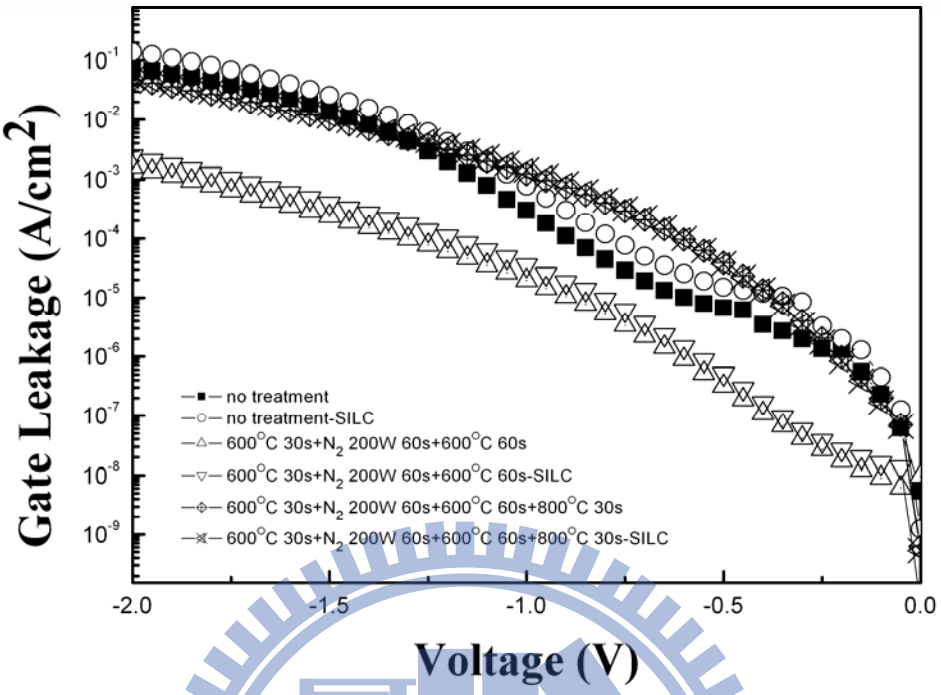

Figure 2.8 The SILC characteristics of the HfO_2 thin films nitrided by ICP N_2 plasma.

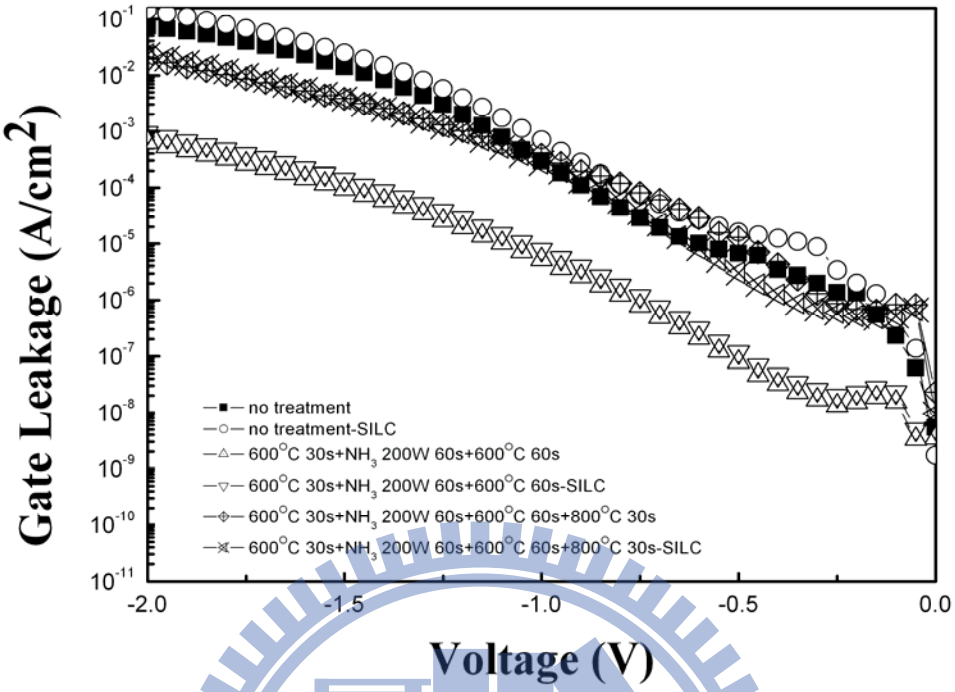

Figure 2.9 The SILC characteristics of the HfO_2 thin films nitrided by ICP NH_3 plasma.

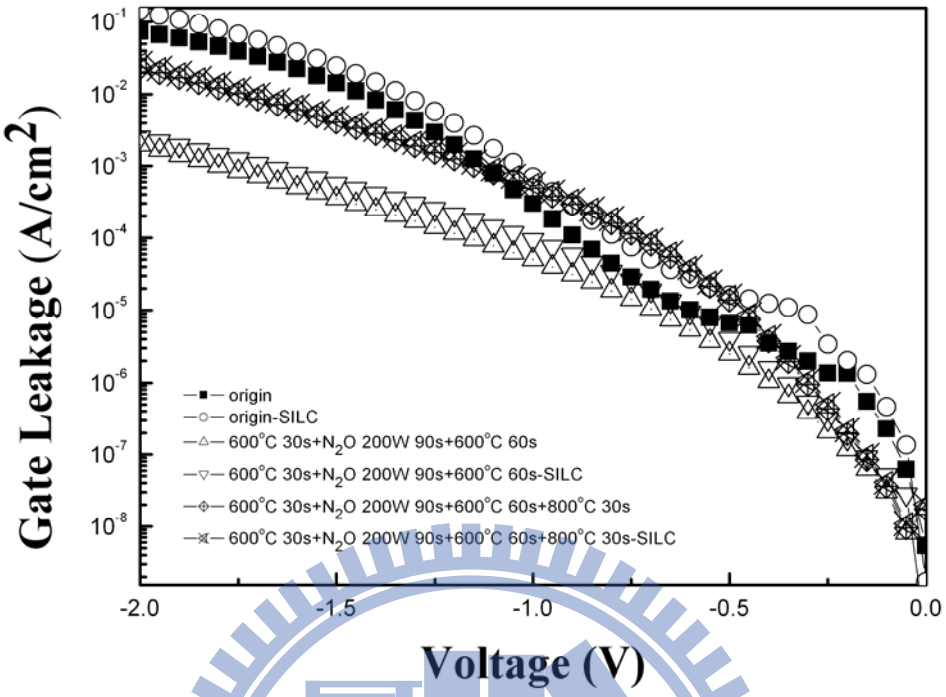

Figure 2.10 The SILC characteristics of the HfO_2 thin films nitrided by ICP N_2O plasma.

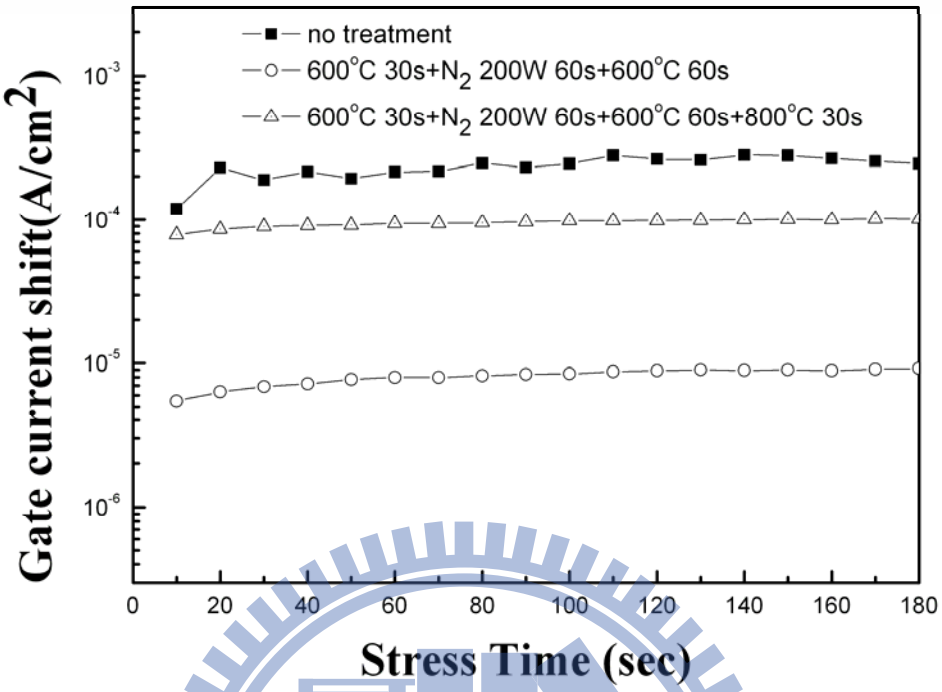

Figure 2.11 The leakage current shift curves of the HfO_2 thin films nitrided by ICP N_2 plasma.

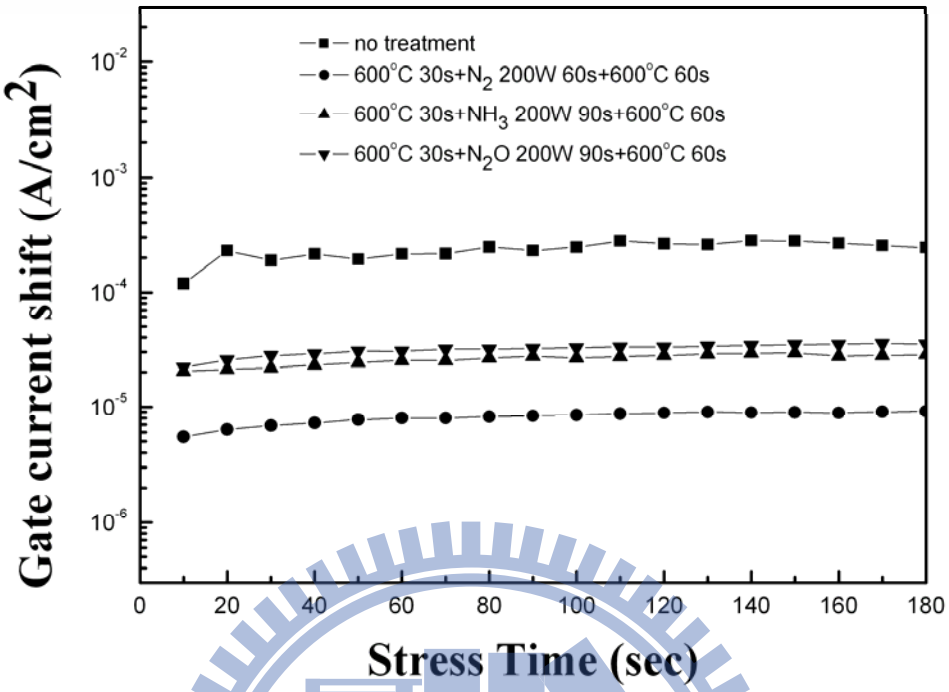

Figure 2.12 The leakage current shift curves of the HfO_2 thin films nitrided by different plasma.

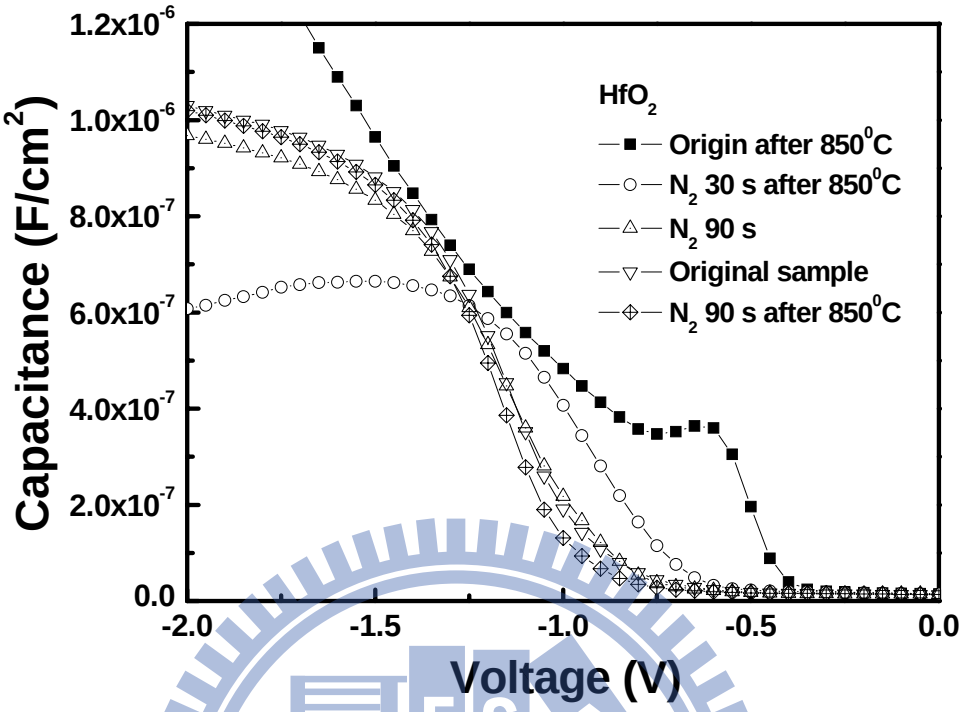

Figure 2.13 The C-V characteristics of the HfO_2 gate dielectrics treated by different plasma nitridation process and PDA.

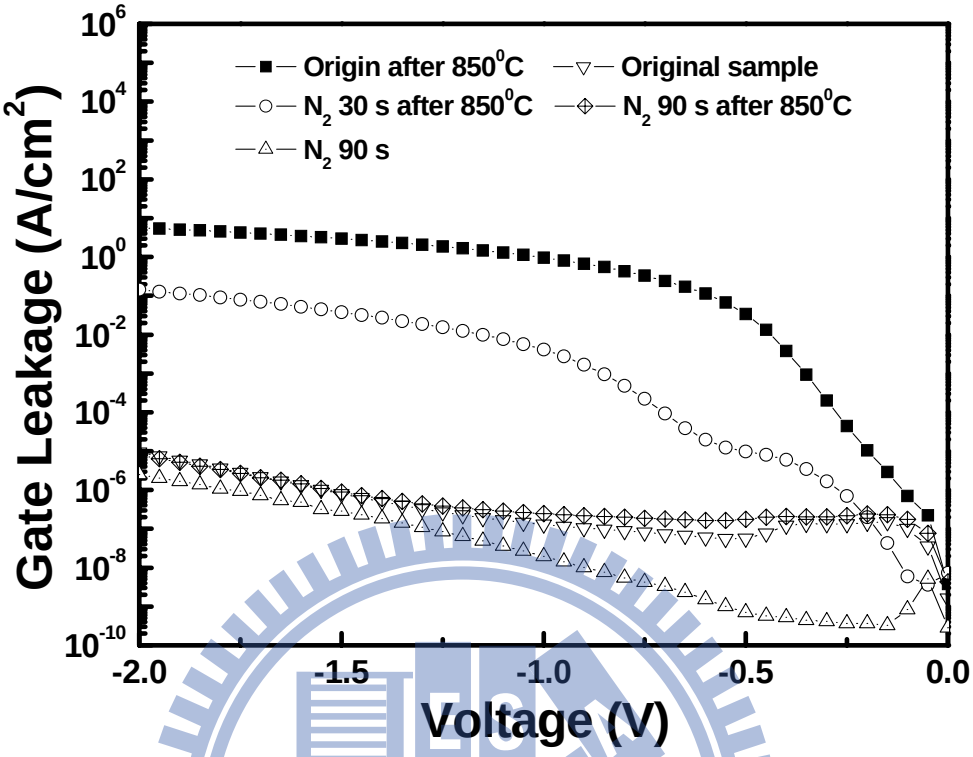

Figure 2.14 The J-V characteristics of the HfO_2 gate dielectrics treated by different plasma nitridation process and PDA.

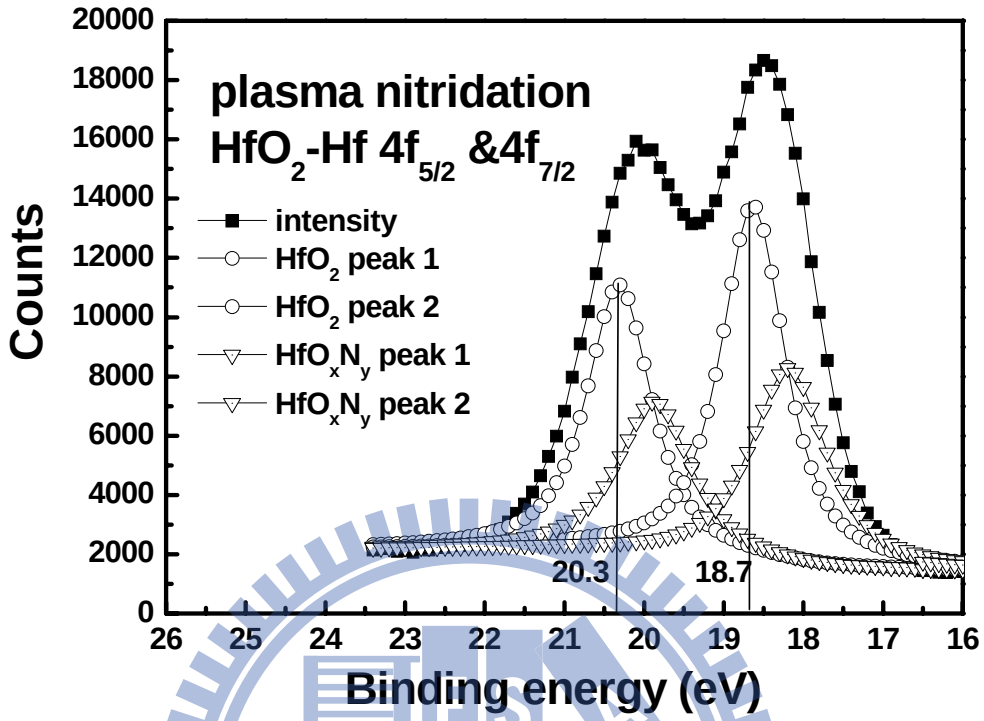

Figure 2.15 The XPS analysis of the Hf 4f electronic spectra of the samples treated in ICP N_2 plasma for 60 sec.

Chapter 3

The Improvement Effect of the Plasma Nitridation Process to the Electrical Properties, the Reliability and the Thermal Stability of $HfAlO_x$ thin films

3.1 Introduction

Gate dielectric scaling of complementary metal-oxide-semiconductor (CMOS) structure accomplishes increase in speed and pack density for modern integrated circuits. However, dielectric layer scaling companies the excessive off-state leakage current that could cause intolerable power consumption and overheat of the devices. To solve the issue about leakage current, a major resolution is to replace the silicon dioxide with a thicker dielectric layer that has a higher dielectric constant and maintains relatively low equivalent oxide thickness (EOT) [1]. There are many kinds of high-k dielectrics have been considered to substitute as the gate dielectrics for the advanced CMOS technologies [2-4]. Among these dielectrics, HfO_2 is considered as a suitable gate dielectric material because of the acceptable band gap (~ 5.7 eV), the large dielectric constant (~ 25) and relatively high free energy of reaction with Si (47.6 kcal/mole at 727 ^oC) [2-4, 6]. However, there are still some issues which have to be solved in order to integrate these Hf-based dielectrics into an industrial CMOS process flow like the thermal instability and the reliability of these dielectrics [7, 30]. The crystallization temperature of pure HfO_2 is quite low, so the thermal process, such as Source/Drain activation, would cause the high leakage current after the deposition of HfO_2 thin films. In order to increase the crystallization temperature, Al could be added to HfO_2 to form Hf aluminates [8].

Recently, several studies have used nitrogen incorporation in high-k gate stacks to improve thermal stability and increase dielectric constant [16, 38, 46]. However, thermal nitridation is usually performed at high temperature and hydrogen-containing species that act as electron traps could be added into the thin film. On the other hand, nitrogen could be incorporated into the dielectric layer by plasma nitridation process at lower temperature than by thermal nitridation process [22]. The objective of this study is to discuss the effect of different ICP plasma nitridation processes to the electrical properties, the reliability and the thermal stability of $HfAlO_x$ thin films.

3.2 Experimental

After a standard initial RCA cleaning, a 6-nm $HfAlO_x$ layer was deposited on the p-type wafers by the MOCVD system. The samples were then annealed at 800 ℃ for 60 sec in pure N_2 gas by rapid temperature annealing (RTA) process and nitrided by an ICP process at the substrate temperature of 300 ℃. The process pressure of the plasma nitridation process was set as 1.33×10^{-4} bar. Ar was added into the chamber to activating the plasma containing nitrogen while the nitridation process was carried out. The flow rate of Ar was set as 10 sccm and the flow rate of the gas containing nitrogen, which is N_2, NH_3 or N_2O, was set as 100 sccm. After the plasma nitridation, there was an annealing process whose condition was at 600 ℃ for 60 sec in pure N_2 to eliminate the plasma damage caused by nitridation process [35]. A 40-nm Ti film was deposited by dual e-gun evaporation and an Al film of 400 nm was thermally evaporated. The top electrodes were defined by a lithography process. Finally, the backside native oxide was stripped with diluted HF solution and the backside aluminum electrodes were evaporated by a thermal evaporation. The gate area of the $Al/Ti/HfAlO_x/Si$ MOS capacitors is 5000 μm^2. The capacitance-voltage (C-V) and the current density-voltage (J-V) characteristics of the MOS structures were measured by using a C-V measurement (HP

4284) and an Agilent 4156C semiconductor parameter analyzer. The experimental condition of the SILC measurement that was carried out in this study was set as constant voltage of -3 V for 180 sec. The stress condition of CVS measurement implemented in this study was set as -3 V.

3.3 Results and Discussion

In the beginning of this study, different process times were tested to determinate the most suitable process condition to the C-V and the J-V characteristics of the samples for various plasma nitridation processes. After the process time had been decided, we would examine the effect of the plasma nitridation process to the reliability of $HfAlO_x$ thin films.

3.3.1 The Most Suitable Process Time

Figure 3.1 presents the C-V characteristics of the $HfAlO_x$ gate dielectrics nitrided in ICP N_2 plasma for different process times. The frequency used in the high frequency C-V measurement was set as 50 kHz. The capacitors treated for 10 and 30 sec perform the larger capacitance density among these samples. The factor of improvement might be from that the nitrogen incorporation in the $HfAlO_x$ dielectrics. First, the incorporated nitrogen could enhance the electronic polarization as well as the ionic polarization, so the dielectric constant of the $HfAlO_x$ thin films increases just as Hf-silicate thin films and SiO_2 thin films [40-41]. Secondly, the growth of the interfacial layer between $HfAlO_x$ thin film and silicon could be suppressed by incorporated nitrogen [47]. A properly nitrided Hf-based dielectric could act as an oxygen diffusion barrier, perhaps by filling grain boundaries or vacancies [20]. Besides, the capacitance density of the samples treated for 60 sec and 90 sec is degraded because of the damage caused by the N_2 plasma.

The J-V characteristics of the $HfAlO_x$ capacitors nitrided by ICP N_2 plasma with different process times from 0 V to -2 V are shown in Fig. 3.2. The gate leakage current density is restrained apparently while the treatment condition was 30 sec. The reduction of the leakage current could be attributed to that the defects in Hf-based dielectric could be passivated in nitridation process and the post deposition annealing (PDA) [37-38]. The gate leakage current density of the samples not treated in ICP N_2 plasma at V_g of -1 V is about 2.5×10^{-4} A/cm^2 and the gate leakage current density of the capacitors treated in ICP N_2 plasma for 30 sec at V_g of -1 V is about 1.36×10^{-5} A/cm^2. Moreover, the leakage current densities of the samples treated in N_2 plasma for shorter or longer time are larger than the one treated for 30 sec. The improvement effect of the nitridation process with shorter process time might be not enough. On the other hand, while the nitridation process time is longer than 30 sec, the plasma damage from the plasma nitridation could be obvious. In summary, the best process time of the plasma nitridation for ICP N_2 process is set as 30 sec. The samples treated in N_2 plasma for 30 sec display the best value (the EOT of the samples is about 2.6 nm).

For ICP NH_3 and ICP N_2O nitridation process, the best process time of the plasma nitridation could be set as 30 sec from similar analysis process.

In Fig. 3.3 and Fig. 3.4, the C-V and the J-V characteristics of the $HfAlO_x$ gate dielectrics treated by three kinds of ICP plasma are demonstrated. The EOT of $HfAlO_x$ thin films changes from 3.7 nm to 2.9 nm after NH_3 plasma nitridation and changes from 3.7 nm to 2.6 nm after N_2O plasma nitridation. For the N_2O plasma nitridation process, a high concentration of oxygen vacancies would cause electrons to be generated and a large leakage current to flow, so treatment with plasma that contains oxygen could reduce oxygen vacancies to improve the quality of dielectric films [34]. As mentioned above, the gate leakage current density of the

samples treated in ICP N_2O plasma for 30 sec would be the smallest among all samples. It is about 4.40×10^{-6} A/cm^2 at V_g of -1 V. Besides, the gate leakage current density of $HfAlO_x$ thin films changes from 2.50×10^{-4} A/cm^2 to 7.98×10^{-6} A/cm^2 at -1 V after NH_3 plasma nitridation. In summary, the C-V and the J-V characteristics of the samples with various ICP nitridation processes are better than the one with simply PDA.

3.3.2 Reliability

Figure 3.5 displays the hysteresis characteristics of the $HfAlO_x$ gate dielectrics treated in different kinds of plasma containing nitrogen. Hysteresis measurement was started from positive to negative bias, and then swept back from negative to positive bias at a frequency of 50 kHz. The hysteresis phenomenon of the C-V curves is caused by the existence of negative charges trapped in the dielectric defect states when the samples are stressed. These defect states are called slow trapping sites [45]. The reason for the lower hysteresis is the thin film has lower number of defects, and consequently there is less charge trapped. The voltage shift in the C-V curve of the samples nitrided by N_2 or N_2O plasma is about 6 mV and the voltage shift in the C-V curve of the sample nitrided by NH_3 plasma is about 7 mV. That is, the hysteresis phenomenon of pure $HfAlO_x$ dielectrics could be restrained to be less than 10 mV by various nitridation processes.

The SILC curves of p-type $HfAlO_x$ gate dielectrics treated with N_2 plasma process are shown in Fig. 3.6. After the sample was stressed by constant voltage of -3 V for 180 sec, the degradation of the leakage current could reflect the reliability of the MOS structures. Figure 3.6 performs that the degradation could be suppressed effectively by N_2 plasma nitridation process with suitable process time. The increase of gate leakage current at -1 V of $HfAlO_x$ thim film changes from 94.00 % to 60.29 % after N_2 plasma nitridation. On the other hand,

when the nitridation process time is too long, the leakage current would increase and the variation of leakage current caused by the stress voltage would be apparent again due to the plasma damage.

The SILC curves of p-type $HfAlO_x$ gate dielectrics nitrided with NH_3 plasma process and N_2O plasma process are displayed in Fig. 3.7 and Fig. 3.8. As shown in Fig. 3.7, the SILC characteristics of p-type $HfAlO_x$ gate dielectrics nitrided by NH_3 plasma process present that the shift of leakage current because of the CVS could also be restrained by NH_3 plasma nitridation. But the improvement effect of the NH_3 plasma nitridation process to the SILC phenomenon of the $HfAlO_x$ thin films seems unapparent in comparison with other plasma nitridation process. Figure 3.8 describes the SILC curves of p-type $HfAlO_x$ gate dielectrics treated with N_2O plasma process. As Fig. 3.8 demonstrates, the shift of leakage current due to the CVS could also be restrained obviously by N_2O plasma nitridation.

The CVS characteristics of samples nitrided by N_2 plasma are described in Fig. 3.9. The stress voltage was set as -3 V. All the gate current shifts of the samples with nitridation could be decreased. Among several process times, the N_2 plasma nitridation process for 30 sec performs the best result. After N_2 plasma nitridation 30 sec, the gate leakage shift shrinks as 7.71 %. This result could correspond to the electrical characteristics that have been discussed above.

Figure 3.10 demonstrates the gate current shift of p-type $HfAlO_x$ capacitors treated with NH_3 plasma for different process time. Comparing to other samples, the gate current shift of the sample treated for 30 sec is the smallest. After NH_3 plasma nitridation 30 sec, the gate leakage shift shrinks as 8.86 %. This result is consistent with the above discussion about the C-V and the J-V characteristics. Figure 3.11 presents the gate current shift of p-type $HfAlO_x$

thin films treated with N_2O plasma for different process time. The current shift of the sample nitrided for 30 sec is the slightest and shrinks as 7.29 %. This result is also consistent with the C-V and the J-V characteristics.

In summary, the improvement effect of the various ICP nitridation processes to the reliability of $HfAlO_x$ thin films has been verified. According the above discussions, although there is not enormous difference, the improvement effect of the ICP N_2O nitridation process would be the most obvious to both the electrical characteristics and the reliability of $HfAlO_x$ thin films.

3.3.3 Thermal stability

The nitrogen was incorporated into the dielectric could maintain an amorphous homogeneous film without phase separation at high temperature [21]. In Figure 3.12 and Figure 3.13, the C-V and the J-V characteristics of the $HfAlO_x$ gate dielectrics treated by different plasma nitridation processes and thermal treatments are shown. As demonstrated in Figure 3.12, for the samples which were just deposited and not nitrided, the C-V characteristic of the samples with the high temperature process (in N_2 gas at 900 ℃ for 30 sec) degenerated because of the recrystallization of the $HfAlO_x$ thin films. So from the electrical characteristic, the original samples could not sustain the high temperature annealing. In the meantime, for the samples which went through the PDA, N_2 plasma nitridation and the post-nitridation annealing (PNA), the C-V characteristic of the samples without the high temperature process was very similar to the ones with the process. So it seemed to prove that the nitridation process could improve the thermal stability of the $HfAlO_x$ thin films. In Figure 3.13, we observed that the J-V curve of the sample with nitridation which suffered high temperature annealing could maintain a lower value than the one without nitridation. Besides,

while the capacitance density of the samples nitrided by ICP plasma was close to the one of the samples just went through the PDA process, the gate leakage density of the nitrided samples was smaller than the one of the samples without nitridation. The above electrical characteristics could also confirm the improved effect of the plasma nitridation to the thermally stability of the $HfAlO_x$ thin films.

3.4 Summary

Based on above results, the nitridation effect and the plasma damage might need to be traded off to achieve the optimum result. According to our study, the whole plasma nitridation process, which includes the post-deposition annealing and the post-nitridation annealing, could be used to strengthen the HfAlOx thin films in order to enhance the C-V characteristic and suppress the gate leakage from the as-deposited samples. After the process time was decided from the C-V and the J-V characteristics, the improvement effect of the ICP nitridation process to the reliability of $HfAlO_x$ thin films was verified from the hysteresis, the SILC and the CVS characteristics. For different kinds of ICP plasma nitridation processes, the influence would be diverse. In conclusion, for the electrical characteristics and the reliability of $HfAlO_x$ thin films, the ICP N_2O process could be a suitable nitridation process. The EOT of $HfAlO_x$ changes from 3.7 nm to 2.6 nm and the gate leakage current density changes from 2.50×10^{-4} A/cm^2 to 4.40×10^{-6} A/cm^2 after N_2 plasma nitridation. Moreover, the plasma nitridation could be used to improve the thermal stability of the $HfAlO_x$ thin films to bear the high temperature process at 900 ℃ for at least 30 sec.

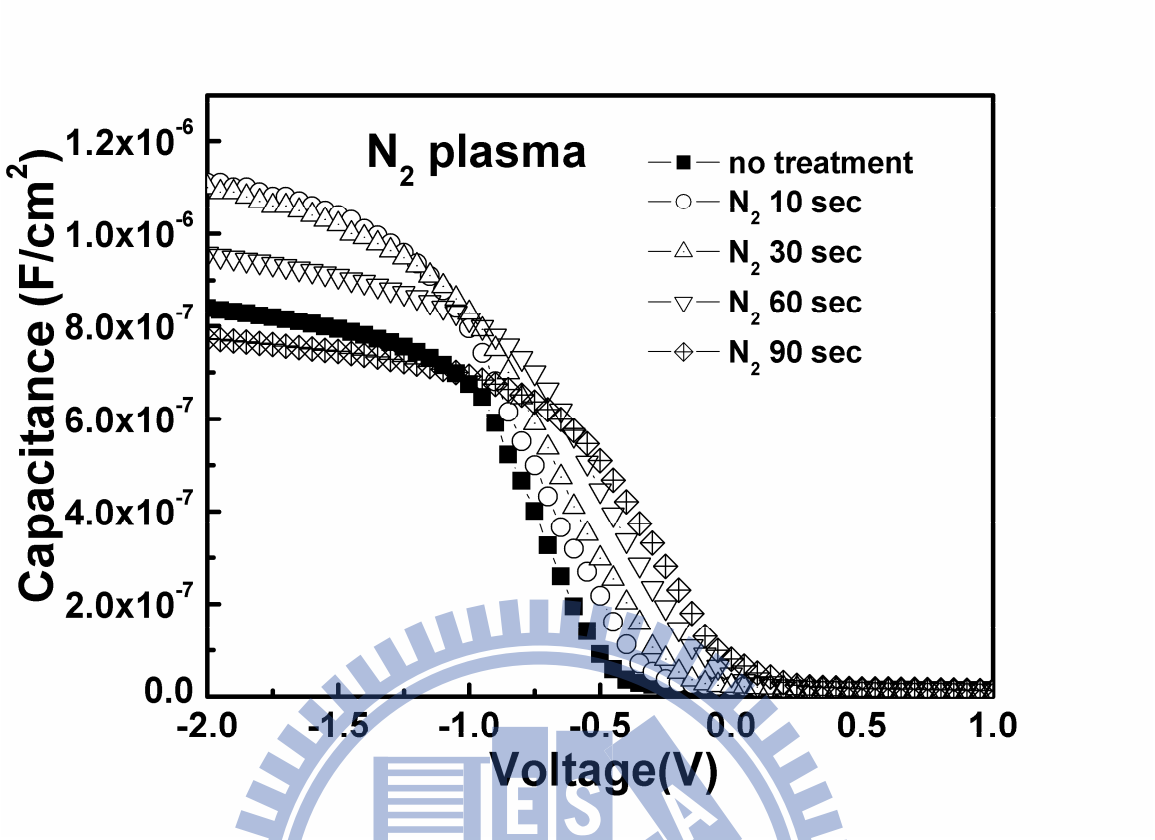

Figure 3.1 The C-V characteristics of the $HfAlO_x$ thin films treated in N_2 plasma for different process times.

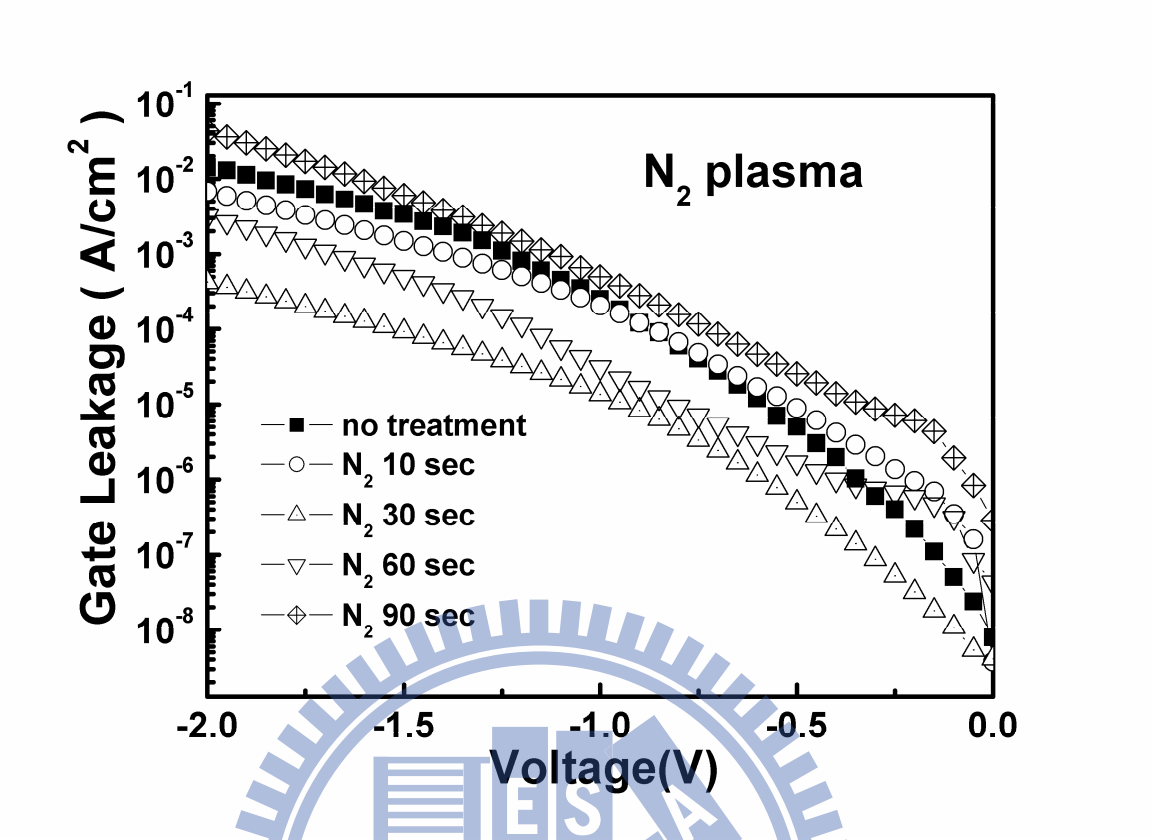

Figure 3.2 The J-V characteristics of the $HfAlO_x$ thin films treated in N_2 plasma for different process times.

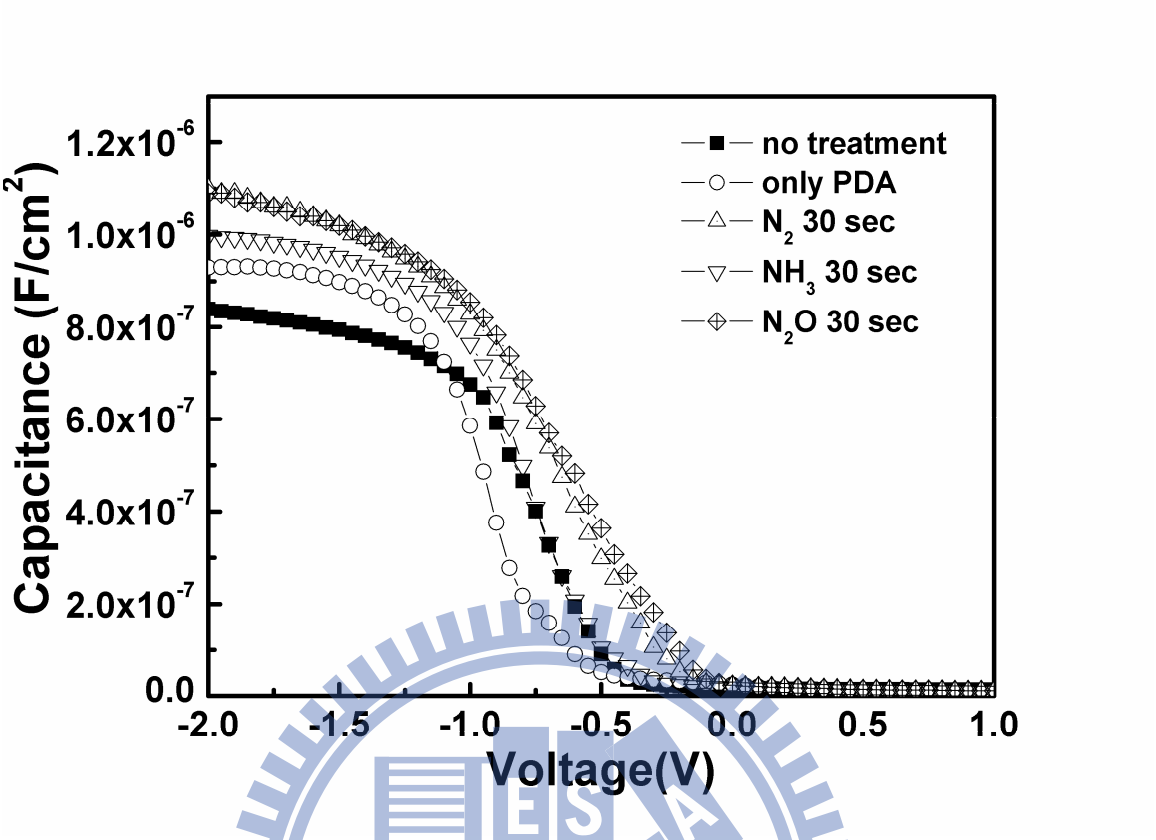

Figure 3.3 The C-V characteristics of the $HfAlO_x$ thin films treated by different kinds of plasma.

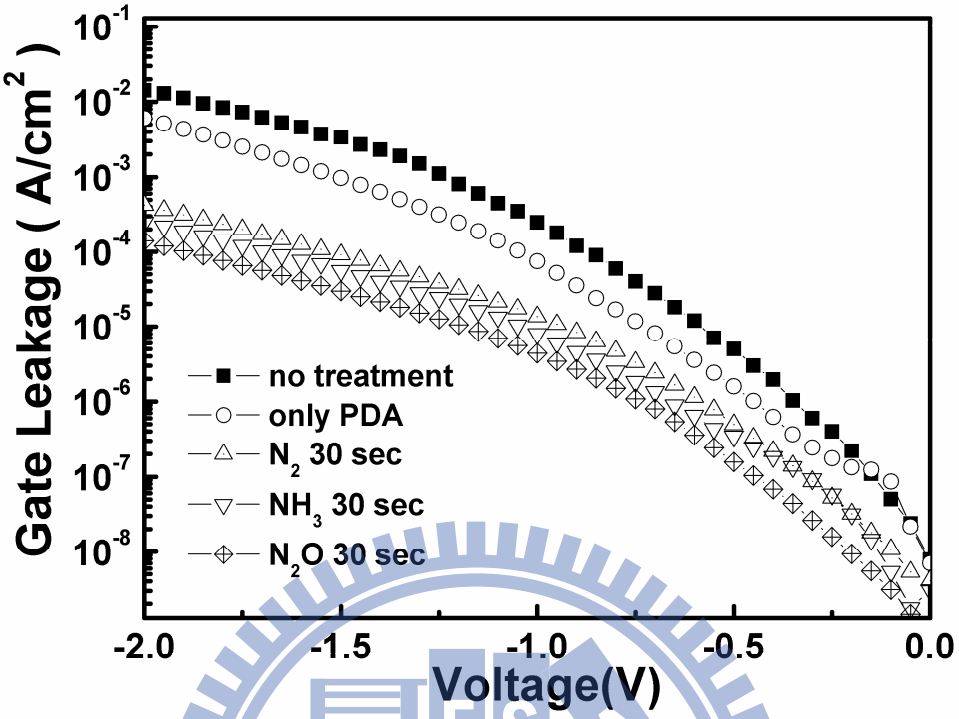

Figure 3.4 The J-V characteristics of the $HfAlO_x$ thin films treated by different kinds of plasma.

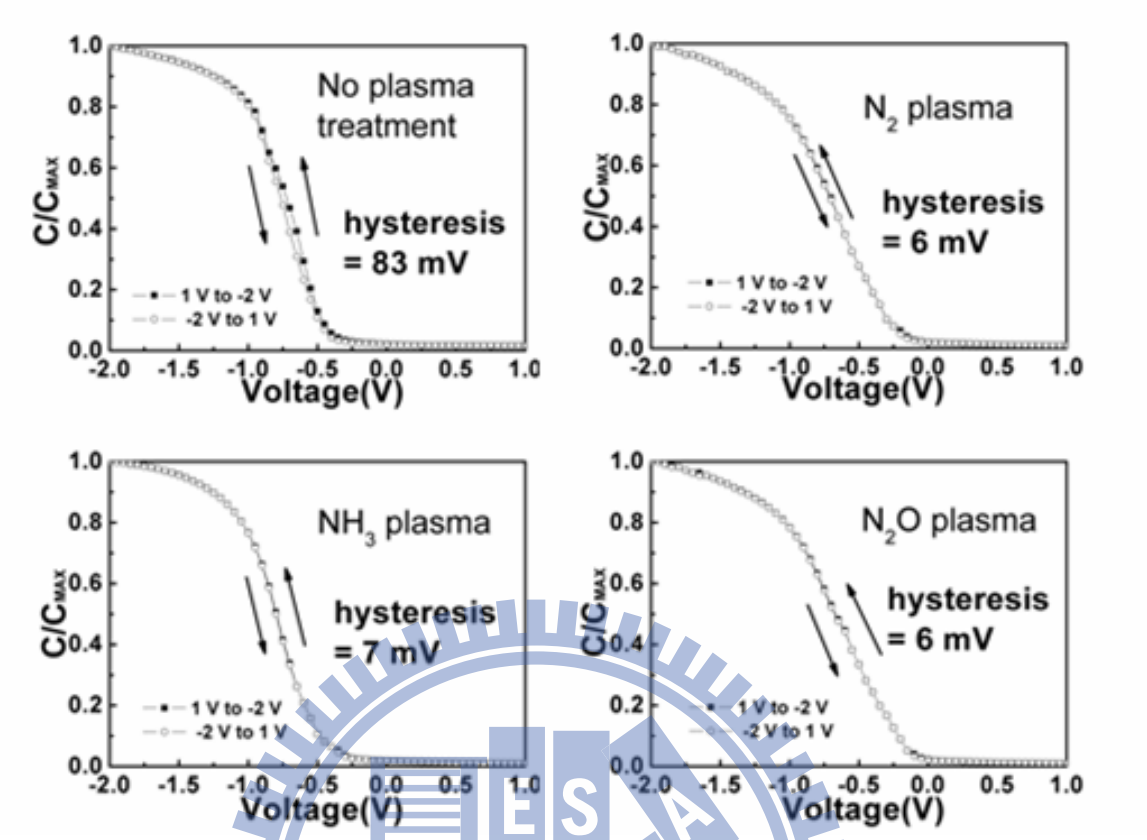

Figure 3.5 The hysteresis characteristics of the samples nitrided by different kinds of plasma containing nitrogen.

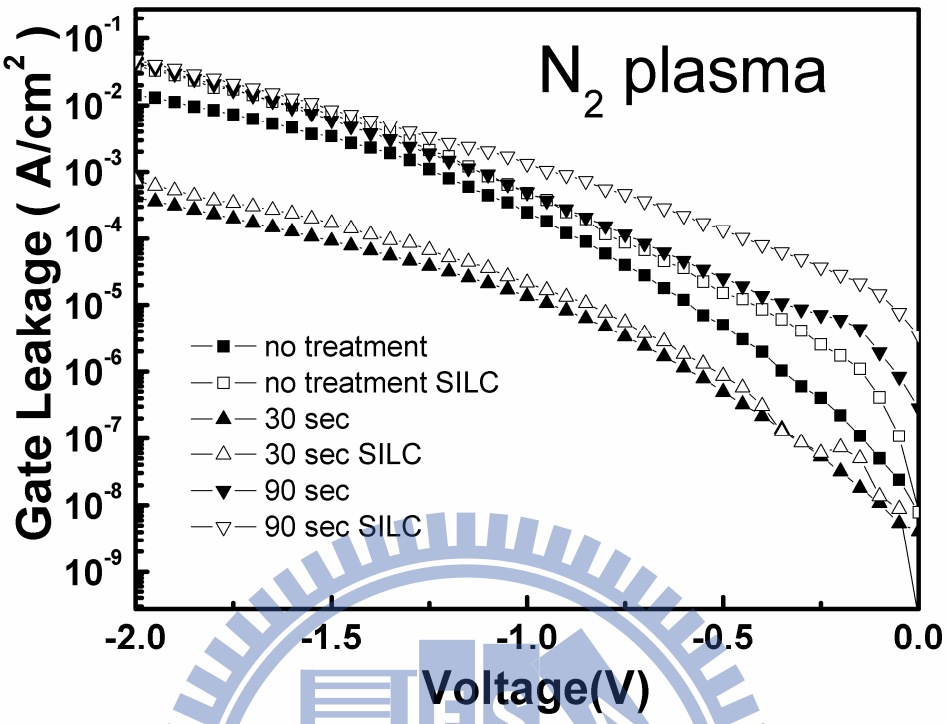

Figure 3.6 The SILC characteristics of the $HfAlO_x$ thin films nitrided by N_2 plasma.

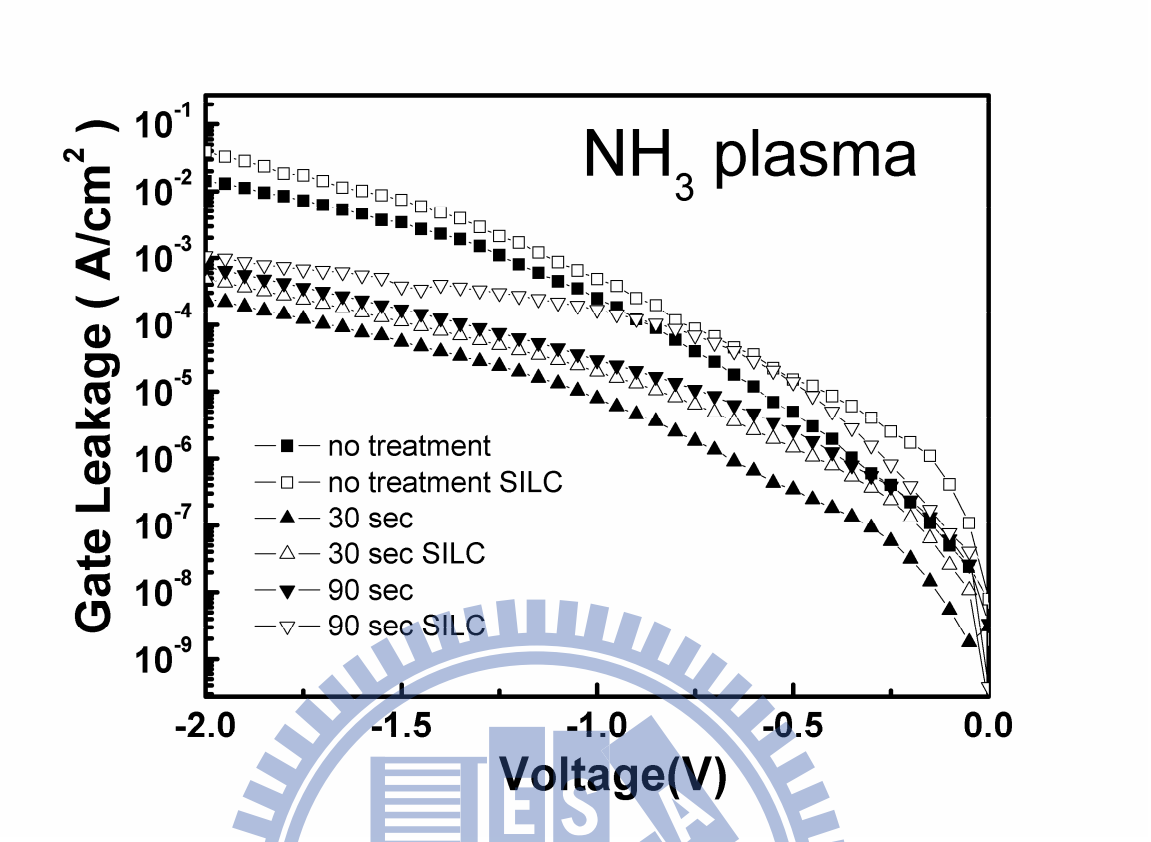

Figure 3.7 The SILC characteristics of the $HfAlO_x$ thin films nitrided by NH_3 plasma.

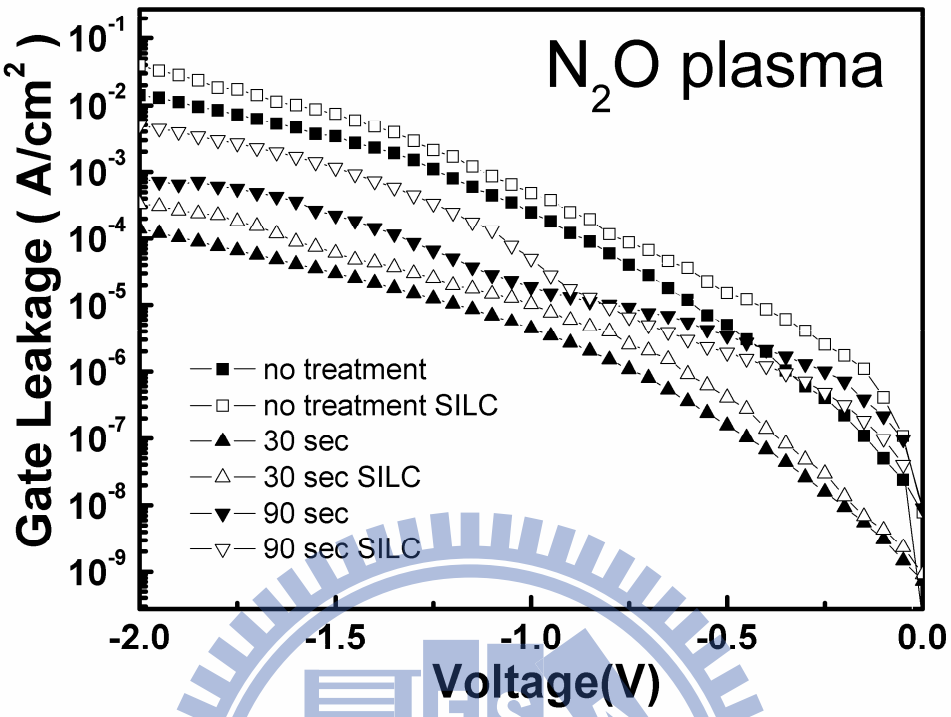

Figure 3.8 The SILC characteristics of the $HfAlO_x$ thin films nitrided by N_2O plasma.

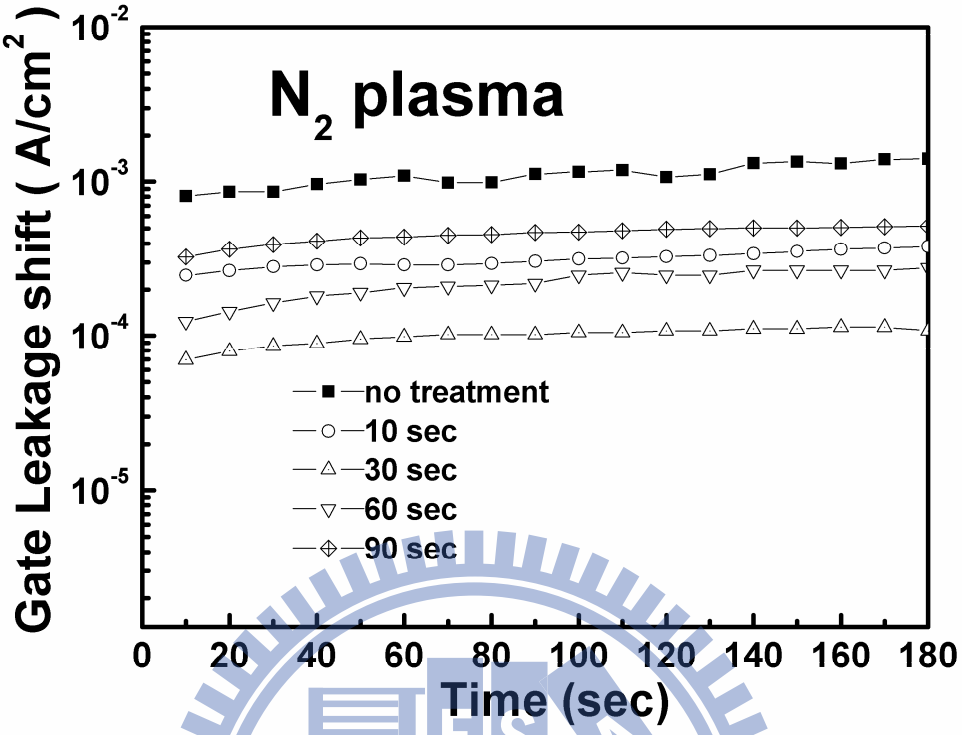

Figure 3.9 The leakage current shift curves of the $HfAlO_x$ thin films nitride by N_2 plasma.

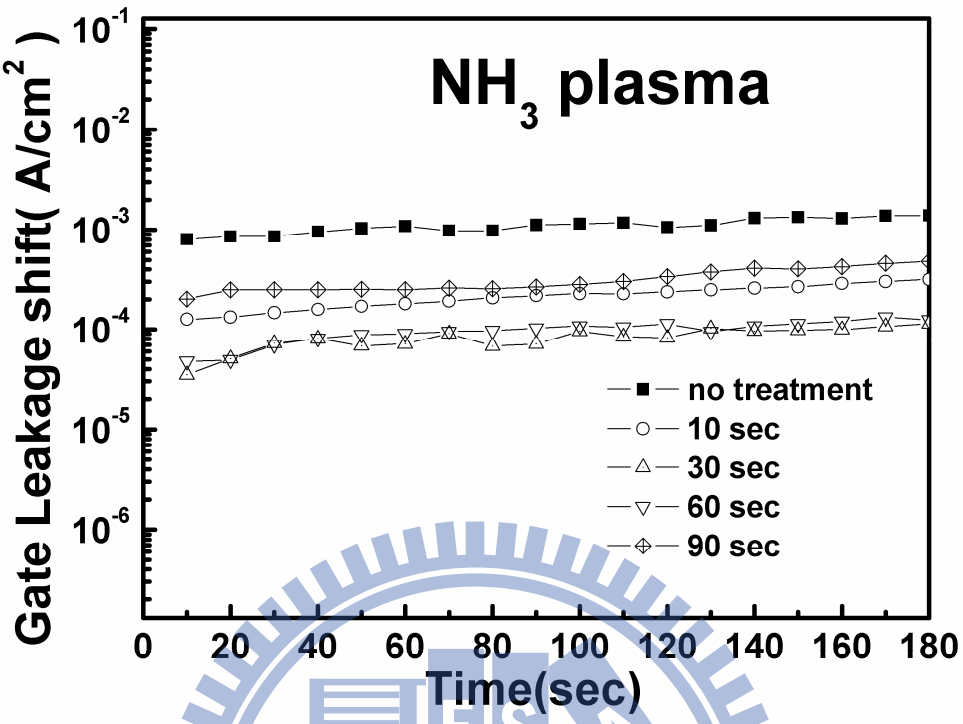

Figure 3.10 The leakage current shift curves of the $HfAlO_x$ thin films nitride by NH_3 plasma.

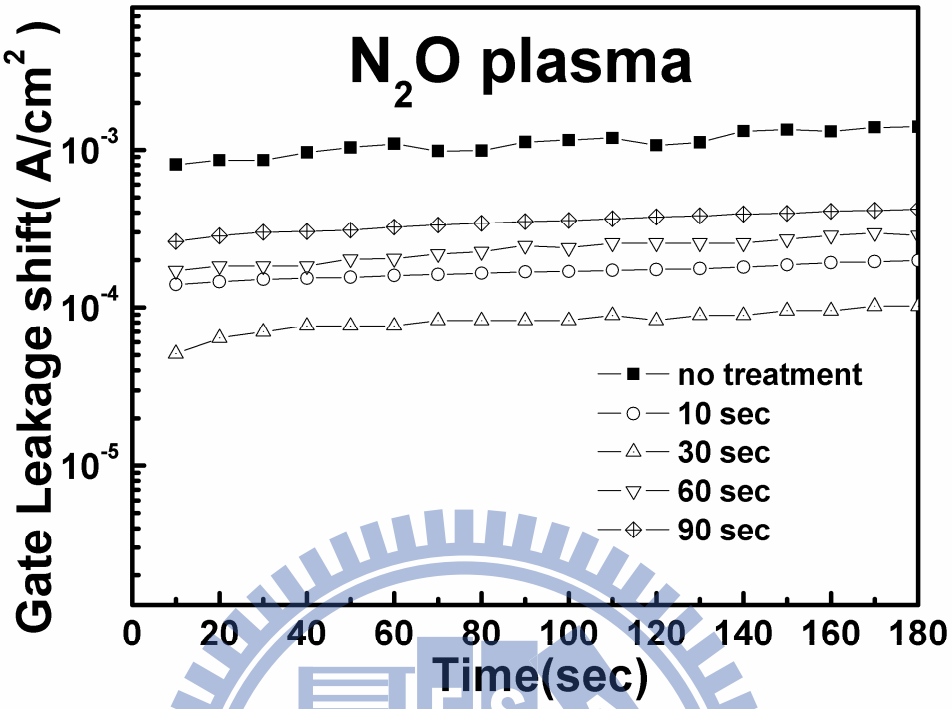

Figure 3.11 The leakage current shift curves of the $HfAlO_x$ thin films nitride by N_2O plasma.

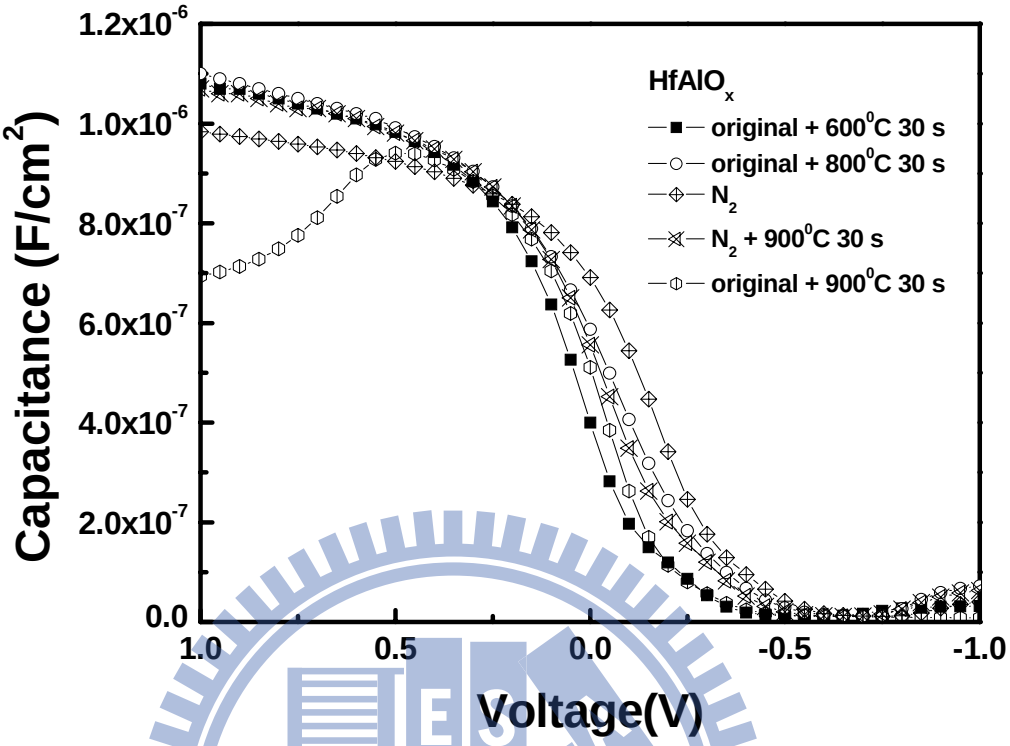

Figure 3.12 The C-V characteristics of the $HfAlO_x$ gate dielectrics treated by different plasma nitridation process, PDA and high temperature process.

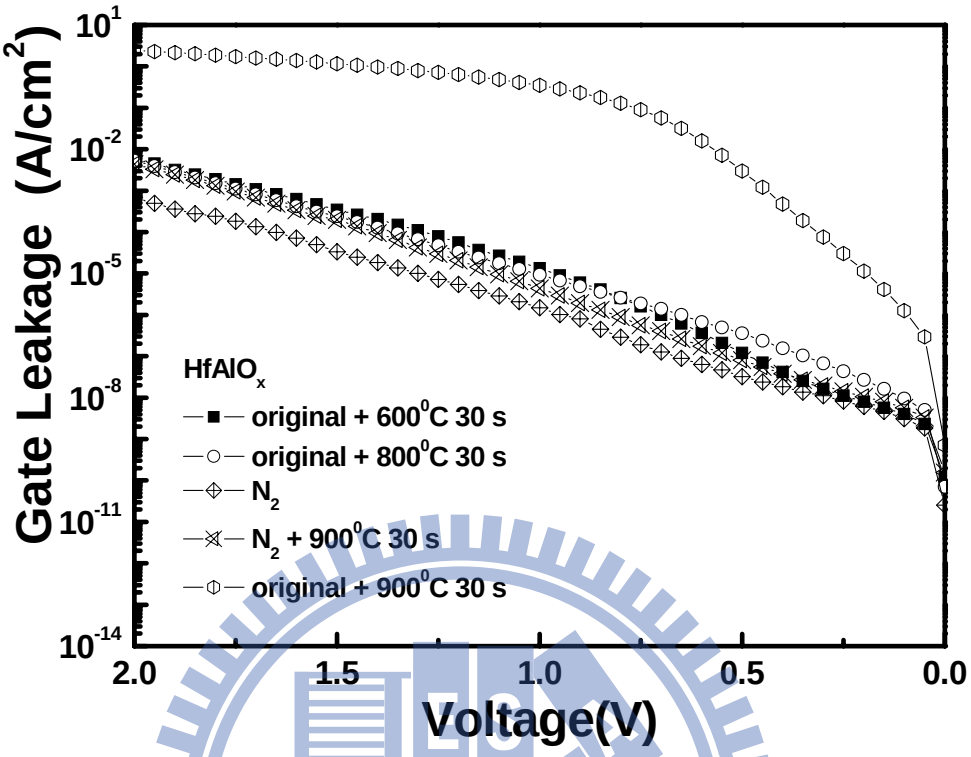

Figure 3.13 The J-V characteristics of the $HfAlO_x$ gate dielectrics treated by different plasma nitridation process, PDA and high temperature process.

Chapter 4

The Improvement Effect of the Plasma Nitridation Process and the Plasma fluorination Process to HfO_2 thin films

4.1 Introduction

To solve the problem of the excessive leakage, Hafnium-based dielectrics have emerged as the promising high-κ candidates to replace the SiON dielectrics for the advanced CMOS technologies [1, 3-4]. The pure HfO_2 is considered as a suitable gate dielectric material because of the acceptable band gap (6 eV) and the large dielectric constant (about 25). The band gap of Hafnium-based dielectrics is not too small to cause the large gate leakage which forms the large power consumption. In the meantime, the dielectric constant of hafnium-based dielectrics is large enough to increase the physical thickness of the gate dielectric and maintain the relatively low effective oxide thickness (EOT). However, there are several challenges which have to be considered in order to integrate these high-κ dielectrics into a conventional CMOS process flow such as the interface SiO_2 regrowth and the thermal stability of these dielectrics [7]. The nitridation process has been shown to improve the thermal stability of hafnium-silicate thin films [21]. On the other hand, there are some recent studies show that fluorine passivation could be use to improve the reliability of high-k dielectric MOS field effect transistors [25, 27, 48]. Plasma fluorination could be an effective method to make incorporation of fluorine into the hafnium-based high-k dielectrics [49-50].

The plasma nitridation effect to pure HfO_2 thin films has already been examined in the chapter 2 of this dissertation. In this chapter, we would try to apply plasma fluorination process to improve the plasma nitridation effect of pure HfO_2 thin films.

4.2 Experimental

After initial standard RCA cleaning, the wafers were placed into the chamber and the HfO_2 layers were deposited on the wafers by the metal organic chemical vapor deposition (MOCVD) system. The precursor used to deposit HfO_2 thin films in MOCVD was 0.05 M solution of $Hf(Tert\text{-}butoxy)_2(MMP)_2$ in octane. The substrate temperature of the MOCVD system is 500 ℃. The flow rate of pure O_2, that is used to react with the precursor to form HfO_2, was 1700 sccm. The process pressure for depositing HfO_2 thin films was set as 1.5 mbar. Then the samples were annealed (post-deposition annealing) at 600 ℃ for 30 sec in pure N_2 gas and nitrided by an additional ICP plasma treatment at the substrate temperature of 300 ℃, the process pressure of the plasma nitridation process was 1.33×10^{-4} bar. The conditions of the nitridation plasma treatment were in N_2 for 60 sec and in N_2O or NH_3 for 90 sec. The process time of the nitridation process is from the chapter 2 of this dissertation. The RF power of the ICP system was set as 200 W, and no DC bias. The condition of the plasma fluorination process was the same as those of the plasma nitridation except the plasma treatment is in CF_4 gas. The process time of fluorination is 30 sec, 60 sec, 90 sec and 120 sec, respectively. After the plasma treatment, there was an annealing process whose condition was at 600 ℃ for 30 sec in pure N_2 to reduce the plasma damage. The 10-nm Ti thin films and the 400-nm Al thin film were deposited on the top side of the samples by the dual e-gun evaporation system. The top electrodes were defined by the mask process. Finally, backside aluminum electrodes were evaporated by the thermal evaporation.

The top area of the $Al/Ti/HfO_2/Si$ MOS capacitors is 5000 μm^2. The capacitance-voltage (C-V) and the current density-voltage (J-V) characteristics of the MOS structures were measured by semiconductor parameter analyzer (HP4156C) and C-V measurement (HP4284) in order to evaluate the improvement effect of the plasma nitridation process and the best

process condition. The stress condition of constant voltage stress (CVS) measurement carried out in this study was set as constant voltage of 5 V to observe the change of the gate leakage current while the stress was applied.

4.3 Results and Discussion

4.3.1 The Electrical Characteristics

Figure 4.1 shows the C-V characteristics of the HfO_2 gate dielectrics treated in ICP N_2 plasma for 60 sec and treated in ICP CF_4 plasma for different process times. The frequency used in the high frequency C-V measurement was set as 50 kHz. The capacitors treated for 60 sec perform the maximum capacitance density among these samples with different process times. In addition, the capacitors treated in CF_4 plasma for 30 sec also present the larger values than the capacitors without whole plasma nitridation process. The factor of improvement might be from that the PDA process [36-38], the nitrogen incorporation in the HfO_2 dielectrics [20, 39-40], and the elimination of oxygen vacancies with optimal nitrogen and fluorine doping [51] and the regrowth of interfacial oxide is also restrained by incorporation of fluorine [52]. On the other hand, there might be etching effect caused by CF_4 treatment to the hafnium oxide thin films. When the etching effect happens, the EOT of samples might degrade or decrease but the leakage current would increase dramatically because of the thinner oxide thickness and the damage caused by CF_4 etching. In Fig. 4.1, the capacitance density of the samples treated for 90 sec and 120 sec is degraded. The reason could be the damage caused by the CF_4 plasma. On the other hand, through comparing Fig. 4.1 and Fig 2.1, the improvement of plasma fluorination to the nitride HfO_2 thin films could be presented. The EOT of HfO_2 thin films could be changed from 2.9 nm to 1.7 nm through N_2 plasma nitridation and CF_4 plasma fluorination treatment.

The J-V characteristics of the HfO_2 capacitors treated in ICP N_2 plasma for 60 sec and treated in ICP CF_4 plasma for different process times from 0 V to -2 V are described in Fig. 4.2. The gate leakage current density of the samples treated in ICP CF_4 plasma for 60 sec at V_g of -1 V is about 1.50×10^{-4} A/cm^2 and the gate leakage current density of the capacitors treated in ICP CF_4 plasma for 30 sec at V_g of -1 V is about 5.85×10^{-5} A/cm^2 while the leakage current density of sample without any plasma treatment is 5.59×10^{-5} A/cm^2 at Vg of -1 V. The reason about reduction of hafnium oxide leakage could be the nitrogen incorporation and the interface charge trapping sites passivated by fluorine introduced by ICP CF_4 plasma treatment [20, 39-40, 51]. Besides, polymer could be produced by CF_4 treatment. If the polymer existed in the MOS structure, not only the leakage current of the samples would be restrained but also the C-V characteristic of the samples would degrade seriously. Because of the etching effect and polymer producing might caused by CF_4 treatment, the process conditions of ICP CF_4 plasma fluorination must be controlled carefully to avoid those unwanted effect.

In Fig. 4.3 and Fig. 4.4, the C-V and the J-V characteristics of the HfO_2 gate dielectrics treated in ICP NH_3 plasma for 90 sec then in ICP CF_4 plasma for different process times are presented. The reason of the improvement effect in the NH_3 nitridation combined CF_4 fluorination process could be similar with the one in the N_2 nitridation combined CF_4 fluorination process. From Fig. 4.3 and Fig 4.1, the effect to the HfO_2 thin films by the NH_3 nitridation and CF_4 fluorination process is worse. It could be from the hydrogen contained in NH_3 plasma degenerate the effect of the fluorination. The gate leakage current density of the samples treated in ICP NH_3 plasma for 90 sec and ICP CF_4 plasma for 60 sec at V_g of -1 V is about 2.38×10^{-4} A/cm^2 and the EOT of the samples is about 1.8 nm. From the similar

analysis, the best process time of the plasma fluorination in CF_4 plasma to the HfO_2 nitrided by NH_3 plasma is set as 60 sec.

In Fig. 4.5 and Fig. 4.6, the C-V and the J-V characteristics of the HfO_2 gate dielectrics treated in ICP N_2O plasma for 90 sec and in ICP CF_4 plasma for different process times are demonstrated. Controlling the process time is for not only the achievement of optimal condition between nitridation and fluorination but also avoiding the unwanted effect caused by CF_4 treatment as polymer that might be produced or etching hafnium oxide thin films. After analyzing the experimental data, the most suitable process time of the ICP fluorination process to the HfO_2 thin films treated by N_2O plasma could be 60 sec. The EOT and gate leakage current density of the samples treated in ICP N_2O plasma for 90 sec and ICP CF_4 plasma for 60 sec at V_g of -1 V is about 2.0 nm and 1.63×10^{-4} A/cm^2, respectively. As the chapter 2, the reduction of the gate leakage density of the samples nitrided by N_2O plasma would be more obvious than the sample nitride by other plasma contain nitrogen [33]. In summary, the N_2O and CF_4 plasma treatment could also be a practicable method to improve the electrical characteristics of HfO_2 gate dielectrics.

4.3.2 Reliability

Figure 4.7, Figure 4.8, Figure 4.9 and Figure 4.10 show the hysteresis characteristics of the HfO_2 gate dielectrics treated in different ICP plasma containing nitrogen then in CF_4 plasma. Hysteresis measurement was started from negative to positive bias (-2.5 V to 0.5 V), and then swept back from positive to negative bias (0.5 V to -2.5 V) at a frequency of 50 kHz. The hysteresis phenomenon is caused by the existence of negative charges trapped in the dielectric defect states, which are called slow trapping sites, when the capacitors are stressed [43-44, 53]. The hysteresis characteristic could be improved by various ICP plasma processes

as presented from Fig. 4.7 to Fig 4.10. According to the Fig. 2.7, the hysteresis characteristic of the HfO_2 thin films nitride by different plasma is basically the same after the CF_4 plasma fluorination. That is, the hysteresis phenomenon of pure HfO_2 dielectrics could be restrained about 10 mV by ICP nitridation and fluorination process.

Figure 4.11 demonstrates the gate current shift of p-type HfO_2 gate dielectrics treated with N_2 plasma for different annealing process during CVS of 5 V. Figure 4.11 indicates that the gate current shift of the thin film treated with N_2 plasma for 60 sec and CF_4 plasma for 60 sec is smaller than the one without plasma treatment, the gate leakage shift shrinks as 7.71 % of original one. In other word, for substrate injection, the gate current shift could be suppressed by N_2 plasma nitridation and CF_4 plasma fluorination. The plasma damage could be the reason why the shift of the leakage current increase by the increase of the CF_4 plasma time.

Figure 4-12 shows gate current shift of p-type HfO_2 gate dielectrics treated with NH_3 plasma treatment 90 sec and CF_4 plasma for different process time during CVS of 5 V. It indicated that the gate leakage current shift of the thin film with NH_3 plasma treatment plus CF_4 60 sec was smaller than the original one as 9.8×10^{-3} %. The reason would be the same with the sample treated by N_2 and CF_4 plasma.

The CVS characteristics of samples nitride ICP N_2O plasma and fluorinated by CF_4 plasma for different times are described in Fig. 4.13. Figure 4.13 presents that the gate current shift of the thin film treated with N_2O plasma for 90 sec and CF_4 plasma for 60 sec is smaller than the thin films without plasma treatment as 2.83 %. The samples with CF_4 plasma treatment for 90 sec and 120 sec also show smaller current shift.

4.3.3 Physical Analysis

The SIMS profile of the HfO_2 sample treated in ICP N_2 plasma for 60 sec and in ICP CF_4 plasma for 60 sec is shown in Fig. 4.14. Fig 4.14 indicates that the incorporation of fluorine, which is induced by the plasma fluorination process, is mainly at the HfO_2/Si interface.

Fig. 4.15 is the XPS F 1s electronic spectra of the HfO_2 samples treated in ICP N_2 plasma for 60 sec and treated in ICP CF_4 plasma for 60 sec. The F1s peak in the spectra is evident for the case with fluorine incorporation [54]. From Fig. 4.15, there is no peak around binding energy of 688 eV, so the fluorine combined with carbon from CF_4 plasma process would be slight enough to ignore [24]. It would be an evidence to prove that carbon would not be induced by the ICP CF_4 plasma treatment we applied. Fig. 4.16 is XPS analysis of the Hf 4f electronic spectra of the samples treated in ICP CF_4 plasma for 60 sec. For the fluorinated HfO_2 thin films, the Hf 4f peaks of the XPS spectra would shift to higher binding energies [58-59]. It indicates that the presence of Hf-F bonds in HfO_2 thin films after ICP CF_4 plasma process.

4.4 Summary

According to this chapter, the electrical characteristics of HfO_2 thin films could be improved effectively by ICP nitridation and fluorination with suitable process time. The improvement effect of the ICP plasma process to the reliability of pure HfO_2 thin films was verified from the hysteresis and CVS characteristics. Comparing to the chapter 2 of this dissertation, plasma nitridation combined with adequate plasma fluorination would be more effective than simply plasma nitridation. After analysis of XPS data, the existence of the Hf-F bonds in HfO_2 thin films after plasma fluorination could be proven. Besides, in XPS spectrum

data of F 1s, the carbon would not be induced by CF_4 plasma treatment. In conclusion, the electrical characteristic of HfO_2 thin films nitrided by ICP plasma could be effectively enhanced by ICP CF_4 plasma fluorination while the reliability would not degrade.

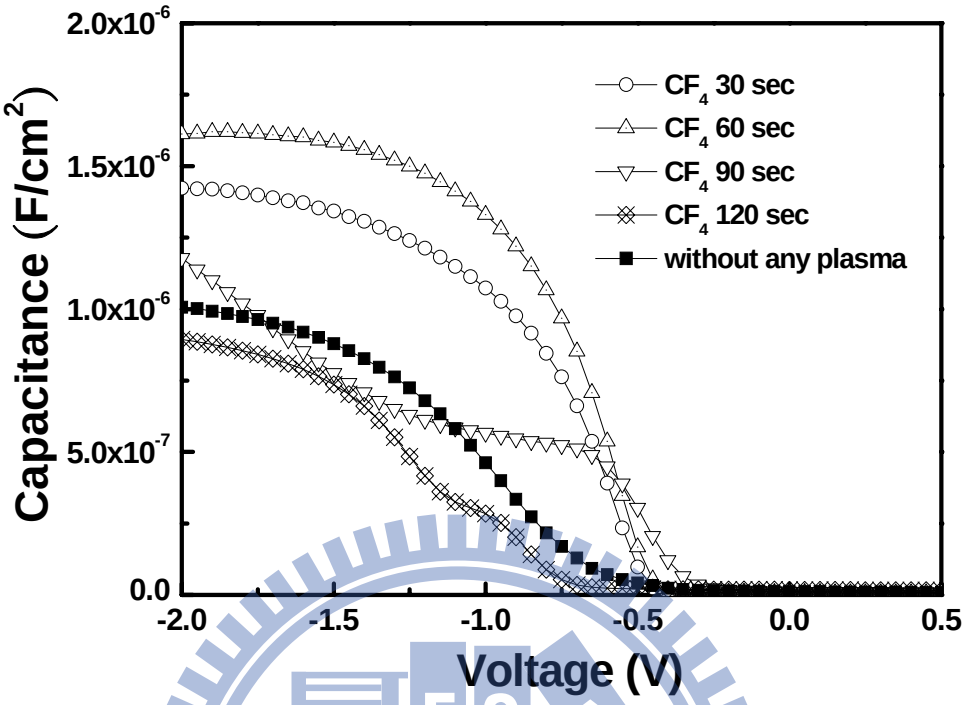

Figure 4.1 The C-V characteristics of the HfO_2 thin films treated in N_2 plasma for 60 sec and then in CF_4 plasma for different process times.

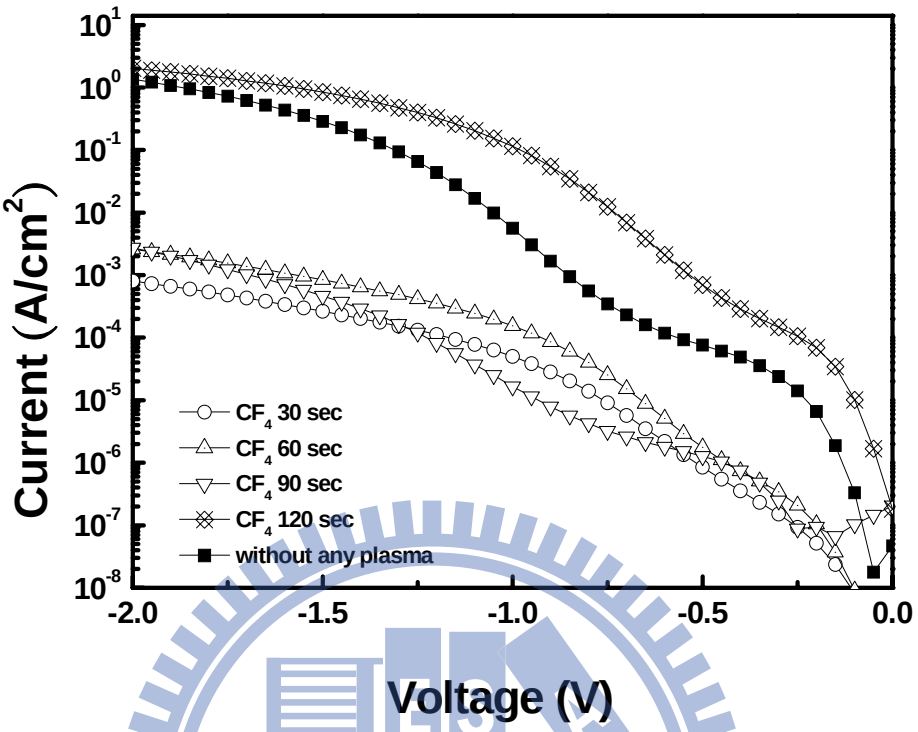

Figure 4.2 The J-V characteristics of the HfO_2 thin films treated in N_2 plasma for 60 sec and then in CF_4 plasma for different process times.

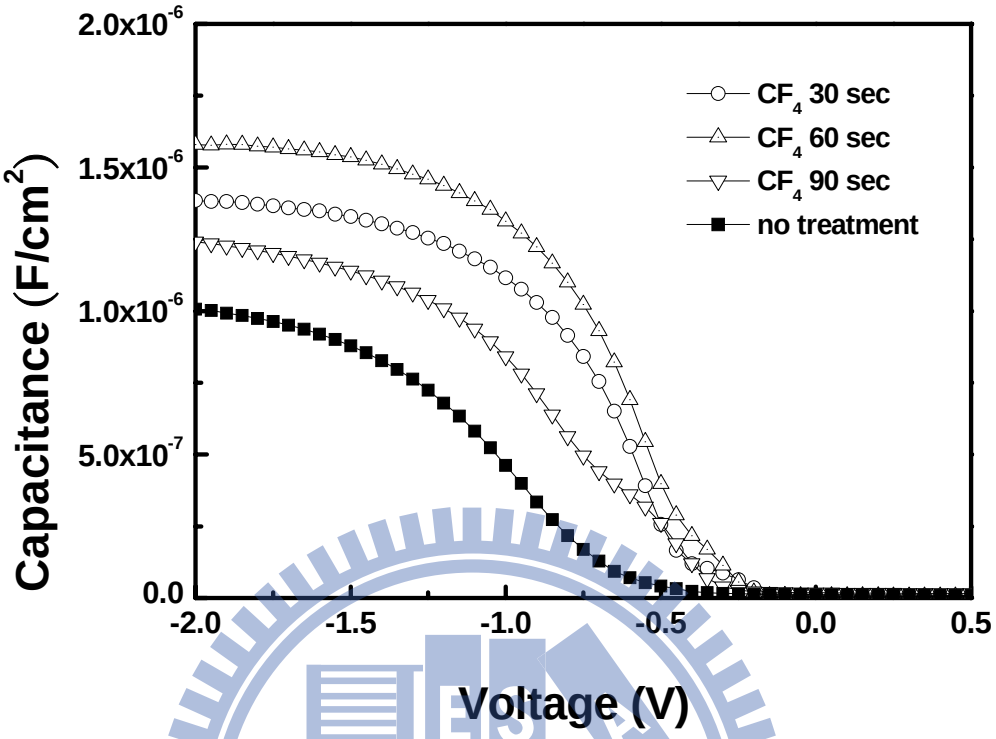

Figure 4.3 The C-V characteristics of the HfO_2 thin films treated in NH_3 plasma for 90 sec and then in CF_4 plasma for different process times.

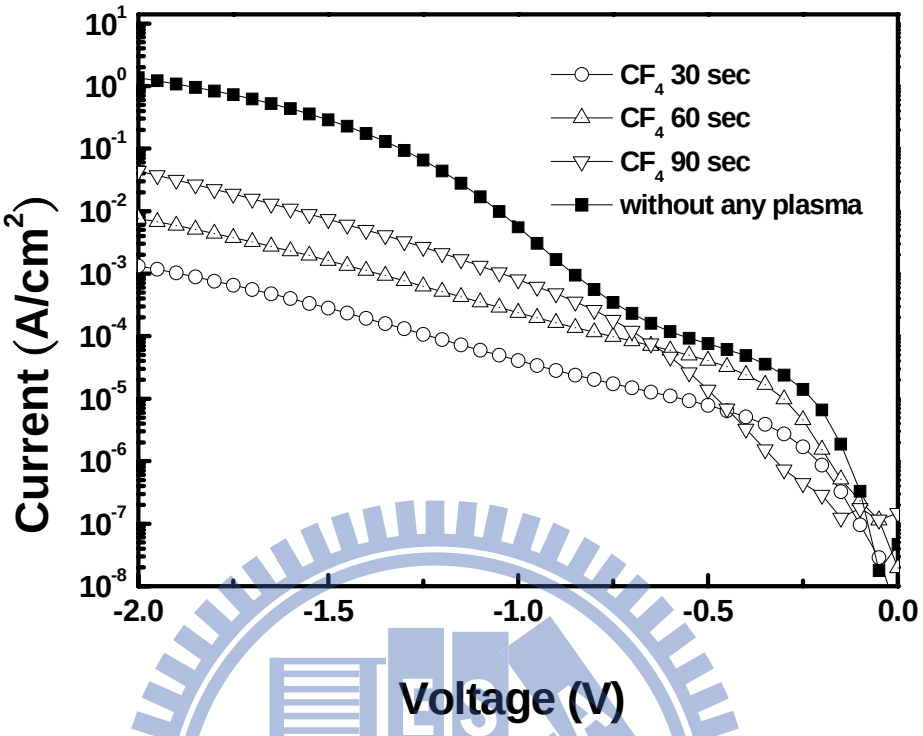

Figure 4.4 The J-V characteristics of the HfO_2 thin films treated in NH_3 plasma for 90 sec and then in CF_4 plasma for different process times.

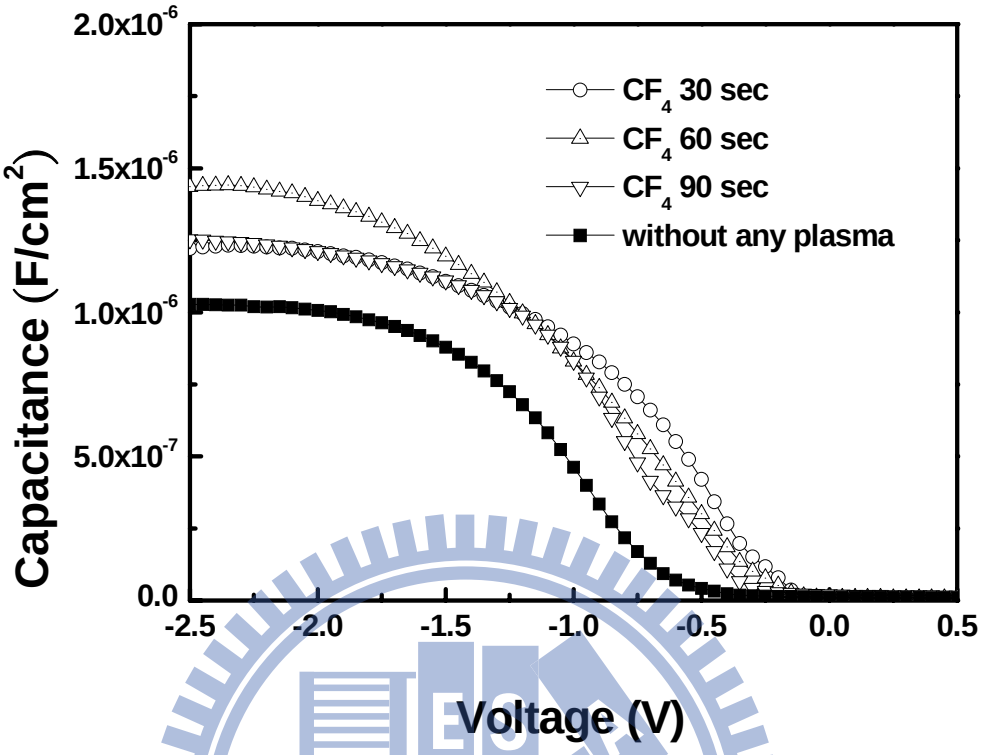

Figure 4.5 The C-V characteristics of the HfO_2 thin films treated in N_2O plasma for 90 sec and then in CF_4 plasma for different process times.

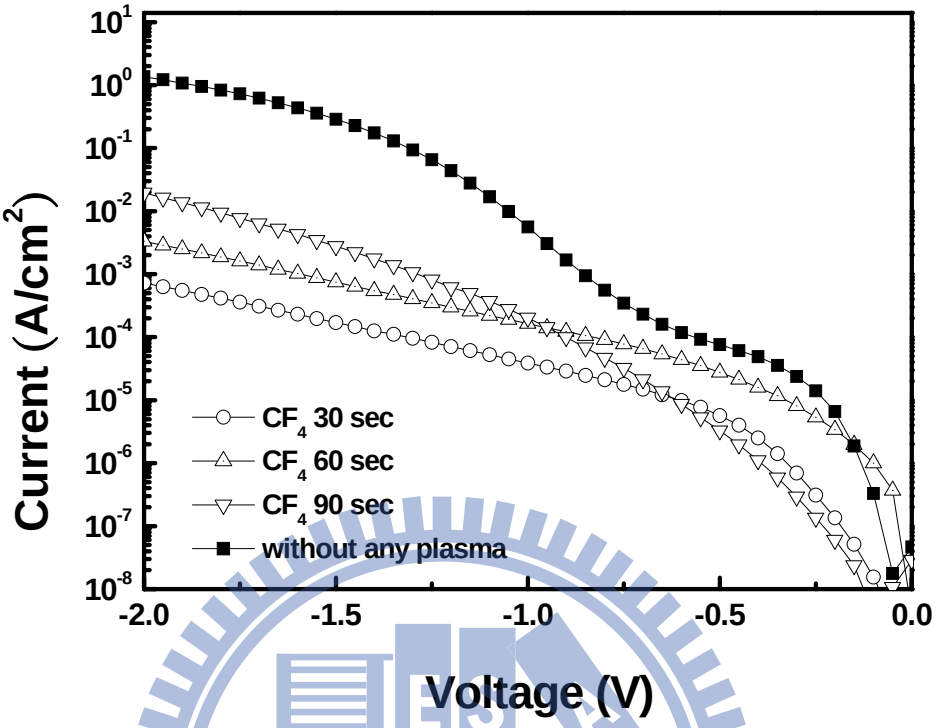

Figure 4.6 The J-V characteristics of the HfO_2 thin films treated in N_2O plasma for 90 sec and then in CF_4 plasma for different process times.

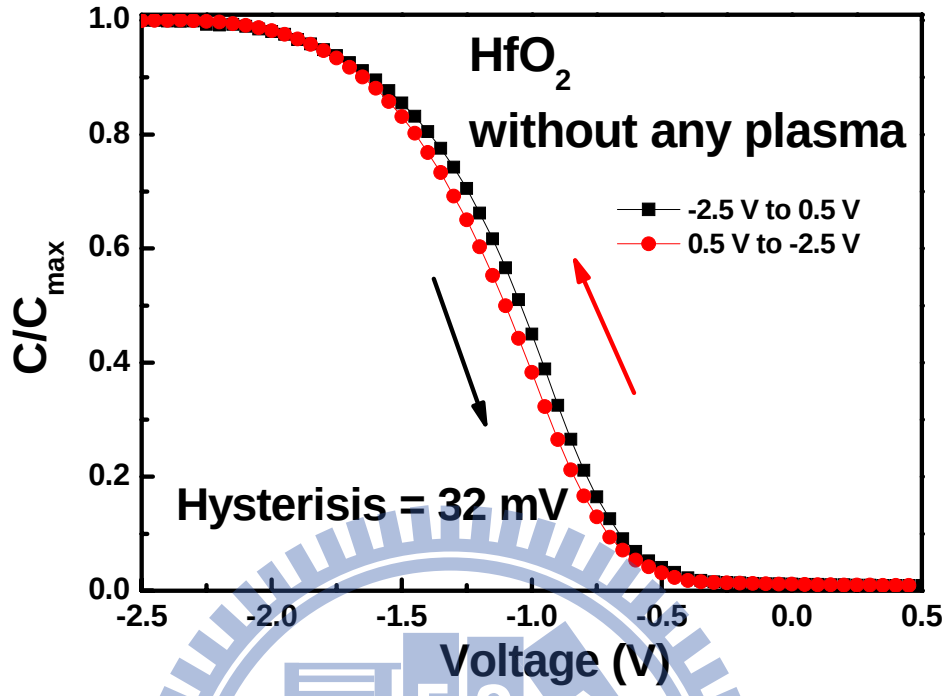

Figure 4.7 The hysteresis characteristics of the HfO_2 thin films without plasma treatment.

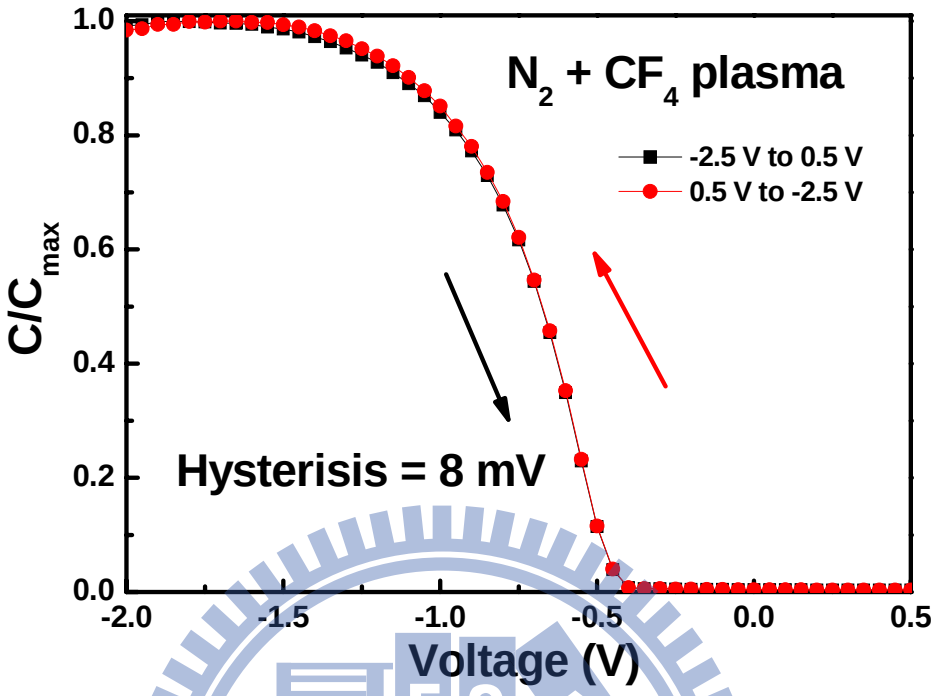

Figure 4.8 The hysteresis characteristics of the HfO_2 thin films treated in N_2 plasma for 60 sec and then in CF_4 plasma for 60 sec.

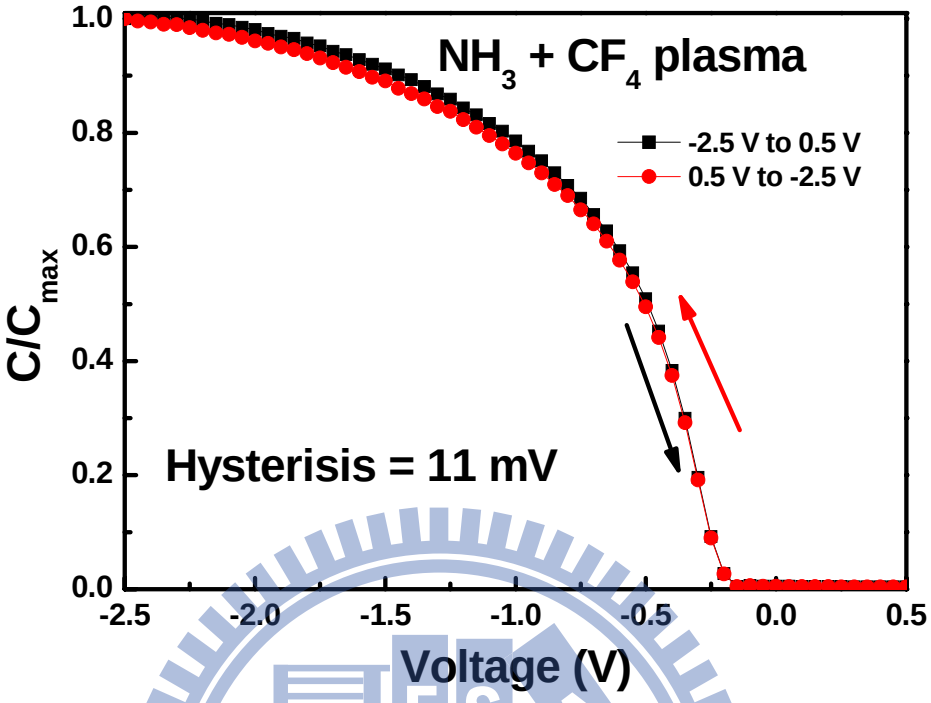

Figure 4.9 The hysteresis characteristics of the HfO_2 thin films treated in NH_3 plasma for 90 sec and then in CF_4 plasma for 60 sec.

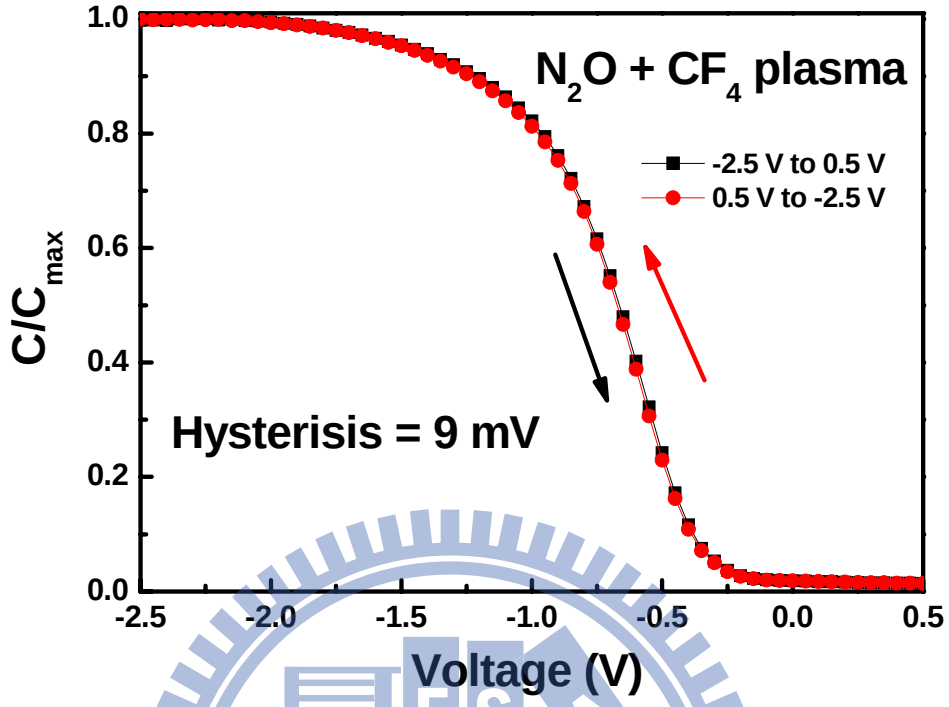

Figure 4.10 The hysteresis characteristics of the HfO_2 thin films treated in N_2O plasma for 90 sec and then in CF_4 plasma for 60 sec.

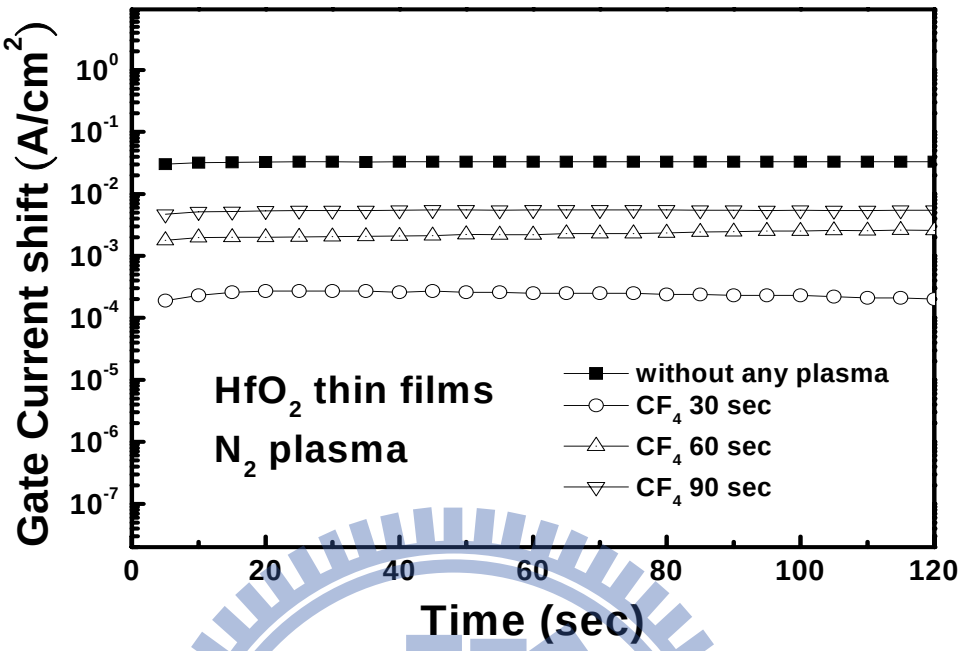

Figure 4.11 The leakage current shift curves of the HfO_2 thin films that were nitrided by ICP N_2 plasma for 60 sec then fluorinated by ICP CF_4 plasma for different time.

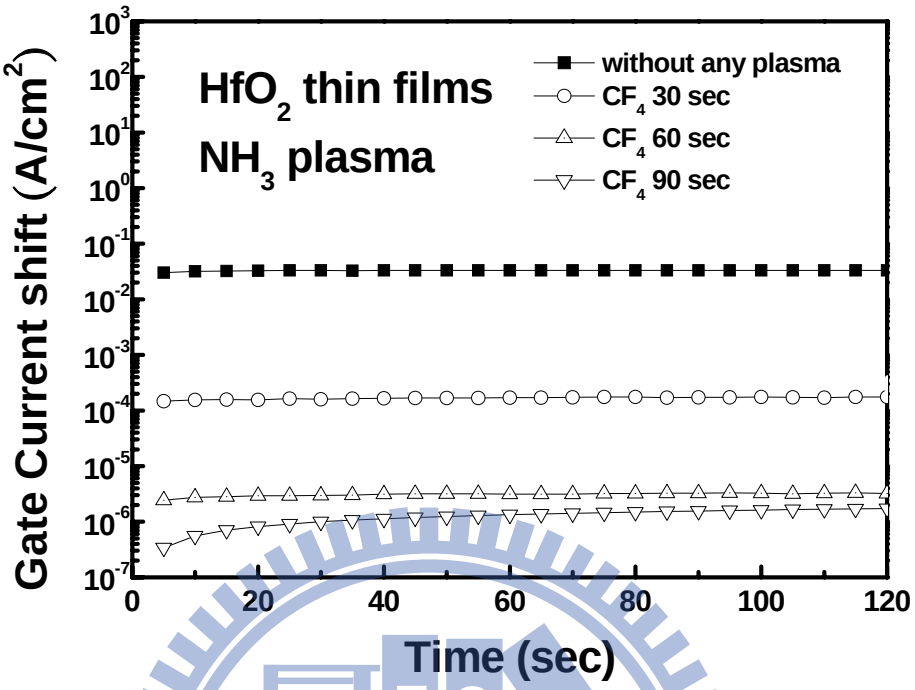

Figure 4.12 The leakage current shift curves of the HfO_2 thin films that were nitrided by ICP NH_3 plasma for 90 sec then fluorinated by ICP CF_4 plasma for different time.

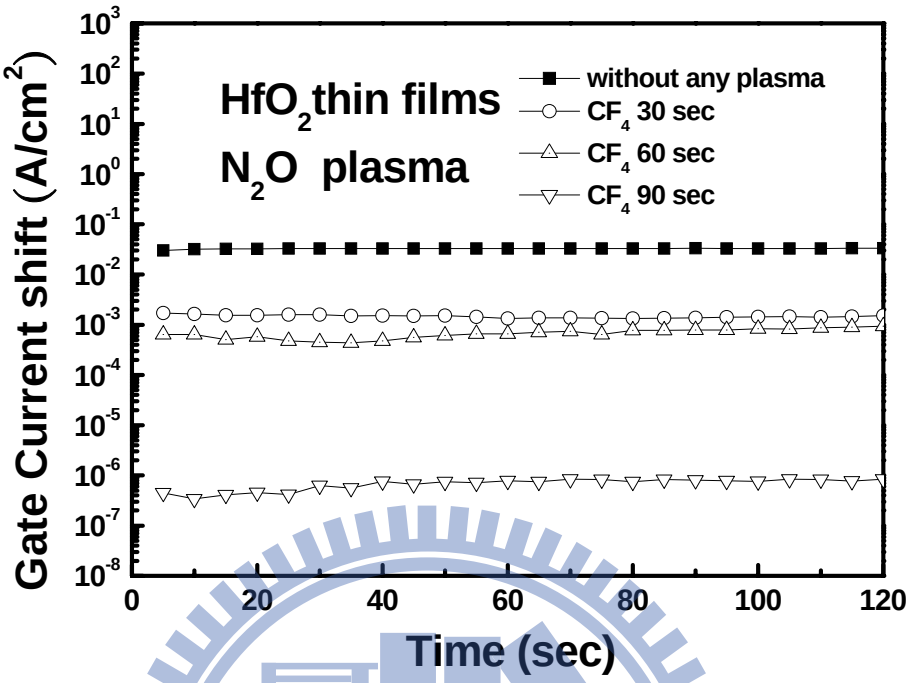

Figure 4.13 The leakage current shift curves of the HfO_2 thin films that were nitrided by ICP N_2O plasma for 90 sec then fluorinated by ICP CF_4 plasma for different time.

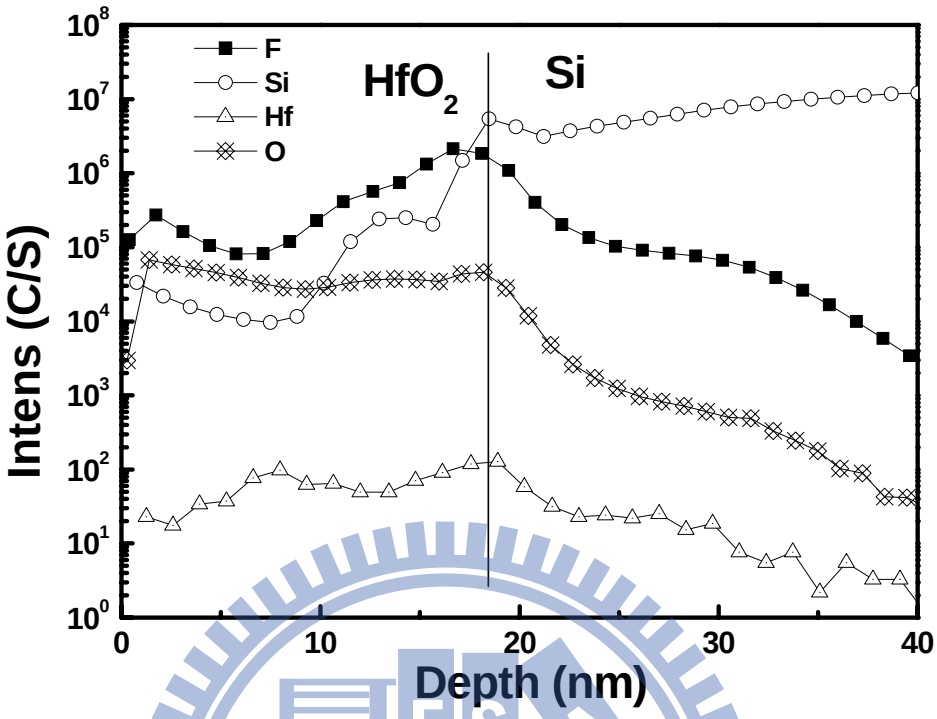

Figure 4.14 The SIMS profile of the HfO_2 thin films treated in ICP N_2 plasma for 60 sec and treated in ICP CF_4 plasma for 60 sec.

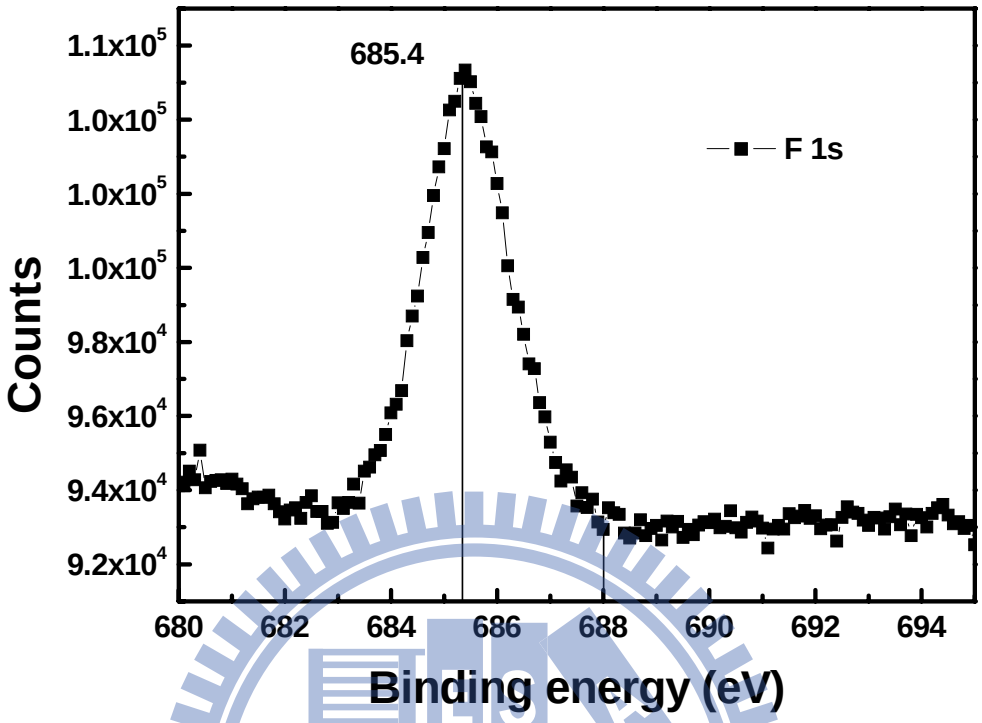

Figure 4.15 The XPS F 1s electronic spectra of the HfO_2 thin films treated in ICP N_2 plasma for 60 sec and treated in ICP CF_4 plasma for 60 sec.

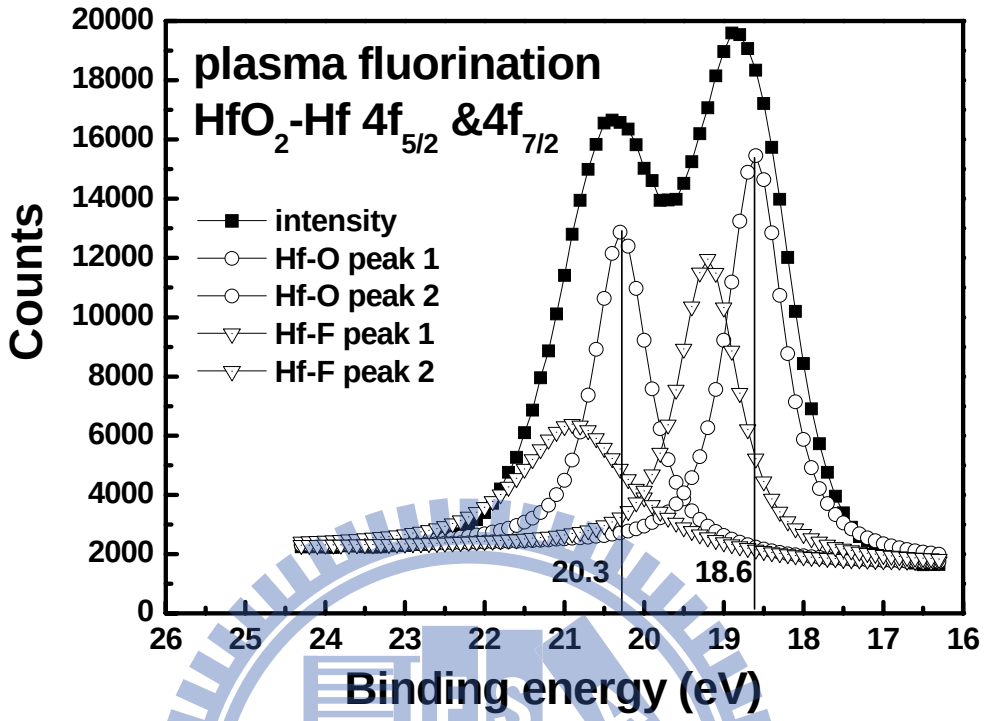

Figure 4.16 The XPS analysis of the Hf 4f electronic spectra of the samples treated in ICP CF_4 plasma for 60 sec.

Chapter 5

The Improvement Effect of the Plasma Nitridation Process and the Plasma Fluorination to $HfAlO_x$ thin films

5.1 Introduction

Considerable effect efforts have been directed in finding the appropriate high-k gate dielectric replacement for the SiON dielectrics for high performance and low stand-by power CMOS [1]. Among all high-k dielectric materials, hafnium-based dielectrics have emerged as the promising high-κ candidates to be used for the advanced CMOS technologies [3-4]. However, there are still several challenges which have to be considered in order to integrate these high-κ dielectrics into a conventional CMOS process flow such as the interface SiO_2 regrowth and the thermal stability of these dielectrics [7]. HfO_2 crystallizes at temperatures less than 500 ˚C. Grain boundaries in crystallized HfO_2 gate dielectrics could be the fast path for oxygen or dopants diffusion into gate dielectric. So the interface layer regrowth and defect generation in the interface between gate dielectric and channel region would appear [55].

The incorporation of aluminium in Hf-based dielectrics has been proven as an effective solution to the issue of thermal stability [8, 19, 37]. The nitridation process also has been shown to improve the thermal stability of hafnium-silicate thin films [21]. Besides, the plasma-nitridation effect to $HfAlO_x$ thin films has been verified in the chapter 3 of this dissertation. Since plasma fluorination could be an effective method to make incorporation of fluorine into the hafnium-based high-k dielectrics [49-50]. In this chapter, we would try to apply plasma fluorination process to examine the improve effect to the electrical properties and the reliabilities of nitrided $HfAlO_x$ thin films.

5.2 Experimental

After a standard initial RCA cleaning, a $HfAlO_x$ layer was deposited on the p-type wafers by the metal organic chemical vapor deposition (MOCVD) system. The precursor used to deposit $HfAlO_x$ thin films in MOCVD was 0.05 M solution of $Hf(Tert\text{-}butoxy)_2(MMP)_2$ in octane and 0.05 M solution of Tris(isopropoxy)Al in octane. The substrate temperature of the MOCVD system is 500 ℃. The flow rate of pure O_2, that is used to react with the precursor to form thin films, was set as 1700 sccm. The process pressure for depositing $HfAlO_x$ thin films was set as 1.5 mbar. The samples were then annealed at 800 ℃ for 60 sec in pure N_2 gas by rapid temperature annealing (RTA) process and nitrided by an ICP process at the substrate temperature of 300 ℃. The process pressure of the plasma nitridation process was set as 1.33×10^{-4} bar. The RF power of the ICP system was set as 200 W, and the DC bias power of the ICP system was set as 0 W to depress plasma damage caused by radical bombardment. The flow rate of the gas containing nitrogen, which is N_2, NH_3 or N_2O, was set as 100 sccm. The condition of the plasma fluorination process was the same as those of the plasma nitridation except the plasma treatment is in CF_4 gas. The process time of the nitridation plasma treatment was in N_2, N_2O or NH_3 for 30 sec, which is from the chapter 3 of this dissertation. The process time of fluorination is 30 sec, 60 sec, 90 sec and 120 sec, respectively. After the plasma treatment, there was an annealing process whose condition was at 600 ℃ for 60 sec in pure N_2 to eliminate the plasma damage caused by plasma treatment [56]. The 10-nm Ti thin films and the 400-nm Al thin film were deposited on the top side of the samples by the dual e-gun evaporation system. The top electrodes were defined by a lithography process. Finally, the backside native oxide was stripped with diluted HF solution and the backside aluminum electrodes were evaporated by a thermal evaporation. The gate area of the $Al/Ti/HfAlO_x/Si$ MOS capacitors is 5000 μm^2. The capacitance-voltage (C-V) and

the current density-voltage (J-V) characteristics of the MOS structures were measured by using a C-V measurement (HP 4284) and an Agilent 4156C semiconductor parameter analyzer.

5.3 Results and Discussion

5.3.1 The Electrical Characteristics

Figure 5.1 presents the C-V characteristics of the $HfAlO_x$ gate dielectrics nitrided in ICP N_2 plasma for 30 sec and fluorinated in ICP CF_4 plasma for different process times. The frequency used in the high frequency C-V measurement was set as 50 kHz. The capacitors treated for 60 sec perform the larger capacitance density among these samples. From figure 5.1, the capacitance density of the samples treated in N_2 plasma for 30 sec could be improved slightly after the additional treatment in CF_4 for 60 sec. The factor of improvement might be the elimination of oxygen vacancies with optimal nitrogen and fluorine doping [51] and the regrowth of interfacial oxide is also restrained by incorporation of fluorine [52]. On the other hand, the nitride samples treated in CF_4 plasma for 30 sec show lower capacitance density because of no optimal nitrogen and fluorine doping. Besides, the capacitance density of the $HfAlO_x$ thin films nitride in N_2 plasma for 30 sec then fluorinated treated for 90 sec is degraded because of the damage caused by the CF_4 plasma. As mentioned in chapter 4, the unwanted effect of CF_4 plasma treatment as polymer production and etching high-k thin films is what we need to avoid by control ling the process conditions.

The J-V characteristics of the $HfAlO_x$ capacitors nitrided by ICP N_2 plasma for 30 sec and fluorinated by CF_4 plasma with different process times from 0 V to -2 V are shown in Fig. 5.2. The gate leakage current density of the capacitors treated in ICP N_2 plasma for 30 sec at V_g of

-1 V is about 9.02 × 10^{-2} A/cm^2 and the gate leakage current density of the capacitors treated in N_2 plasma for 30 sec and in CF_4 plasma for 60 sec is about at V_g of -1 V is about 1.55 × 10^{-4} A/cm^2. The reduction of the leakage current could be attributed to that the defects in Hf-based dielectric might be passivated in fluorination process [50, 57]. Moreover, the gate leakage current density of the nitride samples fluorinated in CF_4 plasma for 30 sec at V_g of -1 V is about 1.20 × 10^{-3} A/cm^2 and the gate leakage current density of the nitride samples fluorinated in CF_4 plasma for 90 sec at V_g of -1 V is about 1.55 × 10^{-4} A/cm^2. Corresponding to Fig. 5.1, although the regrowth of interfacial layer could be restrained by the optimal fluorination dose, the thickness of the bulk gate dielectric layer might increase due to the damage caused by the fluorination process. In summary, the best process time of the plasma fluorination for ICP CF_4 process is set as 60 sec. The EOT of the $HfAlO_x$ thin films nitrided for N_2 plasma for 30 sec and fluorinated for CF_4 plasma for 60 sec could be decreased to 2.6 nm.

In Fig. 5.3 and Fig. 5.4, the C-V and the J-V characteristics of the $HfAlO_x$ gate dielectrics treated in ICP NH_3 plasma for 30 sec and in ICP CF_4 plasma for different times are demonstrated. The samples fluorinated for 60 sec perform the best capacitance density and smaller leakage current due to the trading off between fluorination effect and plasma damage. The reason of the improvement effect in the NH_3 nitridation combined CF_4 fluorination process could be similar with the one in the N_2 nitridation combined CF_4 fluorination process. The EOT of the $HfAlO_x$ thin films nitrided for NH_3 plasma for 30 sec and fluorinated for CF_4 plasma for 60 sec could be decreased to 2.1 nm. The gate leakage current density of the capacitors treated in NH_3 plasma for 30 sec and in CF_4 plasma for 60 sec is about at V_g of -1 V is about 1.33 × 10^{-4} A/cm^2. From above discussion, the optimal NH_3 and CF_4 plasma treatment is also a practicable method to improve the C-V and J-V characteristics of $HfAlO_x$ gate dielectrics.

In Fig. 5.5 and Fig. 5.6, the C-V and the J-V characteristics of the HfO_2 gate dielectrics treated in ICP N_2O plasma for 30 sec and in ICP CF_4 plasma for different process times are demonstrated. From analyzing the experimental data, the leakage current of the $HfAlO_x$ thin films nitrided in N_2O plasma could be restrained by the fluorination process. The EOT of the $HfAlO_x$ thin films nitrided for N_2O plasma for 30 sec and fluorinated for CF_4 plasma for 90 sec could be decreased to 2.6 nm. The capacitance density of the $HfAlO_x$ thin films nitrided in N_2O plasma for 30 sec could be enhanced after fluorinated in CF_4 plasma for 30 sec. The process time of plasma fluorination is longer, the fluorine and nitrogen incorporation is not optimal and plasma damage is severer. The EOT of the $HfAlO_x$ thin films nitrided for NH_3 plasma for 30 sec and fluorinated for CF_4 plasma for 30 sec could be decreased to 2.1 nm. The gate leakage current density of the capacitors treated in N_2O plasma for 30 sec and in CF_4 plasma for 30 sec is about at V_g of -1 V is about 1.28×10^{-3} A/cm^2.

5.3.2 Reliability

The hysteresis characteristics of the HfO_2 gate dielectrics treated in different ICP plasma containing nitrogen then in CF_4 plasma is show in figure 5.7, figure 5.8, figure 5.9 and figure 5.10. Hysteresis measurement was started from negative to positive bias, and then swept back from positive to negative bias at a frequency of 50 kHz. The reason for the lower hysteresis is the thin film has lower number of defects, and consequently there is less charge trapped [50, 53].The voltage shift in the C-V curve of the $HfAlO_x$ thin films without plasma treatment is 98 mV. The voltage shift in the C-V curve of the $HfAlO_x$ thin films treated in N_2 plasma for 30 sec and then in CF_4 plasma for 60 sec is 7 mV. The voltage shift in the C-V curve of the samples nitrided by NH_3 plasma then fluorinated by CF_4 plasma is about 19 mV. The voltage shift in the C-V curve of the samples nitrided by NH_3 plasma then fluorinated by CF_4 plasma

is about 41 mV. That is, the hysteresis phenomenon of pure $HfAlO_x$ dielectrics could be restrained by various nitridation processes and fluorination process. From fig. 3-7, the hysteresis characteristic of $HfAlO_x$ thin films nitrided by N_2 plasma would remain the same quality after the fluorination process.

The CVS characteristics of samples nitrided by N_2 plasma for 30 sec and fluorinated by CF_4 plasma for different times are described in Fig. 5-11. The stress voltage was set as 5 V. Comparing to the samples without plasma treatment, all the gate current shifts of the samples with treatment could be decreased. The current shift of the nitrided sample would decrease with the fluorination process for 30 sec and 60 sec. The gate leakage shift of samples nitride in N_2 plasma for 30 sec and fluorinated in CF_4 plasma for 60 sec shrinks as 4.2×10^{-1} % of original one. It verifies the improve effect of fluorination plasma treatment to the reliability of nitrided $HfAlO_x$ thin films. The damage caused by fluorination plasma would be responsible for the CVS characteristic of the nitrided samples with fluorination for 90 sec. This result could correspond to the electrical characteristics that have been discussed above.

Figure 5.12 demonstrates the gate current shift of p-type $HfAlO_x$ capacitors treated with NH_3 plasma for 30 sec and CF_4 plasma for different process time. The gate leakage shift of samples nitride in NH_3 plasma for 30 sec and fluorinated in CF_4 plasma for 60 sec shrinks as 3.7×10^{-2} % of original one. Comparing to other samples, the gate current shift of the sample treated for 30 sec is the smallest. This result is consistent with the above discussion about plasma damage.

Figure 5.13 presents the gate current shift of p-type $HfAlO_x$ thin films treated with N_2O plasma for 30 sec and CF_4 for different process time. The gate leakage shift of samples nitride in NH_3 plasma for 30 sec and fluorinated in CF_4 plasma for 30 sec shrinks as 2.8×10^{-1} % of

original one. The current shift of the treated sample could also be improved through the plasma treatment.

5.3.3 Physical Analysis

The SIMS profile of the sample treated in ICP N_2O plasma for 30 sec and treated in ICP CF_4 plasma for 30 sec is presented in Fig. 5.14. Fig. 5.14 indicates that aluminium accumulation at the $HfAlO_x$/Si intrerface just like fluorine, which is induced by the plasma fluorination process. However, the aluminium accumulation also might be just from the characteristic of SIMS analysis, that is dopant could tend to accumulate in interface from SIMS data. Fig. 5.15 is the XPS F 1s electronic spectra of the $HfAlO_x$ sample treated in ICP N_2O plasma for 30 sec and treated in ICP CF_4 plasma for 30 sec. The F1s peak in the spectra is evident for the case with fluorine incorporation [54]. Besides, as in Fig. 4.15, there is no peak around binding energy of 688 eV, so the fluorine combined with carbon from CF_4 plasma process would be slight enough to ignore [24]. It would be an evidence to prove that carbon would not be induced by the ICP CF_4 plasma treatment we applied.

In summary, the improvement effect of the ICP fluorination processes to the electrical properties and the reliabilities of nitride $HfAlO_x$ thin films have been verified. According the chapter 4 and above discussions, the fluorination effect to nitride HfO_2 is more obvious. The reason to cause this difference could be the aluminium accumulation at the $HfAlO_x$/Si interface make the fluorine incorporated by the plasma fluorination process at the $HfAlO_x$/Si not form enough Hf-F bonding [24, 55].

5.4 Summary

Based on above results, the fluorination effect and the plasma damage might need to be traded off to achieve the optimum result. According to our study, the whole plasma fluorination process could be used to strengthen the $HfAlO_x$ thin films treated by various plasmas containing nitrogen in order to enhance the C-V characteristic and suppress the gate leakage. After the process time was decided from the C-V and the J-V characteristics, the improvement effect of the ICP fluorination process to the reliabilities of $HfAlO_x$ thin films was verified from the hysteresis and the CVS characteristics. Moreover, from this chapter and the chapter 4 of this dissertation, the effect of fluorination plasma treatment to nitrided $HfAlO_x$ thin films is not so obvious and this difference could be due to the Al accumulation at $HfAlO_x$/Si intrerface.

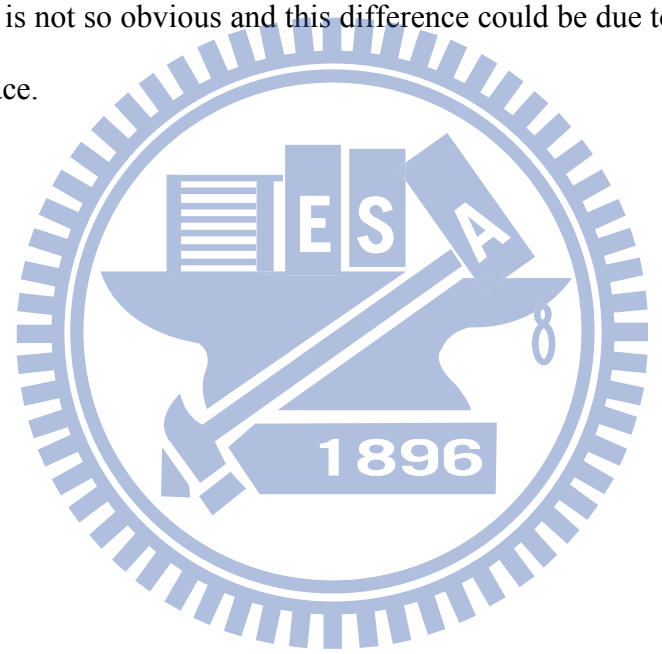

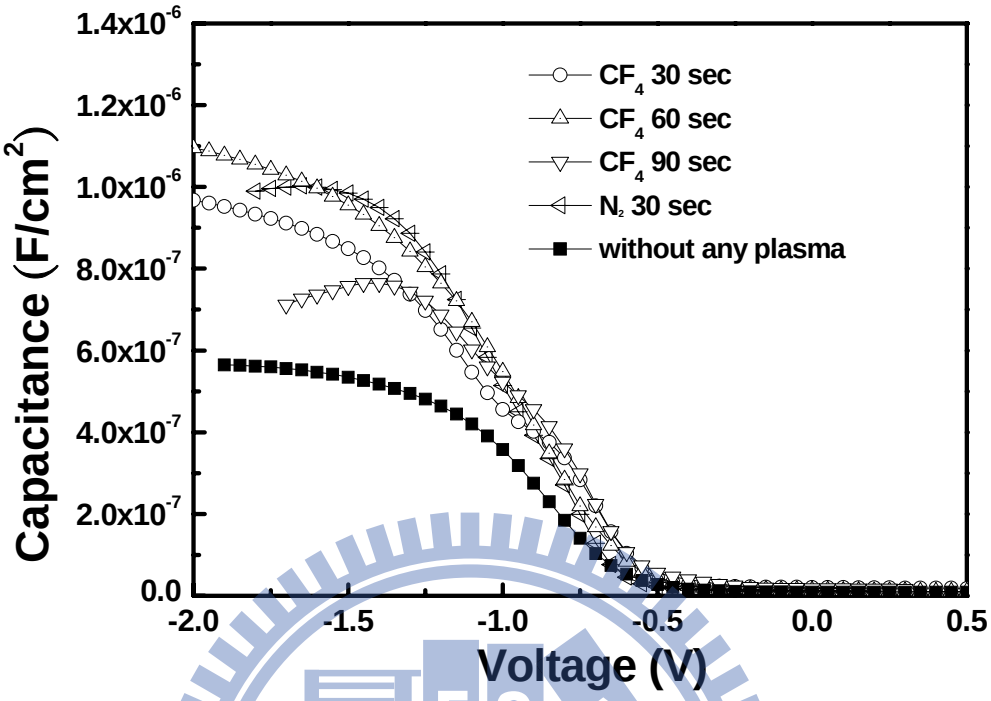

Figure 5.1 The C-V characteristics of the $HfAlO_x$ thin films treated in N_2 plasma for 30 sec and then in CF_4 plasma for different process times.

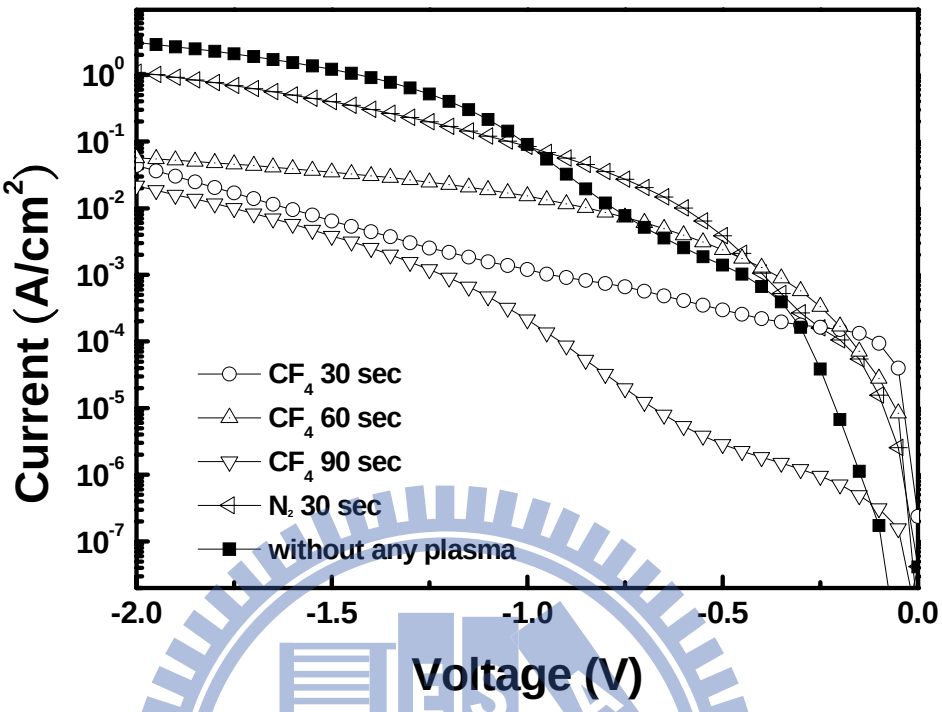

Figure 5.2 The J-V characteristics of the $HfAlO_x$ thin films treated in N_2 plasma for 30 sec and then in CF_4 plasma for different process times.

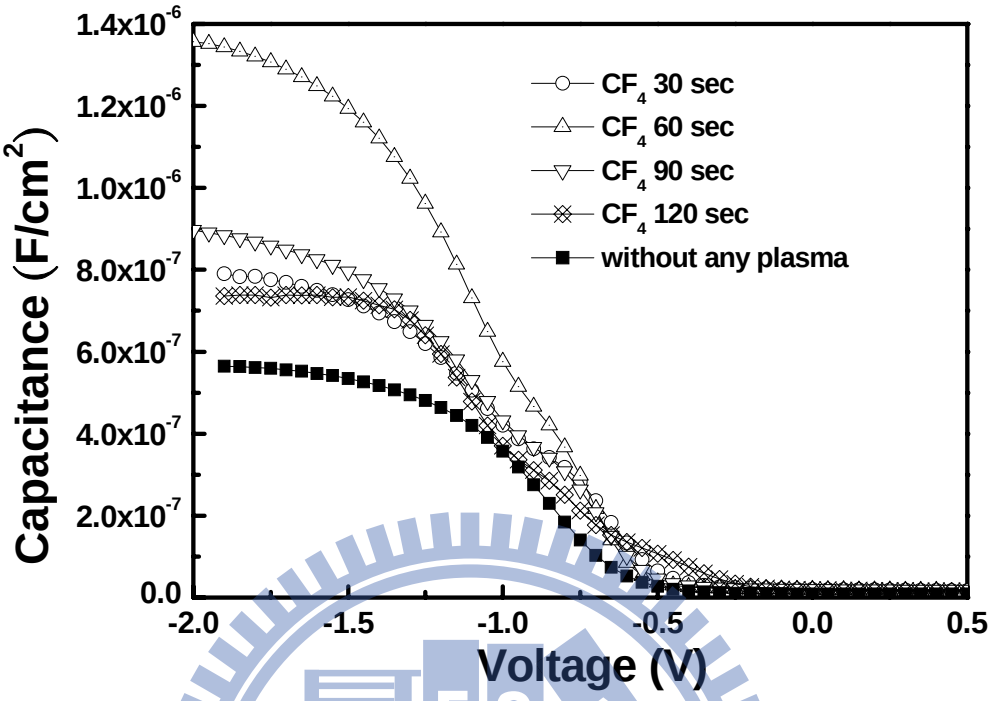

Figure 5.3 The C-V characteristics of the $HfAlO_x$ thin films treated in NH_3 plasma for 30 sec and then in CF_4 plasma for different process times.

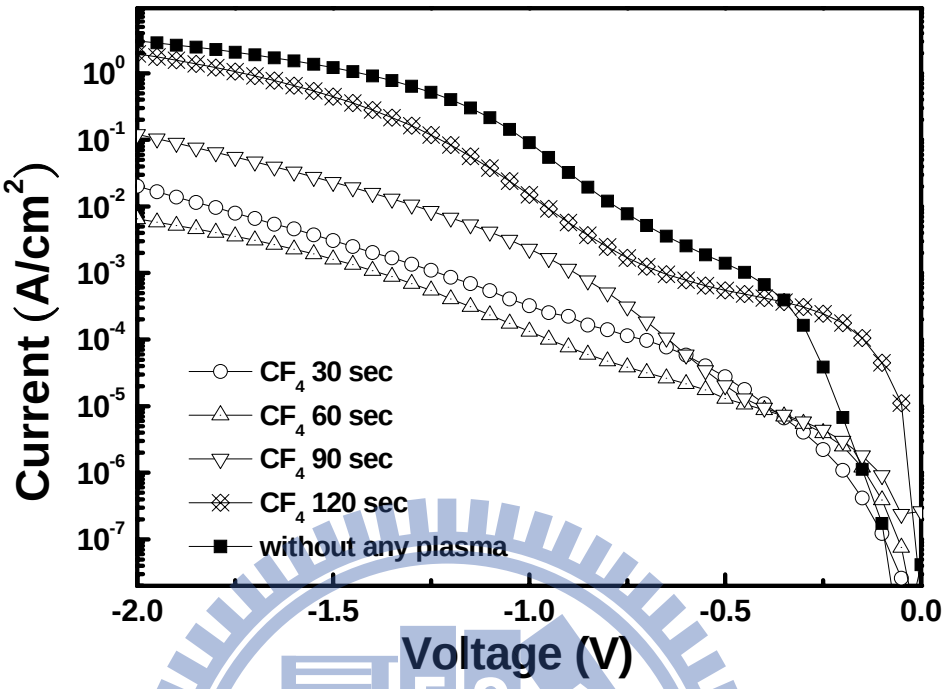

Figure 5.4 The J-V characteristics of the $HfAlO_x$ thin films treated in NH_3 plasma for 30 sec and then in CF_4 plasma for different process times.

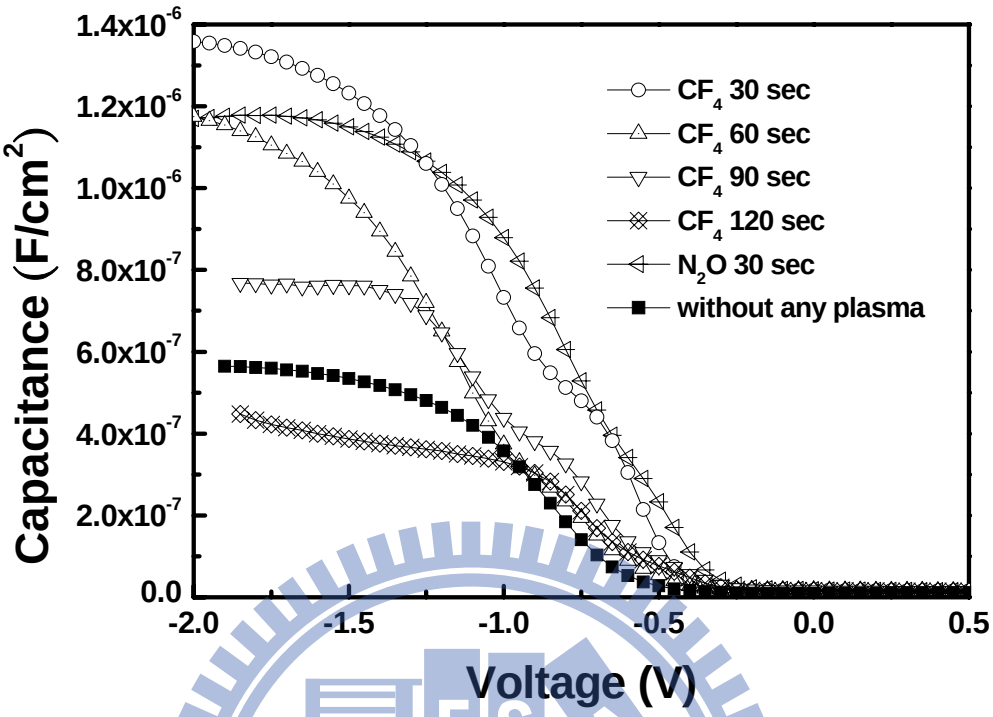

Figure 5.5 The C-V characteristics of the $HfAlO_x$ thin films treated in N_2O plasma for 30 sec and then in CF_4 plasma for different process times.

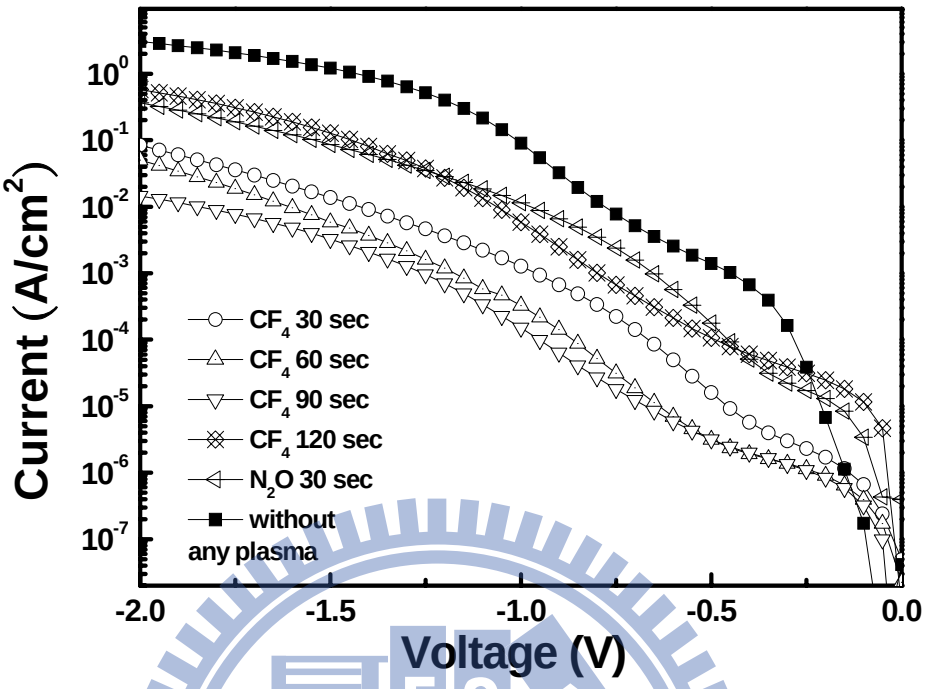

Figure 5.6 The J-V characteristics of the $HfAlO_x$ thin films treated in N_2O plasma for 30 sec and then in CF_4 plasma for different process times.

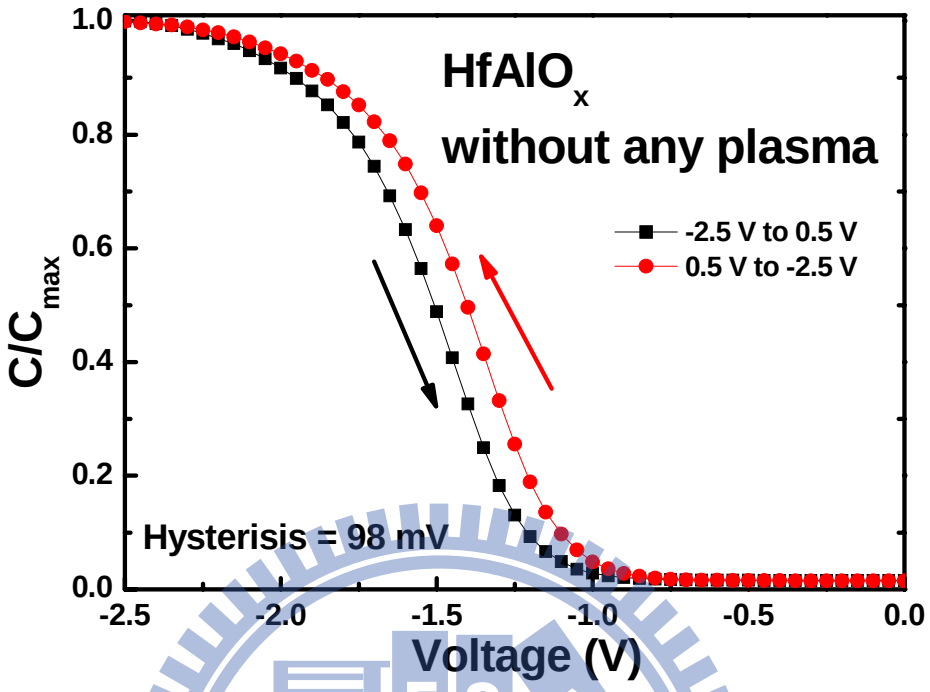

Figure 5.7 The hysteresis characteristics of the $HfAlO_x$ thin films without plasma treatment.

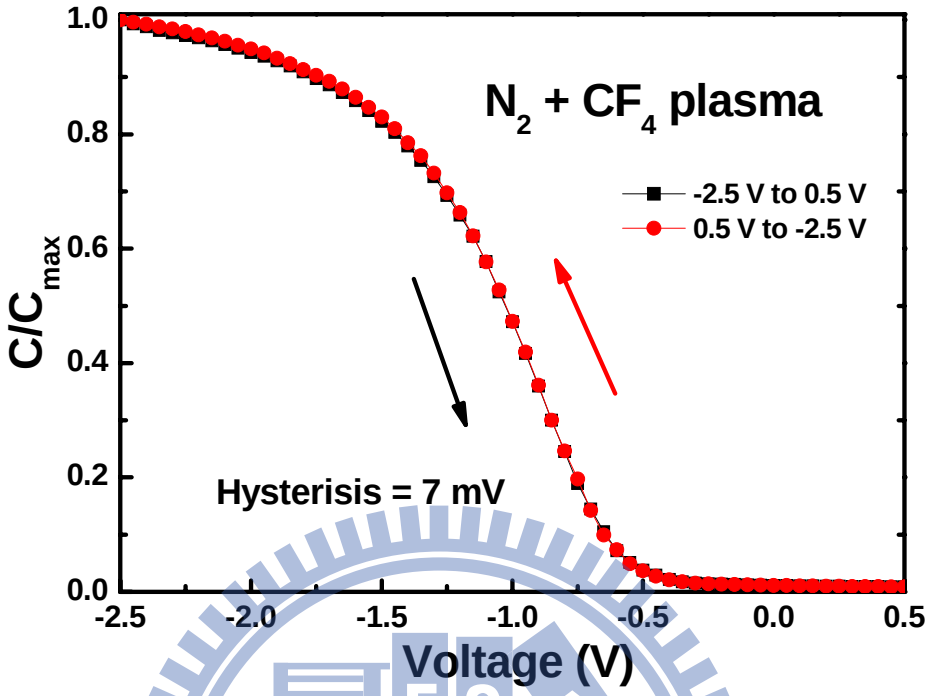

Figure 5.8 The hysteresis characteristics of the $HfAlO_x$ thin films treated in N_2 plasma for 30 sec and then in CF_4 plasma for 60 sec.

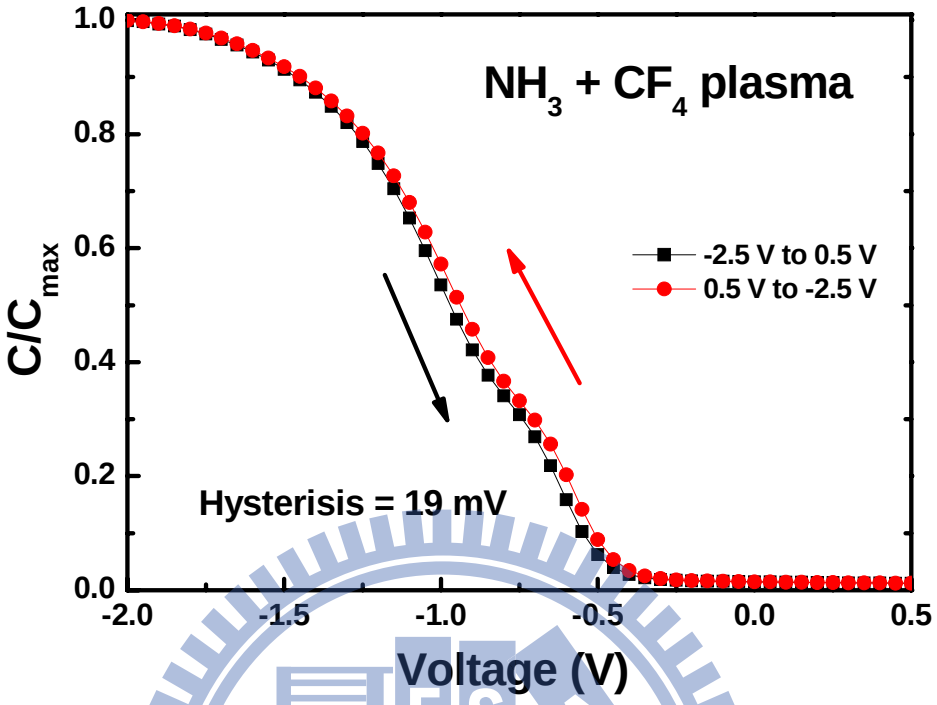

Figure 5.9 The hysteresis characteristics of the $HfAlO_x$ thin films treated in NH_3 plasma for 30 sec and then in CF_4 plasma for 60 sec.

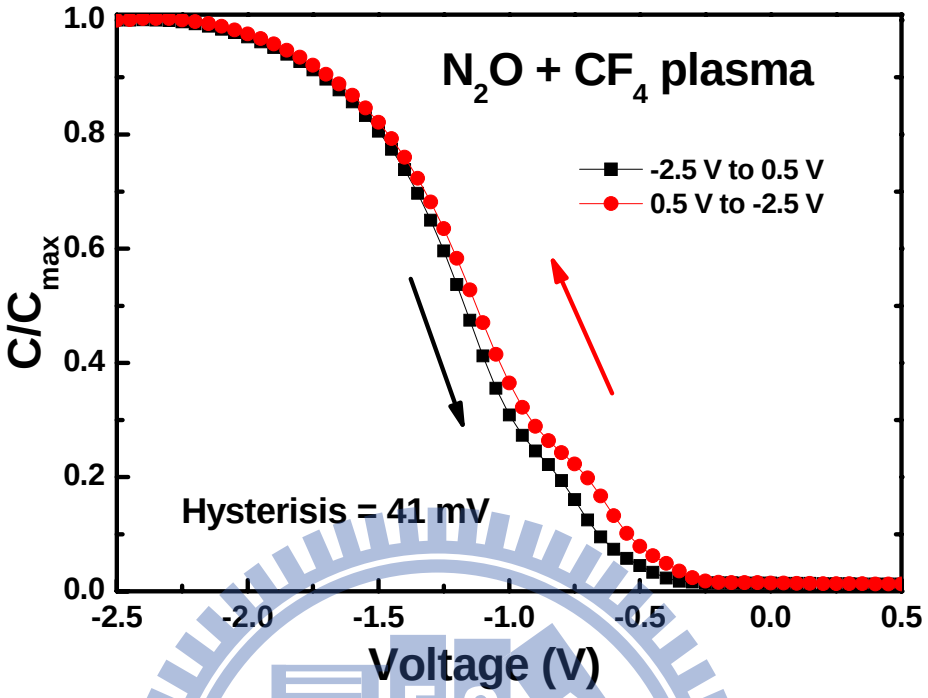

Figure 5.10 The hysteresis characteristics of the HfO_2 thin films treated in N_2O plasma for 30 sec and then in CF_4 plasma for 60 sec.

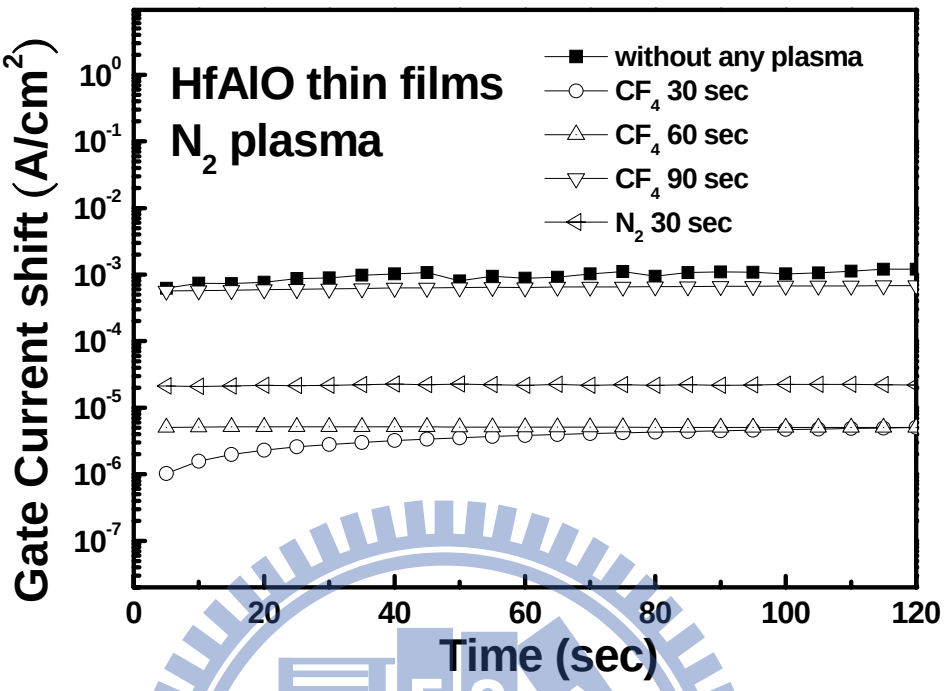

Figure 5.11 The leakage current shift curves of the $HfAlO_x$ thin films that were nitrided by ICP N_2 plasma for 30 sec then fluorinated by ICP CF_4 plasma for different time.

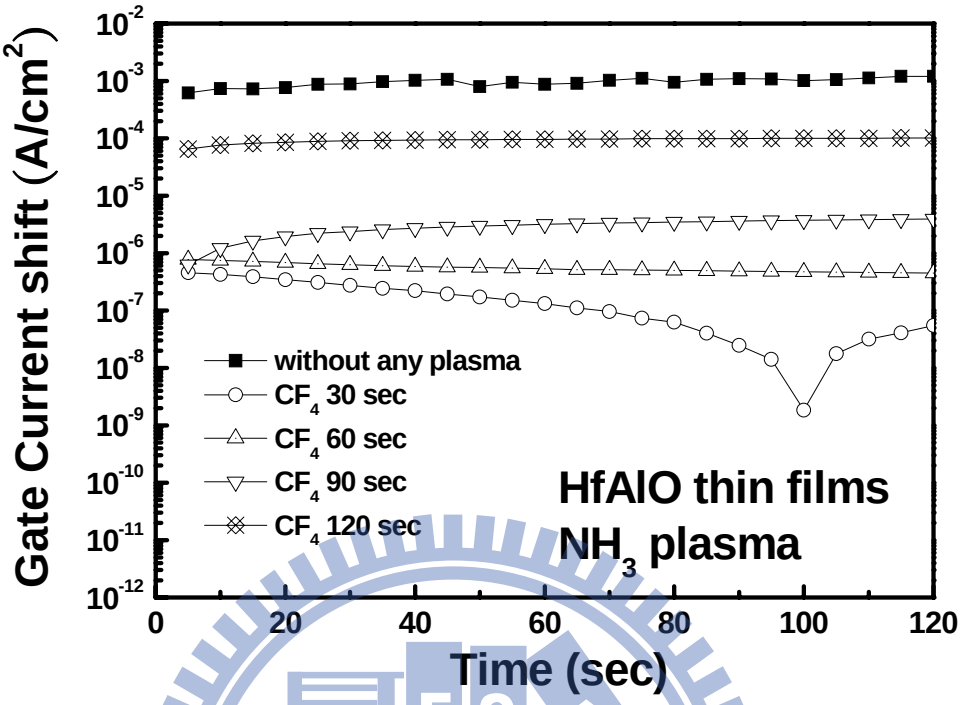

Figure 5.12 The leakage current shift curves of the $HfAlO_x$ thin films that were nitrided by ICP NH_3 plasma for 30 sec then fluorinated by ICP CF_4 plasma for different time.

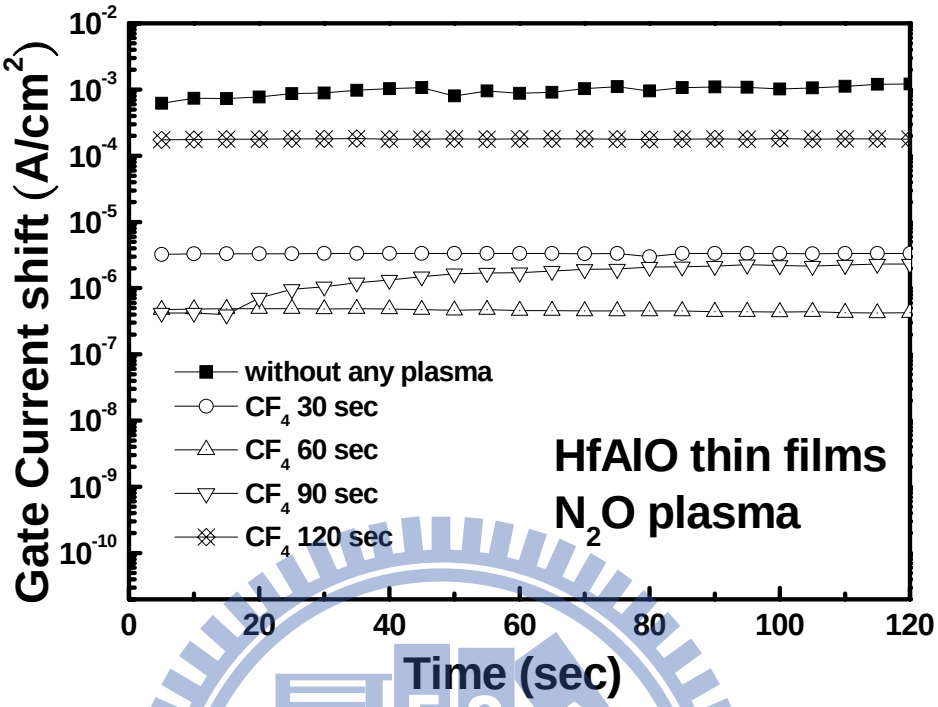

Figure 5.13 The leakage current shift curves of the $HfAlO_x$ thin films that were nitrided by ICP N_2O plasma for 30 sec then fluorinated by ICP CF_4 plasma for different time.

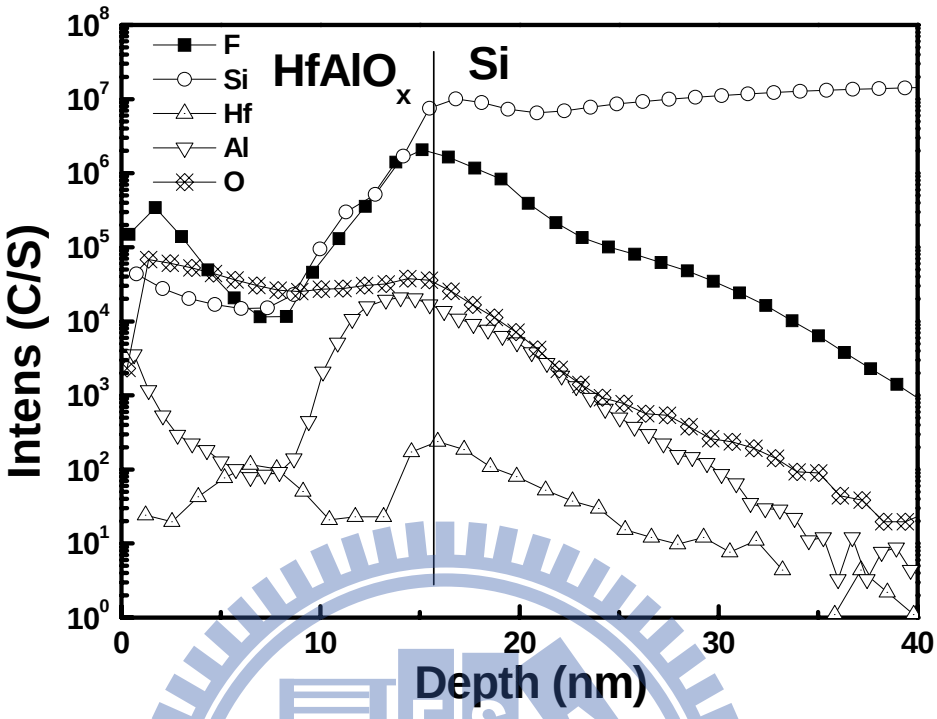

Figure 5.14 The SIMS profile of the $HfAlO_x$ thin films treated in ICP N_2O plasma for 30 sec and treated in ICP CF_4 plasma for 30 sec.

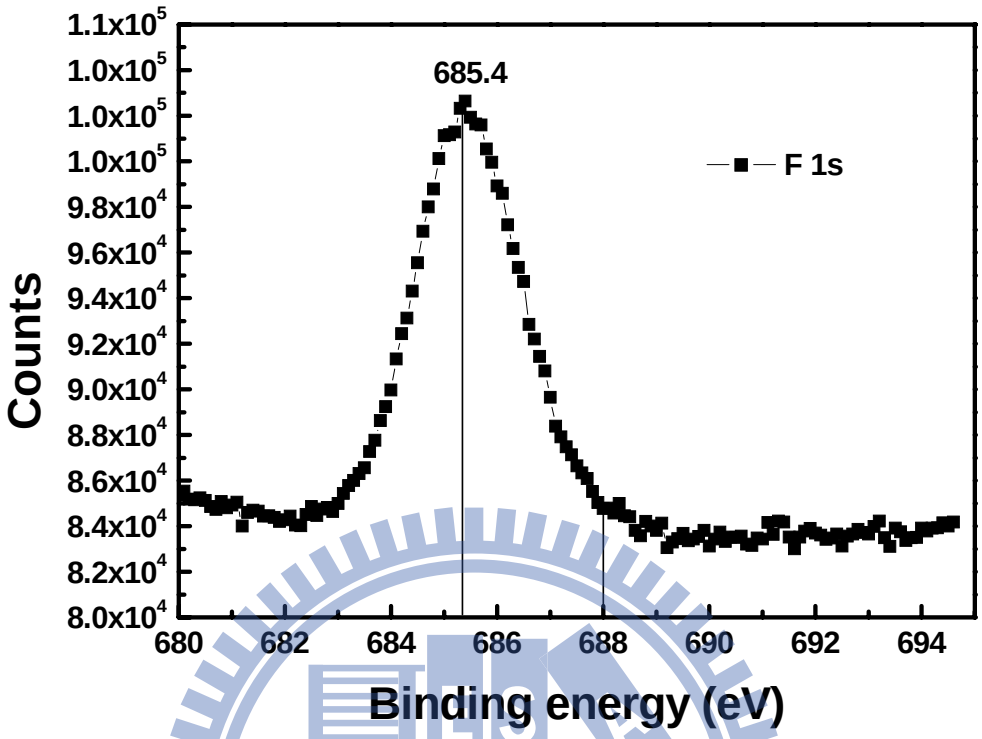

Figure 5.15 The XPS F 1s electronic spectra of the $HfAlO_x$ thin films treated in ICP N_2O plasma for 30 sec and treated in ICP CF_4 plasma for 30 sec.

Chapter 6

Conclusion and Future Work

6.1 Conclusion

In this dissertation, we have applied ICP nitridation process to improve the electrical characteristics, the reliabilities and the thermal stability of HfO_2 thin films and $HfAlO_x$ thin films. Then we have tried to applied ICP fluorination process in order to enhance the improvement effect of the plasma treatment. The electrical characteristics and the reliabilities of HfO_2 thin films and $HfAlO_x$ thin films could be strengthened in adequate plasma treatment.

In the chapter 2 of this dissertation, the ICP nitirdation process has been examine to be an effective method to enlarge the capacitance density and restrain the gate leakage current density of HfO_2 thin films. The reliability of HfO_2 thin films also could be strengthened by the plasma nitirdation treatment from analyzing the hysteresis characteristics, stress-induced leakage current characteristics and constant voltage stress characteristics of the thin films. Besides, the thermal stability of HfO_2 thin films could be enhanced by the incorporation of nitrogen from the nitridation process.

In the chapter 3 of this dissertation, the similar ICP nitridation process has been used to modify $HfAlO_x$ thin films. The electrical characteristics and the reliabilities of $HfAlO_x$ thin films could be improved by the plasma nitirdation treatment. The thermal stability of $HfAlO_x$ thin film is better than HfO_2 thin films because of the Al incorporation in $HfAlO_x$ dielectric layers. Furthermore, the thermal stability of $HfAlO_x$ thin films could increase effectively due to the nitrogen incorporation induced by the plasma nitridation treatment.

In the chapter 4 of this dissertation, the post deposition plasma fluorination process combined with the plasma nitridation process has been applied in HfO_2 thin films. The

fluorine accumulation, which is induced by the plasma fluorination process, at the HfO_2 dielectric layer/silicon substrate interface might restrain the regrowth of interfacial layer. So the EOT of HfO_2 thins film could decrease by optimal nitrogen and fluorination dopant. The reliability of HfO_2 thins film would be not damaged after the additional post deposition fluorination process.

In the chapter 5 of this dissertation, the same fluorination process was integrated into the experimental process of $HfAlO_x$ capacitor. Since the Al incorporation is mainly between the dielectric layers and the silicon substrate, the suppression of interfacial layers regrowth due to the fluorination process is not obvious. Even so, the capacitance density and leakage current density of nitrided $HfAlO_x$ thin films would be strengthened by the fluorination process. The reliability of $HfAlO_x$ thin films would maintain after integrating this fluorination process into the experimental process.

6.2 Future Work

Although the effect of the plasma nitrdation and fluorination to the electrical characteristics and reliabilities of HfO_2 and $HfAlO_x$ thin films has been examined in this research, there are still several issues that could be investigated in the future:

1. We could do more material analysis, like TEM, SIMS and XPS, to study the change of dielectric layers with or without plasma treatment.
2. We could study the leakage current mechanism change of the dielectric layers caused by the plasma treatment.
3. We could integrate the plasma technology to CMOSFET process flow to verify the effect of the plasma nitridation and plasma fluorination to the electrical characteristics of the transistors, like threshold voltage, mobility and sub-threshold swing.
4. We could try to use the plasma nitridation and fluorination technology to treat thinner

dielectric layers, whose EOT are less than 1 nm. The thin films could be made with integrating atomic layer chemical vapor deposition (ALD) technology and pre-deposition CF_4 plasma treatment.

5. The plasma nitridation and fluorination technology could be used to treat thicker dielectric layers, whose physical thickness are about 20 nm. The thicker dielectric layers could be integrated in thin-film-transistors (TFT) and might be able to enhance the electrical characteristics and the reliability of the TFTs.

References

[1] International Technology Roadmap for Semiconductors, presented at public.itrs.net (2009).

[2] G. D. Wilk, R. M. Wallace, and J. M. Anthony, "High-κ gate dielectrics: Current status and materials properties considerations", *J. Appl. Phys.*, **89**, p. 5243 (2001).

[3] Y. Shimamoto, J. Yugami, M. Inoue, M. Mizutani, T. Hayashi, K. Shiga, F. Fujita, M. Yoneda, and H. Matsuoka, "Advantages of gate work-function engineering by incorporating sub-monolayer Hf at SiON/poly-Si interface in low-power CMOS", *Symposium on VLSI Technology Digest of Technical Papers*, IEEE, p. 132, (2005).

[4] C. Hobbs, L. Fonseca, V. Dhandapani, S. Samavedam, B. Taylor, J. Grant, L. Dip, D. Triyoso, R. Hegde, D. Gilmer, R. Garcia, D. Roan, L. Lovejoy, R. Rai, L. Hebert, H. Tseng, B. White, and P. Tobin, "Fermi level pinning at the polySi/metal oxide interface", *Symposium on VLSI Technology Digest of Technical Papers*, IEEE, p. 9, (2003).

[5] R. I. Hegde, "Film and Device Characteristics of Sputter-Deposited Hafnium Zirconate Gate Dielectric", *J. Electrochem. Soc.*, **155**, 5, p. G121 (2008).

[6] K. J. Hubbard and D. G. Schlom, "Thermodynamic stability of binary oxides in contact with silicon", *J. Mater. Res.*, **11**, p. 2757 (1996).

[7] S. Yamaguchi, K. Tai, T. Hirano, T. Ando, S. Hiyama, J. Wang, Y. Hagimoto, Y. Nagahama, T. Kato, K. Nagano, M. Yamanaka, S. Terauchi, S. Kanda, R. Yamamoto, Y. Tateshita, Y. Tagawa, H. Iwamoto, M. Saito, N. Nagashima and S. Kadomura, "High Performance Dual Metal Gate CMOS with High Mobility and Low Threshold Voltage Applicable to Bulk CMOS Technology", *Symposium on VLSI Technology Digest of Technical Papers*, IEEE, p. 152, (2006).

[8] W. J. Zhu, T. Tamagawa, M. Gibson, T. Furukawa, and T. P. Ma, "Effect of Al inclusion in HfO_2 on the physical and electrical properties of the dielectrics", *IEEE Electron Dev. Lett.* **23**, p. 649 (2002).

[9] K. Torii, K. Shiraishi, S. Miyazaki, K. Yamabe, M. Boero, T. Chikyow, K. Yamada, H. Kitajima, and T. Arikado, "Physical model of BTI, TDDB and SILC in HfO_2-based high-k gate dielectrics", *IEDM Tech. Dig.*, p. 129, (2004).

[10] N. Umezawa, K. Shiraishi, T. Ohno, H. Watanabe, T. Chikyow, K. Torii, K. Yamabe, K. Yamada, H. Kitajima, and T. Arikado, "First-principles studies of the intrinsic effect of nitrogen atoms on reduction in gate leakage current through Hf-based high-k dielectrics", *Appl. Phys. Lett.*, **86**, p. 143507 (2005).

[11] G. Shang, P.W. Peacock, and J. Robertoson, "Stability and band offsets of nitrogenated high-dielectric-constant gate oxides", *Appl. Phys. Lett.* **84**, p. 106 (2004).

[12] M. L. Green, E. P. Gusev, R. Degraeve´, and E. L. Garfunkel, "Ultrathin (≪4 nm) SiO_2 and Si–O–N gate dielectric layers for silicon microelectronics: Understanding the processing, structure, and physical and electrical limits", *J. Appl. Phys.*, **90**, p. 2057 (2001).

[13] T. Morimoto, H. S. Momose, Y. Ozawa, K. Yamabe, and H. Iwai, "Relationship between mobility and residual-mechanical-stress as measured by Raman spectroscopy for nitrided-oxide-gate MOSFETs", *Tech. Dig. Int. Electron. Device Meet.*, p. 429, (1990).

[14] H. S. Momose, T. Morimoto, Y. Ozawa, K. Yamabe, and H. Iwai, "Electrical characteristics of rapid thermal nitrided-oxide gate n and p-MOSFET's with less than 1 atom% nitrogen concentration", *IEEE Trans. Electron Devices*, **41**, p. 546 (1994).

[15] K. Yamamoto, W. Deweerd, M. Aoulaiche, M. Houssa, S. De Gendt, S. Horii, M. Asai,

A. Sano, S. Hayashi, and Masaaki Niwa, “Electrical and physical characterization of remote plasma oxidized HfO_2 gate dielectrics”, *IEEE Trans. Electron Devices*, **53**, p. 1153 (2006).

[16] S. Lee, S. Bang, S. Jeon, S. Kwon, W. Jeong, S. Kim, and H. Jeon, “Film and Device Characteristics of Sputter-Deposited Hafnium Zirconate Gate Dielectric”, *J. Electrochem. Soc.*, **155**, 7, p. H516 (2008).

[17] M. S. Akbar, S. Gopalan, H.-J. Cho, K. Onishi, R. Choi, R. Nieh, C. S. Kang, Y. H. Kim, J. Han, S. Krishnan, and J. C. Lee, “High-performance TaN/HfSiON/Si metal-oxide-semiconductor structures prepared by NH3 post-deposition anneal”, *Appl. Phys. Lett.*, **82**, p. 1757 (2003).

[18] V. S. Chang, L.-Å. Ragnarsson, H. Y. Yu, M. Aoulaiche, T. Conard, K. M. Yin, T. Schram, J. W. Maes, S. De Gendt, and S. Biesemans, “Effects of Al_2O_3 Dielectric Cap and Nitridation on Device Performance, Scalability, and Reliability for Advanced High- κ/Metal Gate pMOSFET Applications”, *IEEE Trans. Electron Devices*, **54**, p. 2738 (2007).

[19] C. H. Choi, S. J. Rhee, T. S. Jeon, N. Lu, J. H. Sim, R. Clark, M. Niwa, and D. L. Kwong, “Thermally stable CVD HfO_xN_y advanced gate dielectrics with poly-Si gate electrode”, *Tech. Dig. Int. Electron. Device Meet.*, p. 857 (2002).

[20] M. Koyama, A. Kaneko, T. Ino, M. Koike, Y. Kamata, R. Iijima, Y. Kamimuta, A. Takashima, M. Suzuki, C. Hongo, S. Inumiya, M. Takayanagi, and A. Nishiyama, “Effects of nitrogen in HfSiON gate dielectric on the electrical and thermal characteristics”, *Tech. Dig. Int. Electron. Device Meet.*, p. 849 (2002).

[21] M. A. Quevedo-Lopez, J. J. Chambers, M. R. Visokay, A. Shanware, and L. Colombo, “Thermal stability of hafnium–silicate and plasma-nitrided hafnium silicatefilms studied by Fourier transform infrared spectroscopy”, *Appl. Phys. Lett.*, **87**, p. 12902 (2005).

[22] C.-C. Cheng, C.-H. Chien, J.-H. Lin, and C.-Y. Chang, G.-L. Luo, C.-H. Yang, and S.-L. Hsu, "Thermochemical reaction of $ZrO_x(N_y)$ interfaces on Ge and Si substrates", *Appl. Phys. Lett.*, **89**, p. 12905 (2006).

[23] T. Schimizu, and N. Fukushima, *Int. Conf. Phys. Semicond.*, p. 297 (2006).

[24] K.-i. Seo, R. Sreenivasan, P. C. McIntyre, and K. C. Saraswat, "Improvement in High-k (HfO_2/SiO_2) Reliability by Incorporation of Fluorine", *IEEE Electron Dev. Lett.* **27**, p. 821 (2006).

[25] M. Inoue, S. Tsujikawa, M. Mizutani, K. Nomura, T. Hayashi, K. Shiga, J. Yugami, J. Tsuchimoto, Y. Ohno, and M. Yoneda, "Fluorine incorporation into HfSiON dielectric for V_{th} control and its impact on reliability for poly-Si gate pFET", *Tech. Dig. Int. Electron. Device Meet.*, p. 425 (2004).

[26] H.H. Tseng, P.J. Tobin, E.A. Hebert, S. Kalpat, M.E. Ramon, L. Fonseca, Z.X. Jiang, J.K. Schaeffer, R.I. Hegde, D.H. Triyoso, D.C. Gilmer, W.J. Taylor, C.C. Capasso, O. Adetutu, D. Sing, J. Conner, E. Luckowski, B.W. Chan, A. Haggag, S. Backer, R. Noble, M. Jahanbani, Y.H. Chili, and B.E. White, "Defect passivation with fluorine in a Ta_xC_y high-K gate stack for enhanced device threshold voltage stability and performance", *Tech. Dig. Int. Electron. Device Meet.*, p. 713 (2004).

[27] K.I. Seo, R. Sreenivasan, P.C. McIntyre, and K.C. Saraswat, "Improvement in High-k (HfO_2/SiO_2) Reliability by Incorporation of Fluorine", *Tech. Dig. Int. Electron. Device Meet.*, p. 429 (2005).

[28] K. Tse, and J. Robertson, "Defect passivation in HfO_2 gate oxide by fluorine", *Appl. Phys. Lett.* **89**, p. 142914 (2006).

[29] T. Schimizu, and M. Koyama, "Control of electronic properties of HfO_2 with fluorine doping from first-principles", *Applied Surface Science*, **254**, 19, p. 6109 (2008).

[30] J.-P. Han, E. M. Vogel, E. P. Gusev, C. D'Emic, C. A. Richter, D. W. Heh, and J. S. Suehle, "Asymmetric energy distribution of interface traps in n- and p-MOSFETs with

HfO_2 gate dielectricon ultrathin SiON buffer layer", *IEEE Electron Device Lett.*, **25**, p. 126 (2004).

[31] G. S. Lujan, S. Kubicek, S. De Gendt, M. Heyns, W. Magnus, and K. De Meyer, "Mobility degradation in high-k transistors: the role of the charge scattering", *Proc. ESSDERC*, p. 399, (2003).

[32] M.-H. Cho, K. B. Chung, and D.-W. Moon, "Electronic structure and thermal stability of nitrided Hf silicate films using a direct N plasma", *Appl. Phys. Lett.*, **89**, p. 182908 (2006).

[33] C. X. Li, P. T. Lai, J. P. Xu and X. Zou, "Effects of annealing gas on electrical properties and reliability of Ge MOS capacitors with HfTiON as gate dielectric", *IEEE EDSSC*, p. 185, (2007).

[34] K.-C. Tsai, W.-F. Wu, C.-G. Chao, and C.-C. Wu, "Improving Electrical Characteristics of Ta/Ta_2O_5/Ta Capacitors Using Low-Temperature Inductively Coupled N_2O Plasma Annealing", *J. Electrochem. Soc.*, **154**, 6, p. H512 (2007).

[35] S. Kim, S. Woo, H. Hong, H. Kim, H. Jeon, and C. Baeb, "Effect of Buffer Layer for HfO_2 Gate Dielectrics Grown by Remote Plasma Atomic Layer Deposition", *J. Electrochem. Soc.*, **154**, 2, p. H97 (2007).

[36] J. Y. Kim, S. Seo, D. Y. Kim, H. Jeon, and Y. Kim, "Remote plasma enhanced atomic layer deposition of TiN thin films using metalorganic precursor", *J. Vac. Sci. Technol. A*, **22**, 1, p. 8 (2004).

[37] G. D. Wilk, M. L. Green, M.-Y. Ho, B. W. Busch, T. W. Sorsch, F. P. Klemens, B. Brijs', R. B. van Dover, A. Komblit, T. Gustafsson, E. Garfunkel, S. Hillenius, D. Monroe, P. Kalavade, and J.M. Hergenrother, "Improved film growth and flatband voltage control of ALD HfO_2 and Hf-Al-O with n^+ poly-Si gates using chemical oxides and optimized post-annealing", *Symposium on VLSI Technology Digest of Technical Papers*, IEEE, p. 88, (2002).

[38] J. Molina, K. Tachi, K. Kakushima, P. Ahmet, K. Tsutsui, N. Sugii, T. Hattori, and H. Iwai, "Effects of N_2-Based Annealing on the Reliability Characteristics of Tungsten/La_2O_3/Silicon Capacitors", *J. Electrochem. Soc.*, **154**, 5, p. G110 (2007).

[39] C.-C. Cheng, C.-H. Chien, C.-W. Chen, S.-L. Hsu, C.-H. Yang, and C.-Y. Chang, "Effects of Postdeposition Annealing on the Characteristics of HfO_xN_y Dielectrics on Germanium and Silicon Substrates", *J. Electrochem. Soc.*, **153**, 7, p. F160 (2006).

[40] M. R. Visokay, J. J. Chambers, A. L. P. Rotondaro, A. Shanware, and L. Colombo, "Application of HfSiON as a gate dielectric material", *Appl. Phys. Lett.*, **80**, p. 3183 (2002).

[41] H. Takashi, I. Hiroshi, N. Yasushi, and E. Hideya, "Effect of nitrogen distribution in nitrided oxide prepared by rapid thermal annealing on its electrical characteristics", *IEEE Trans. Electron Devices* **34,** p. 2238 (1987).

[42] I.-C. Chen, S. E. Holland, and C. Hu, "Electrical breakdown in thin gate and tunneling oxides", *IEEE Trans. Electron Devices*, **32**, p. 413 (1985).

[43] S. Yamamichi, A. Yamamichi, D. Park, T.-J. King, and C. Hu, "Impact of time dependent dielectric breakdown and stress-induced leakage current on the reliability of high dielectric constant (Ba,Sr)TiO_3 thin-film capacitors for Gbit-scale DRAMs", *IEEE Trans. Electron Devices*, **46**, p. 342 (1999).

[44] A. Goetzberger and J. C. Irvin, "Low-temperature hysteresis effects in metal-oxide-silicon capacitors caused by surface-state trapping", *IEEE Trans. Electron Devices*, **15**, p. 1009 (1968).

[45] J.-G. Hwu and M.-J. Jeng, "C-V Hysteresis Instability in Aluminum/Tantalum Oxide/Silicon Oxide/Silicon Capacitors due to Postmetallization Annealing and Co-60 Irradiation", *J. Electrochem. Soc.*, **135**, 11, p. 2808 (1988).

[46] K.-M. Chang, B.-N. Chen, and S.-M. Huang, "The effects of plasma treatment on the thermal stability of HfO_2 thin films", *Applied Surface Science,* **254**, 19, p. 6116 (2008).

[47] J. Huang, P. D. Kirsch, J. Oh, S. H. Lee, P. Majhi, H. R. Harris, D. C. Gilmer, G. Bersuker, D. Heh, C. S. Park, C. Park, H.-H. Tseng, and R. Jammy, "Mechanisms Limiting EOT Scaling and Gate Leakage Currents of High-k /Metal Gate Stacks Directly on SiGe", *IEEE Electron Device Lett.*, **30**, p. 285 (2009).

[48] H.-H. Tseng, P. J. Tobin, E. A. Hebert, S. Kalpat, M. E. Ramon, L. Fonseca, Z. X. Jiang, J. K. Schaeffer, R. I. Hedge, D. H. Triyso, C. C. Capasso, O. Adetutu, D. Sing, J. Conner, E. Luckowski, B.W. Chan, A. Haggag, S. Backer, R. Noble, M. Jahanbani, Y. H. Chiu, and B. E. White, "Defect passivation with fluorine in a Ta_xC_y high-K gate stack for enhanced device threshold voltage stability and performance", *Tech. Dig. Int. Electron. Device Meet.*, p. 696 (2005).

[49] W.-C. Wu, C.-S. Lai, S.-C. Lee, M.-W. Ma, T.-S. Chao, J.-C. Wang, C.-W. Hsu, P.-C. Chou, J.-H. Chen, K.-H. Kao,W.-C. Lo, T.-Y. Lu, L.-L. Tay, and N. Rowell, "Fluorinated HfO_2 gate dielectrics engineering for CMOS by pre- and post-CF_4 plasma passivation", *Tech. Dig. Int. Electron. Device Meet.*, p. 1 (2008).

[50] C.-S. Lai, W.-C. Wu, J.-C. Wang, and T.-S. Chao, "Characterization of CF_4-plasma fluorinated HfO_2 gate dielectrics with TaN metal gate", *Appl. Phys. Lett.*, **86**, p. 222905 (2005).

[51] Tatsuo Schimizu, and Masato Koyama, "Control of electronic properties of HfO_2 with fluorine doping from first-principles", *Applied Surface Science*, **254**, p. 6109 (2008).

[52] C.-S. Lai, W.-C. Wu; H.-H. Hsu, P.-C. Chou, and S.-J. Wu, "The polarity dependence of capacitances for HfO_2 affected by post-CF_4 plasma treatment", *IEEE International Conference on Semiconductor Electronics*, p. 565 (2004).

[53] C. S. Chang, Seok Kang, H.-J. Cho, K. Onishi, R. Choi, R. Nieh, S. Goplan, S. Krishnan, and J. C. Lee, "Improved thermal stability and device performance of ultra-thin (EOT<10 Å) gate dielectric MOSFETs by using hafnium oxynitride (HfO_xN_y)", *VLSI Tech. Dig.*, p. 146 (2002).

[54] M. Inoue, S. Tsujikawa, M. Mizutani, K. Nomura, T. Hayashi, K. Shiga, J. Yugami, J. Tsuchimoto, Y. Ohno, and M. Yoneda, "Fluorine incorporation into HfSiON dielectric for V_{th} control and its impact on reliability for poly-Si gate pFET", *Tech. Dig. Int. Electron. Device Meet.*, p. 413 (2005).

[55] S. H. Bae, C. H. Lee, R. Clark, and D. L. Kwong, "MOS characteristics of ultrathin CVD HfAlO gate dielectrics", *IEEE Electron Device Lett.*, **24**, p. 556 (2003).

[56] K.-M. Chang, B.-N. Chen, and S.-M. Huang, "The Effects of Plasma Treatment on the Thermal Stability of $HfAlO_x$ Thin Films", *International Semiconductor Device Reaserch Symposium, IEEE*, p. 1, (2007).

[57] W. C. Wu, C.-S. Lai, T.-M. Wang, J.-C. Wang, C. W. Hsu, M. W. Ma, W.-C. Lo, and T. S. Chao, "Carrier Transportation Mechanism of the TaN/HfO_2/IL/Si Structure With Silicon Surface Fluorine Implantation", *IEEE Trans. Electron Devices*, **55**, p. 1639 (2008).

[58] W. C. Wu, C. S. Lai, J. C. Wang, J. H. Chen, M. W. Ma, and T. S. Chao, "High-Performance HfO_2 Gate Dielectrics Fluorinated by Postdeposition CF_4 Plasma Treatment", *J. Electrochem. Soc.*, **154**, 7, p. H561 (2007).

[59] C. S. Lai, W. C. Wu, T. S. Chao, J. H. Chen, J. C. Wang, L.-L. T, and N. Rowell, "Suppression of interfacial reaction for HfO_2 on silicon by pre-CF_4 plasma treatment", *Appl. Phys. Lett.*, **89**, p. 072904 (2006).

[60] T. J. Park, J. H. Kim, J. H. Jang, K. D. Na, C. S. Hwang, and J. H. Yoo, "Dependences of nitrogen incorporation behaviors on the crystallinity and phase distribution of

atomic layer deposited Hf-silicate films with various Si concentrations", *J. Appl. Phys.*, **104**, p. 054101 (2008).

個人學經歷資料表

姓名：陳柏寧

出生地：基隆市

性別：男

生日：民國 68 年 5 月 9 日

學歷：

高中：國立師範大學附屬高級中學

大學：國立清華大學電機工程學系

碩士：國立交通大學電子研究所固態組

博士：國立交通大學電子研究所固態組

學號：9311802

博士論文題目：

中文：電感耦合電漿氮化製程與氟化製程對鉿系高介電常數材料薄膜之效果

英文：The Effect of Inductively-Coupled Plasma Nitridation and Fluorination Process to Hf-based Dielectric Thin Films